uOttawa

L'Université canadienne
Canada's university

**FACULTÉ DES ÉTUDES SUPÉRIEURES ET POSTDOCTORALES**

uOttawa

L'Université canadienne
Canada's university

**FACULTY OF GRADUATE AND POSTDOCTORAL STUDIES**

Mahsa Fathi

AUTEUR DE LA THÈSE / AUTHOR OF THESIS

M.Sc. (Chemical and Environmental Toxicology)

GRADE / DEGREE

Department of Biology

FACULTÉ, ÉCOLE, DÉPARTEMENT / FACULTY, SCHOOL, DEPARTMENT

Benthic Flux of Mercury Between Sediments and the Overlying Water in the St. Lawrence River Near Cornwall, Ontario

TITRE DE LA THÈSE / TITLE OF THESIS

J. Blais

DIRECTEUR (DIRECTRICE) DE LA THÈSE / THESIS SUPERVISOR

CO-DIRECTEUR (CO-DIRECTRICE) DE LA THÈSE / THESIS CO-SUPERVISOR

EXAMINATEURS (EXAMINATRICES) DE LA THÈSE / THESIS EXAMINERS

D. Lean

J. Ridal

D. Fortin

Gary W. Slater

Le Doyen de la Faculté des études supérieures et postdoctorales / Dean of the Faculty of Graduate and Postdoctoral Studies

# Benthic Flux of Mercury Between Sediments and the Overlying Water in the St. Lawrence River Near Cornwall, Ontario

**Mahsa Fathi**

Thesis submitted to the

Faculty of Graduate and Postdoctoral Studies

In partial fulfillment of the requirements for the

M.Sc. degree in

Chemical and Environmental Toxicology

Ottawa-Carleton Institute of Biology

Thèse soumise à la

Faculté des études supérieures et postdoctorales

en vue de l'obtention de la maitrise en

Toxicologie chimique et environnementale

L'Institut de biologie d'Ottawa-Carleton

University of Ottawa

*Your file Votre référence*
*ISBN:* 978-0-494-58210-7
*Our file Notre référence*
*ISBN:* 978-0-494-58210-7

# ABSTRACT

Sediments, located near Cornwall have been historically contaminated with Hg and other metals by local industries. Cornwall was designated an area of concern by the International Joint Commission (IJC) in 1985. The concentrations of mercury in these sediments exceeded the sediment quality guideline (SQG), of 170 ng $g^{-1}$ set by Environment Canada for the protection of aquatic biota. To identify the role of these contaminated sediments on mercury dynamics in the river, I measured concentrations of total mercury (THg) and methyl mercury (MeHg) in both the porewater and solid phase of sediment cores and in the overlying water to determine whether sediments are a net source or sink for Hg. A comparison of porewater profiles in June, July and August of 2007 revealed little seasonal variation in MeHg concentrations. I also compared THg and MeHg vertical profiles in sediments with complimentary redox-dependent variables, including sulfate, sulfide, and $Fe^{2+}$ distributions which showed that zones of active sulfate reduction and Fe reduction have little effect on the distribution of dissolved MeHg in the sediments. THg in sediment cores was related to the sediment accumulation rates by $^{210}Pb$ radiochronology which showed the history of industrial Hg emissions to the river. MeHg contributed 4% to 100% of the THg in the porewater samples, whereas in the solid phase it contributed less than 1% of the THg. There was little to no diffusion of THg and MeHg from sediments to the overlying water. I have concluded that sediments are a major sink for THg and MeHg to the St. Lawrence River near Cornwall.

# RÉSUMÉ

Les sédiments marins, de la région de Cornwall, ont été contaminés au mercure (Hg) et autres métaux par les industries historiquement locales. Cornwall a été désignée comme étant une région problématique par la Commission Mixte Internationale (CMI) en 1985. La concentration de mercure dans ces sédiments excédait les recommandations canadiennes pour la qualité des sédiments (RCQSe) de 170 ng $g^{-1}$ établies par Environnement Canada pour la protection de la faune aquatique. Afin d'établir le rôle de ces sédiments contaminés sur la dynamique du mercure dans le fleuve, j'ai mesuré les concentrations de mercure total (THg) et de mercure méthyle (MeHg) dans les eaux interstitielles et dans la phase solide des sédiments, ainsi que dans les eaux superficielles pour déterminer si les sédiments étaient une source nette ou un lieu de dépôt de mercure. Une comparaison des profils d'eaux interstitielles en juin, juillet et août 2007 a révélé peu de variations saisonnières dans les concentrations de MeHg. J'ai aussi comparé les profils verticaux de THg et de MeHg dans les sédiments avec des variables redox-dépendantes complémentaires, incluant des distributions de sulfates, sulfides et $Fe^{2+}$, qui ont démontré que les zones de réduction de sulfates actives et de réduction de Fe ont peu d'effet sur la distribution de MeHg dissous dans les sédiments. Le THg dans la phase solide des sédiments a été associé au taux d'accumulation des sédiments par radiochronologie $^{210}Pb$ qui a montré l'histoire des émissions industrielles de Hg dans le fleuve. Le MeHg a constitué de 4% à 100% du THg dans les échantillons d'eaux interstitielles tandis que dans la phase solide il constituait moins de 1% du THg. Il n'y avait pas ou peu de diffusion de THg et de MeHg des sédiments vers les eaux superficielles. J'en conclus

donc que les sédiments sont un lieu de dépôt majeur de THg et de MeHg dans le fleuve St-Laurent près de Cornwall.

# ACKNOWLEDGEMENTS

I would like to express my deepest gratitude to my supervisor, Dr. Jules Blais for his wise advice, inspiration as well as professional, scientific and financial support. I would also like to extend most sincere thanks to all my committee members, Dr. Danielle Fortin and Dr. Jeff Ridal for their guidance and advice and a very special "thank you" to Dr. David Lean for his utmost enthusiasm, care, encouragement and his believing in me.

This work was sponsored and supported by a strategic grant to Dr. David Lean, Dr. Jules Blais, Dr. Peter Hodson, Dr. Jeff Ridal and Dr. Laurier Poissant from Natural Sciences and Engineering Research Council of Canada and Best in Science grant from the Ministry of the Environment.

I would like to thank all Blais Lab personnel especially Linda Kimpe for their help and guidance. My sincere thanks are also extended to Dr. Emmanuel Yumvihoze for his assistance and sound advice which were critical for my work as well as Dr. A. Morin for his assistance for statistical analysis.

I would like to thank all individuals at St. Lawrence River Institute and Environmental Science and all the members of Best in Science project (BIS) for their ideas and help during this research. Much of the field work would not have been possible without the help of many other researchers, technicians, fellow graduate and summer undergraduate students including Roxanne Razavi, Trevor Arnason, Laura Hill, and Willy de Witt.

Many thanks to other graduate students such as: Emily Choy, Tim Seabert, Shinjini Pal, Jamie Doyle, Matthieu Delcourt, Raphael Lavöi, and Lucia Kwan who made my daily life more pleasant at the university.

I also wish to thank my parents, Azar and Khosrow Fathi who raised me, taught me, and guided me without whose support none of this would have been possible.

Last but not least, I would like to gratefully thank my sole mate in life, my husband Nima, whose dedication, encouragement, support and inspiration makes my life joyful and filled with happiness. I would like to dedicate this thesis to him!

# TABLE OF CONTENTS

Abstract ..... ii

Résumé ..... iii

Acknowledgements ..... v

Table of Contents ..... vii

List of Figures ..... xi

List of Tables ..... xiv

List of Abbreviations ..... xvi

1 Introduction ..... 1

1.1 Mercury as a Global Contaminant ..... 1

1.2 Mercury Speciation ..... 2

1.2.1 Atmospheric Mercury ..... 3

1.2.2 Aquatic Mercury ..... 4

1.3 Sediment Quality Guidelines ..... 9

1.4 Background Mercury Concentration ..... 10

1.5 Sediment Chronology ..... 11

1.5.1 The $^{210}$Pb Cycle ..... 11

1.5.2 $^{210}$Pb Dating Models ..... 12

1.6 Mercury Mobility at the Sediment-Water Interface ..... 15

1.6.1 Mercury Sedimentation and Accumulation ..... 15

1.6.2 Diffusion ..... 16

1.7 Mercury Contamination in the St. Lawrence River Near Cornwall ..... 18

1.7.1 Hg Hotspots in the St. Lawrence River ..... 21
1.8 Objectives: ..... 25
2 Materials and Methods ..... 27
2.1 Study Site ..... 27
2.2 Sediment Sampling ..... 28
2.2.1 Sediment Appearance ..... 28
2.2.2 Analytical Methods ..... 29
2.3 Porewater Peepers ..... 31
2.3.1 Porewater Sampling and Analytical Methods ..... 33
2.4 Benthic Chamber Sampling ..... 38
2.5 Statistical Analysis ..... 39
3 Results ..... 40
3.1 Mercury in Solid Phase ..... 40
3.1.1 Total Mercury ..... 40
3.1.2 Methyl Mercury ..... 42
3.1.3 Methyl Mercury Distribution to Total Mercury in Sediment ..... 44
3.1.4 Organic Content ..... 46
3.1.5 Inventories of $^{210}$Pb, Sedimentation Rates and Mercury Accumulation Rates 49
3.2 Mercury and Complimentary Redox Profiles in Porewater and the Water Column ..... 55
3.2.1 Total Mercury in Porewater ..... 55
3.2.2 Methyl Mercury in Porewater ..... 59

3.2.3 Hg Diffusion ..... 61
3.2.4 Sulfate in Porewater ..... 64
3.2.5 Sulfide in Porewater ..... 68
3.2.6 Ferrous Iron in Porewater ..... 72
3.2.7 Manganese in Porewater ..... 75
3.2.8 Redox Measurement in Porewater ..... 77
3.3 Benthic Chamber *In situ* Dialysis ..... 79
4 Discussion ..... 81
4.1 Mercury in the Solid Phase ..... 81
4.1.1 Total Mercury ..... 81
4.1.2 Methyl Mercury ..... 83
4.1.3 Organic Content ..... 86
4.1.4 $^{210}$Pb Inventories, Sedimentation Rates and Mercury Accumulation Rates 86
4.2 Mercury and Complimentary Redox-dependent Variables in Porewater and Water Column ..... 88
4.2.1 Total Mercury in Porewater ..... 88
4.2.2 Methyl Mercury in Porewater ..... 89
4.2.3 Hg Deposition and Diffusion ..... 90
4.2.4 Redox-dependent Variables in Porewater ..... 93
5 Conclusions ..... 96
5.1 General Conclusion ..... 96
5.2 Future Recommendations ..... 99

5.3 Significance of Findings ..... 100

6 References ..... 102

Appendix A ..... 124

Appendix B ..... 131

Appendix C ..... 156

Appendix D ..... 166

# LIST OF FIGURES

Figure 1-1. Location of mercury hotspots (Zone 1, Zone2, and Zone 3) in the St. Lawrence River near Cornwall, ON. High wood fiber site is indicated by ( ◈ ) and the Low wood fiber site by ( ◇ ) ..... 24

Figure 3-1. Depth profile of total mercury in sediment in the HWF (A) and LWF (B) cores. ..... 41

Figure 3-2. Depth profile of log of methylmercury in sediment in the HWF (A) and LWF (B) cores. ..... 44

Figure 3-3. MeHg/THg ratio in sediment in the HWF (A) and LWF (B) cores. ..... 45

Figure 3-4. Correlation between MeHg and THg in the HWF (A) and LWF (B) sediment cores. ..... 45

Figure 3-5. Depth profile of log of organic content in the HWF (A) and LWF (B) cores. ..... 47

Figure 3-6. Correlation between mercury species and organic matter in the HWF (A, C), and LWF (B, D) cores. ..... 48

Figure 3-7. Profiles of the natural log of unsupported $^{210}Pb$ activity versus cumulative dry mass. Mean sedimentation rate (g $cm^{-2}$ $yr^{-1}$) can be calculated by dividing $\lambda$ by the slope (a), where $\lambda$ is the $^{210}Pb$ radioactive decay constant (0.03114 $yr^{-1}$) ..... 50

Figure 3-8. Total mercury concentration in cores from the HWF and LWF sites versus year. $^{210}Pb$ year is based on the constant rate of supply (CRS) model. ..... 52

Figure 3-9. Total mercury accumulation rate versus year (determined by $^{210}Pb$ activities and the CRS model) in the HWF and LWF sites. ..... 54

Figure 3-10. Vertical distribution of THg concentration in triplicate porewater profiles in the HWF (A, B, C) and LWF (D, E) sites. The black solid line shows the position of the sediment-water interface. ..... 56
Figure 3-11. Vertical distribution of THg concentration in triplicate porewater profiles in the HWF (A, B, C) and LWF (D, E, F) sites. The black solid line shows the position of the sediment-water interface. ..... 57
Figure 3-12. Vertical distribution of THg concentration in triplicate porewater profiles in the HWF (A, B, C) and LWF (D, E, F) sites. The black solid line shows the position of the sediment-water interface. ..... 58
Figure 3-13. Vertical distribution of MeHg concentration in porewater profiles in June (A, B, E), July (C, F) and August (D, G) in the HWF and LWF sites. The black solid line shows the position of the sediment-water interface. ..... 60
Figure 3-14. Vertical distribution of sulfate concentration in porewater profiles in the HWF and LWF sites. The black solid line shows the position of the sediment-water interface ..... 67
Figure 3-15. Vertical distribution of sulfide concentration in porewater profiles in the HWF and LWF sites. The black solid line shows the position of the sediment-water interface ..... 71
Figure 3-16. Vertical distribution of $Fe^{2+}$ concentration in porewater profiles in the HWF and LWF sites. The black solid line shows the position of the sediment-water interface. 74
Figure 3-17. Vertical distribution of Mn concentration in porewater profiles in the HWF and LWF sites. The black solid line shows the position of the sediment-water interface. 76

Figure 3-18. Redox (Eh) values with depth in the HWF (A) and LWF (B) sites. The black solid line shows the position of the sediment-water interface. ..... 78

Figure 3-19. Concentration of THg (B, D) and MeHg (A, C) in benthic chambers over time in the HWF and LWF sites. ..... 80

# LIST OF TABLES

Table 1-1. Sediment quality guideline for Hg in freshwater environment which reflects PECs* (modified from McDonald et al. 2000). ..... 10

Table 3-1. Mercury concentration range (mean ± (SD) if n>2) in surface sediments of Zone 1 of the St. Lawrence River from 1970 to 2007. The bold values in 1979 and 2003 are the median values since mean values were unavailable (modified from Richman and Dreier, 2001). ..... 42

Table 3-2. $^{210}$Pb inventories, fluxes and focus factors in cores from the LWF site. ..... 51

Table 3-3. Sediment-water diffusion flux of THg in the HWF site. A positive value shows diffusion is from sediment to water. ..... 62

Table 3-4. Sediment-water diffusion flux of THg in the LWF site. A negative value shows diffusion is from water to sediment and a positive value shows diffusion is from sediment to water. ..... 63

Table 3-5. Sediment-water diffusion flux of MeHg in the HWF site. A positive value shows diffusion is from sediment to water. ..... 64

Table 3-6. Sulfate reduction rate in the HWF and LWF sites. ..... 65

Table 3-7. Sediment-water diffusion flux of sulfate in the HWF and LWF sites. A negative value shows diffusion is from water to sediments. ..... 66

Table 3-8. Sulfide production rate in the HWF and LWF sites. ..... 69

Table 3-9. Sediment-water diffusion flux of sulfide in the HWF and LWF sites. A positive value shows diffusion is from sediment to water. ..... 70

Table 3-10. $Fe^{2+}$ production rate in the HWF and LWF sites. ..... 73

Table 3-11. Sediment-water diffusion flux of $Fe^{2+}$ in the HWF and LWF sites. A positive value shows diffusion is from sediment to water..... 73

# LIST OF ABBREVIATIONS

| | |
|---|---|
| AOC | Area of Concern |
| AVS | Acid Volatile Sulfide |
| CCME | The Canadian Council of Ministers of the Environment |
| CFCS | Constant Flux Constant Sedimentation |
| CRS | Constant Rate of Supply |
| CSQG | Canadian Sediment Quality Guideline |
| CV | Coefficient of Variation |
| CV-AFS | Cold Vapor- Atomic Fluorescence Spectroscopy |
| DIW | De-ionized Water |
| DW | Dry Weight |
| DOC | Dissolved Organic Carbon |
| EPA | Environmental Protection Agency |
| GC-AFS | Gas Chromatography-Atomic Fluorescence Spectrometry |
| Hg | Mercury |
| Hg (II) | Inorganic Mercury |
| $Hg^0$ | Elemental Mercury |
| HWF | High Wood Fiber |
| ICP-AES | Inductively Coupled Plasma- Atomic Emission Spectrometer |
| IJC | International Joint Commission |
| LEL | Lowest Effect Level |

| | |
|---|---|
| LWF | Low Wood Fiber |
| MDL | Method Detection Limit |
| MeHg | Methyl Mercury |
| MOE | Ministry of Environment |
| NEL | No Effect Level |
| PCB | Polychlorinated Biphenyls |
| PEL | Probable Effect Level |
| PSQG | Provincial Sediment Quality Guideline |
| SD | Standard Deviation |
| SE | Standard Error |
| SEL | Severe Effect Level |
| SQG | Sediment Quality Guideline |
| SRBs | Sulfate Reducing Bacteria |
| THg | Total Mercury |
| UV | Ultraviolet |

# 1 INTRODUCTION

## 1.1 Mercury as a Global Contaminant

Mercury (Hg) is one of the most toxic elements in the environment. It is released to the environment naturally and anthropogenically (Pirrone et al. 2001). The combustion of fossil fuels, which is one of the main anthropogenic sources of Hg to the environment, accounts for about two thirds of the global anthropogenic emissions (Pacyna et al. 2006). Natural sources of mercury, including volcanic eruptions and the weathering of rocks, can release mercury into water, soils, and the atmosphere. Nriagu et al. (1989) found that emissions from coal fired generating stations exceeded 30% of global emissions while volcanoes accounted for only 2% of the emissions. Mercury has the capacity of long range atmospheric transport as elemental mercury ($Hg^0$) (Munthe and McElroy, 1992).

Methyl mercury (MeHg) is the most toxic form of mercury (Scheuhammer et al. 2007) and the only form to biomagnify in aquatic food webs leading up to fish and ultimately humans (Lindqvist et al. 1991). Although the concentration of MeHg in the environment is relatively low, it has neurotoxic effects on humans that vary according to the dose and the exposure time (Gilbert and Grantwebster, 1995). Low level chronic exposure to mercury can affect memory and language skills and it may cause attention deficit disorder (Davidson et al. 2004). MeHg accumulation may also affect reproductive success of birds (Wolfe et al. 1998) and fish (Hammerschmidt et al. 2002).

The consumption of mercury contaminated fish is one of the main pathways for mercury exposure in humans. Due to the bioaccumulation potential of methyl mercury and its adverse effects on human health, some countries such as Canada, Europe and the

United States have placed advisories on individual fish species, lakes, and in some cases, entire regions in order to prevent excessive mercury exposures to consumers.

High Hg in humans is known to cause symptoms such as trembling, ataxia, hearing and speech impediments, and in severe cases it may even lead to death (Harada, 1995). For example, major outbreaks of severe mercury poisoning occurred in Japan during the 1950s and early 1960s. The disaster in Minamata Bay in 1956 was related to the release of MeHg to industrial wastewater from a chemical plant (Chisso Co. Ltd). Human consumption of MeHg contaminated fish and shelfish in this bay caused the Minamata disease (Bunce, 1991; Harada, 1995). Another methyl mercury poisoning happened in Iraq from consumption of seed grains that had been treated with an organomercurial fungicide containing methyl mercury (Mahaffey, 2004).

Due to adverse effects of mercury on human health, it is important to understand the origin of Hg and its cycle in the environment.

The work presented in this thesis is an attempt to measure the diffusion of mercury in the sediment-water interface and to identify whether sediments in the St. Lawrence River act as a source or a sink of Hg. In order to establish the framework for the thesis and to quantify the importance of Hg flux at the sediment-water interface, the introduction includes a literature review, presenting an overview of Hg cycling and some of factors that affect it.

## 1.2 Mercury Speciation

Mercury typically occurs in three oxidation states: elemental mercury $Hg^0$ (metalic mercury), monovalent mercury ($Hg^{1+}$ [mercurous salts]), and divalent mercury ($Hg^{2+}$

[mercuric salts]). Organic forms of divalent mercury include methylmercury, ethylmercury, and phenylmercury (Parsons and Percival, 2005).

Chemical speciations of Hg are key factors affecting its distribution and transport in the environment. The toxicity and bioaccumulation potential of Hg also depends on its chemical forms (Bunce, 1994). For example, inorganic mercury is much less toxic than organomercurials, especially MeHg (Bunce, 1991).

### 1.2.1 Atmospheric Mercury

Hg in the atmosphere occurs primarily in the form of $Hg^0$, which is highly volatile and has a relatively long atmospheric residence time of 6 months to 3 years (Schroeder and Munthe, 1998; Parsons and Percival, 2005). Due to its long range atmospheric transport, there is evidence of anthropogenic mercury input in remote areas according to historical records from lake sediments (Fitzgerald et al. 1998). Burning fossil fuels is considered to be the largest single source of atmospheric mercury (Pacyna et al. 2006). Approximately, 95% of the total mercury in the atmosphere is composed of $Hg^0$ (Morel et al. 1998). Elemental mercury ($Hg^0$) moves with wind in the atmosphere where it is oxidized to Hg (II) and returns to the earth surface via adsorption to aerosols such as soot and dust (dry deposition) (Muir et al. 1999), as well as scavenging by rain or snow (wet deposition) (Iverfeldt, 1991; Perry et al. 2005).

Although anthropogenic Hg emissions are decreasing in some countries (Pacyna et al. 2003) and global anthropogenic emissions have decreased between 1995 and 2000 (Pacyna et al. 2006), there is ample evidence that Hg has increased in the environment in the last century. Mason et al. (1994) showed that Hg emissions increased in the

atmosphere by about 1% per year over past 150 years. Fitzgerald, (1995), showed the same increase per year in atmospheric Hg emission over 100 years.

## 1.2.2 Aquatic Mercury

### *1.2.2.1 Mercury in Water*

Mercury concentrations range between 5 and 100 pM (1 and 20 ng $L^{-1}$) in surface freshwaters in uncontaminated sites (Morel et al. 1998). In general, mercury methylation occurs less in the water column than in the sediment (Korthals and Winfrey, 1987). Even though methylation in the water column occurs at a much lower rate per unit volume, due to the larger volume of water than the surfacial sediments, methylation in the water column could still be significant to the overall MeHg balance. Moreover, MeHg from sediments may only reach overlying water slowly due to its slow rate of diffusion. As a result, MeHg in the water column may be more available for entry to the aquatic food web. The mechanism of Hg methylation in surface water is still unclear, although microbial processes (similar to those observed near the sediment) are likely the primary sources (Meili, 1997).

Dissolved Hg species in the aquatic systems includes various complexes of Hg (II) with organic and inorganic ligands. Approximately 95% of the inorganic oxidized mercury (Hg (II)) binds to dissolved organic matter (Meili, 1997) in lakes. Hg (II) may also be bound to sulfides ($S^{2-}$ and $HS^{-}$) in surface waters (Morel et al. 1998). Elemental mercury ($Hg^0$) is the major dissolved mercury species which usually occurs from the reduction of Hg (II) compounds by aquatic microorganisms (Mason et al. 1994) or by photoreduction of Hg (II) (Nriagu, 1994).

Elemental mercury has a high volatility which is responsible for loss of mercury from the aquatic environment (Amyot et al. 2000). Volatilization of elemental mercury from water to the atmosphere is important in the global Hg cycle (Mason et al. 1994).

Photoreduction of Hg (II) is another mechanism to release $Hg^0$ to the atmosphere (Amyot et al. 2000). The photoreduction efficiency depends on the reducible Hg (II) levels, wavelength and intensity of the radiation. In addition, high dissolved organic carbon concentrations (DOC) inhibit the penetration of solar radiation, particularly in the UV range by scavenging UV radiation prior to Hg (II) reduction (Morel et al. 1998; Parson and Percival, 2005). Photoreduction of mercury is the predominant mechanism of Hg (II) reduction in unpolluted areas (at the natural low mercury concentration (pM)); whereas, in contaminated waters (Hg>50 pM or 10 ng $L^{-1}$) microbial reduction of Hg (II) is likely the predominant mechanism (Morel et al. 1998).

#### *1.2.2.2 Mercury in Oxic Freshwater Sediments*

Sediments are the main Hg reservoir in the aquatic environment (Benoit et al. 1998) and they play a major role in Hg cycling in aquatic systems (Ramalhosa et al. 2001). Once mercury enters an aquatic system, it can bind to inorganic ligands such as $Cl^-$ or $OH^-$, dissolved organic carbon (DOC) (Hintelmann et al. 1995) or be absorbed by particulate matter (Hurley et al. 1994) and settle to the bottom. Infact, more than 90% of all Hg in the aquatic environment settles to the bottom (Kroenke, 2003).

#### *1.2.2.3 Mercury Methylation in Anoxic Freshwater Sediments*

Mercury methylation in the aquatic environment may be biotic (microbially mediated) or abiotic. Abiotic methylation of mercury is only possible if suitable methyl

donors are present. Transmethylation of organometallic complexes such as methylcobalamin, methyltin and methyllead are also considered as likely abiotic methyl donors in the aquatic systems (Celo et al. 2006; Craig, 1986). Biotic methylation usually occurs under low oxygen or anoxic conditions near the sediment-water interface (Siciliano et al. 2001; Gilmour et al. 1991). Sulfate reducing bacteria (SRBs) are believed to be primary mercury methylators (Compeau and Bartha, 1985, King et al. 2001; Cleo et al. 2006; Jensen and Jernelov, 1969; Drott et al. 2007) as well as the principal Hg demethylators (Oremland et al. 1991) in freshwater and estuarine sediments. Factors that control the activity of SRBs, and consequently the concentration of MeHg in the sediments, include sulfate concentration (e- acceptor), the abundance and type of energy-rich organic matter (e- donor), temperature, and the availability of inorganic mercury (Drott et al. 2007).

Sulfate concentration is one of the most important factors affecting microbial Hg methylation (Lambertsson and Nilsson, 2006). The optimum sulfate concentration at which sulfate-reducers produce MeHg is ca 0.3 mM (~ 29 mg $L^{-1}$) (Gilmour et al. 1992). Sulfate concentrations higher than 5 mM (~ 480 mg $L^{-1}$) stop the methylation most likely due to complexation of Hg and sulfide from sulfide ions produced by the activity of sulfate reducing bacteria (Gilmour et al. 1998; Weber, 1993; Compeau and Bartha, 1983; Mason et al. 1996; Fagerstrom and Jernelov, 1971; Bisogni and Lawrence, 1975). Recent studies have shown that high sulfide concentrations reduce the Hg methylation rate, not due to the precipitation of HgS, but because of less bioavailable charged Hg-S. Sulfate influences SRBs activities while sulfide controls mercury speciation and its bioavailability for methylation. MeHg production is inhibited beyond a sulfide

concentration of about 1.8 mg $g^{-1}$ (Craig and Moreton, 1983). The optimal condition for Hg methylation in solid phase occurs when sulfide concentration is mild, generally below 10 μM (0.32 mg $L^{-1}$) and dissolved organic carbon (DOC) is high (Benoit et al. 2001).

Dissolved organic matter is an important factor in determining Hg speciation, bioavailability and its fate and transport in the aquatic environment (Ravichandran, 2004). Hg can bind to dissolved organic carbon (DOC) in the aquatic environment (Hintelmann et al. 1995), often by binding to thiol groups which facilitates the transfer of Hg from soils to surface waters (Ravichandran, 2004). Typically, a positive relationship is observed between Hg methylation and organic carbon concentration (Furutani and Rudd, 1980; Lee et al. 2000; Olson, 1976) probably due to the stimulating effect of DOC on microbial methylation activity (Ullrich et al. 2001). However, some studies have shown a reduction in Hg methylation at high carbon content probably since DOC inhibits the bioavailiblity of Hg (II) at a specific pH; hence, reducing MeHg production (Miskimmin et al. 1992; Barkay et al. 1997; Jackson, 1991).

Demethylation of Hg is the decomposion of MeHg to inorganic mercury and it has been shown to occur both biotically and abiotically (Weber, 1993; Ullrich et al. 2001; Craig, 1986). In the biotic processes, Hg demethylation is mainly accomplished by aerobic organisms, whereas Hg methylation occurs by both anaerobic and aerobic bacteria (Oremland et al. 1991). Photochemical Hg demethylation in surface waters is considered to be the most important abiotic pathway (Sellers et al. 1996).

Other factors such as dissolved organic carbon, pH, and microbial respiration rates may also affect mercury demethylation (Miskimmin et al. 1991). The concentration of

MeHg in the aquatic environments reflects the net Hg methylation because of the simultaneous production and degradation of MeHg (Weber, 1993; Ullrich et al. 2001).

As mentioned above, sulfate reducing bacteria (SRBs) are the primary mercury methylators in anoxic sediments. Other microorganisms, such as methanogens and iron reducing bacteria, may also be responsible for Hg methylation (Pak and Bartha, 1998; Fleming and Nelson, 2006). Iron reducing bacteria methylate mercury in sediments where iron reduction was the dominant terminal electron acceptor. The by-product of iron reducing bacteria is $Fe^{2+}$ through the reduction of $Fe^{3+}$ to $Fe^{2+}$. The rate of Hg methylation by iron reducing bacteria was observed to be lower than the rate of Hg methylation by sulfate reducing bacteria (Warner et al. 2003).

Iron can also affect Hg methylation by altering the chemistry of Hg and consequently its bioavailability in the aquatic environment. Fe and Mn oxides which are known as scavengers of trace metals in the environment (Lockwood and Chen, 1973) can scavenge Hg from surface waters to surface sediments and form stable complexes (Murray, 1975). They can alter the profile of Hg due to their high capacity to adsorb (because of their large surface areas) and co-precipitate Hg (Gobeil et al. 1999; Jenne, 1977). Reduction of Fe and Mn oxides and their dissolution as a consequence of the microbial degradation of the organic matter, may remobilize Hg to the porewater (Froelich et al. 1977). Although both Fe and Mn oxides are responsible for the distribution and transport of Hg, Mn redox cycling is considered to be of less importance (Hurley et al. 1994; Bloom et al. 1999; Gagnon et al. 1996; Gobeil et al. 1999).

## 1.3 Sediment Quality Guidelines

The Ontario Ministry of Environment's Provincial Sediment Quality Guideline (PSQG) describes three effect levels of contaminated sediments on benthic organisms (Persaud et al. 1993); (1) no effect level (NEL), (2) the lowest effect level (LEL), which is the level that can be tolerated by the majority of benthic organisms and, (3) the severe effect level (SEL), which is the concentration that can be harmful for most benthic species. The LEL and PEL (probable effect level) for mercury are 200 ng $g^{-1}$ and 2000 ng $g^{-1}$ (Persuad et al. 1993). However, Canadian sediment quality guidelines for the protection of aquatic life (CSQG) reported SQG of 170 ng $g^{-1}$ and PEL of 486 ng $g^{-1}$ for Hg in the aquatic ecosystems (CCME, 2005).

Sediment quality guideline criteria (SQGs) have been developed in some countries; however, because of uncertainties in bioavailibility of Hg, it has been suggested to apply it with caution in different sites (Chapman et al. 1999).

Table 1-1. Sediment quality guideline for Hg in freshwater environment which reflects PECs* (modified from McDonald et al. 2000).

| Probable Effect Concentrations | Hg (ng $g^{-1}$dw) | Study |
|---|---|---|
| Probable Effect Level | 486 | Smith et al. 1996 |
| Severe Effect Level | 2000 | Persaud et al. 1993 |
| Toxic Effect Level | 1000 | EC and MENVIQ, 1992 |
| Effect Range Median | 1300 | Long and Morgan, 1991 |
| Consensus Based PEC* | 1060 | |

*PEC is a level above which adverse effects are expected to occur.

## 1.4 Background Mercury Concentration

Mercury in sediments is not only from anthropogenic sources, but it can also be deposited naturally in the sediments. The background Hg concentration, which refers to the concentration of Hg in sediments in the absence of anthropogenic sources, has been estimated in several studies. Lockhart et al. (1998) found the background Hg concentration in pre-industrial sediments ranged between 20 and 130 ng $g^{-1}$ in 18 lakes across northern and central Canada. Another study measured the background Hg concentration in pre-industrial sediments of 12 lakes in northern Quebec to range between 30 and 200 ng $g^{-1}$ (Lucotte et al. 1995). Although Hg background concentration in pre-industrial sediments is low compared to the Hg concentration in anthropogenically

contaminated sediments, it may still exceed the SQG of 170 ng $g^{-1}$, and may even reach the LEL of 200 ng $g^{-1}$ for the protection of aquatic biota set by Environment Canada.

## 1.5 Sediment Chronology

Sediment cores are natural repositories that could be used to provide historical information in lakes and rivers. Accurate chronology of the sediment is crucial for the interpretation of these archives. Dating of sediments can be used to connect certain events in the sediment with the known historical milestones of the area. The introduction of using $^{210}$Pb and anthropogenic radioisotopes ($^{137}$Cs, $^{241}$Am) as dating methods began in the early 1970s and was one of the key developments used to record events in these natural archives (Appleby, 2008). In the past twenty years, $^{210}$Pb became the most important means of dating recent sediments (0-150 years) and its application is to assess erosion rate and water quality (Appleby et al. 2001) as well as to monitor contaminants (Fitzgerald et al. 1998; Yamashita et al. 2000; Appleby et al. 2001). In order to use these methods effectively, it is necessary to understand $^{210}$Pb accumulation processes.

### 1.5.1 The $^{210}$Pb Cycle

$^{210}$Pb is a naturally occurring daughter isotope of $^{238}$U (uranium). $^{238}$U decays in the environment to $^{226}$Ra (radium) with a half life of $4.51\times10^{9}$ years; then $^{226}$Ra decays to the gaseous $^{222}$Rn (radon), which has a short half life of 3.82 days. A fraction of $^{222}$Rn escapes to the atmosphere, decaying to form the unsupported $^{210}$Pb, a fraction of which returns to the ground. *In situ* decay of $^{226}$Ra from weathered materials forms the supported $^{210}$Pb in the lake sediments. The unsupported $^{210}$Pb is used for the calculation of sedimentation rates and sediment dates, and is calculated by subtracting the supported

$^{210}$Pb from the total $^{210}$Pb activities (Oldfield and Appleby, 1984). The unsupported $^{210}$Pb has a half life of 22.26 years. As a result, $^{210}$Pb can be used to date sediments from recent times to 150 years in age (Oldfield and Appleby, 1984; Appleby, 2001).

Radionuclides delivered to the bed of the lake sediments may be redistributed in the sediment phase because of physical or biological mixing of the sediment at or near the water-sediment interface, as well as the chemical diffusion within porewater (Appleby, 2001). Therefore, interpretation of $^{210}$Pb dating must be done carefully, especially in fluvial environments and should be confirmed by independent evidence (Carignan and Lorrain, 2000).

$^{210}$Pb activities in this study were measured by gamma spectrometry, which is the most widely used method for measuring $^{210}$Pb profiles.

## 1.5.2 $^{210}$Pb Dating Models

Several dating models are applicable for interpreting $^{210}$Pb profiles, including the CFCS model (constant flux constant sedimentation rate), the CRS (constant rate of supply), and the CIC model (constant initial concentration) (Appleby and Oldfield, 1978; Appleby, 2001).

### *1.5.2.1 CFCS Model*

The CFCS model (constant flux constant sedimentation rate) is applicable in lakes where erosive processes in the catchment and the productivity in the water column are steady. This method requires the validity of two assumptions; the supply of unsupported $^{210}$Pb and sedimentation rates must remain constant (Oldfield and Appleby, 1984).

The sediment age can be calculated using the following formula:

$$t = \frac{m}{r}$$

Where m= cumulative dry mass at depth x (g $cm^{-2}$) and r = dry mass sedimentation rate (g $cm^{-2}$ $yr^{-1}$).

In the CFCS model, the unsupported $^{210}Pb$ activity $C_{(x)}$ (Bq $Kg^{-1}$) at depth $_{(x)}$ is described by the following formula:

$$C_{(x)} = C_{(0)}\, e^{-\lambda m/r}$$

Where $\lambda$ = the radioactive decay constant of $^{210}Pb$ (0.03114 $yr^{-1}$) and $C_{(0)}$ = the unsupported $^{210}Pb$ activity at the surface of the core.

### *1.5.2.2 CRS Model*

The CRS model (constant rate of supply) is applicable in lakes with variable sediment accumulation and production rates. This model assumes that the rate of unsupported $^{210}Pb$ delivered to the sediments from the atmosphere is constant, whereas sediment accumulation rate is variable. Variability in sediment accumulation rate can dilute or concentrate the $^{210}Pb$ in sediments (Blais et al. 1995).

The application of this method was used in particular sites and was validated in studies done by Oldfield et al. (1978) and Appleby et al. (1979). A summary of detailed methodology of this method can be found in Appleby, (2001).

The sediment age (t) in this method can be calculated using the following formula:

$$A_{(x)} = A_{(0)} e^{-\lambda t}$$

Where $A_{(x)}$ = $^{210}$Pb inventory (Bq $m^{-2}$) below depth x, $A_{(0)}$ = the full unsupported $^{210}$Pb activity of the sediment profile and $\lambda$ = the radioactive decay constant of $^{210}$Pb (0.03114 $yr^{-1}$)

$$t = 1 / \lambda \ln (A_{(0)} / A)$$

### *1.5.2.3 CIC Model*

The CIC model (constant initial concentration) is applicable for a system with variable sedimentation rate, while the initial $^{210}$Pb is constant (Oldfiels and Appleby, 1984; Appleby, 2001). This model assumes that the initial surface $^{210}$Pb concentration is constant regardless of the sedimentation rate. A summary of detailed methodology of this method is given in Appleby, (2001).

The age of the sediments in this method is obtained using the following formulas:

$$C_{(x)} = C_{(0)} e^{-\lambda t}$$

Where $C_{(0)}$ = C at a depth zero

$$t = 1 / \lambda \ln (C_{(0)} / C)$$

## 1.6 Mercury Mobility at the Sediment-Water Interface

### 1.6.1 Mercury Sedimentation and Accumulation

Sedimentation refers to the accumulation of sediment at the sediment-water interface measured from a fixed stratum (such as the level of bedrock) and the rate at which sediment accumulates is called the sedimentation rate. The most common tool to measure the sedimentation rate is vertical distribution of radionuclides such as $^{210}Pb$, $^{137}Cs$, as well as pollen grains (Di Toro, 2001).

Over the past century, industrial agricultural and domestic sources have introduced a multitude of toxic substances including Hg into the water bodies by their discharging of liquid and solid waste. Many of these contaminants have a tendency to bind to the suspended particles in water which then deposit on the bottom sediments according to particle size and the speed of the current (Marvin and Pelletier, 2005). The accumulation of these particles in the sediment represents a historical record of the natural and anthropogenic events. In order to interpret sediment accumulation accurately, it is necessary to assume the presence of negligible diagenetic processes. The term diagenesis refers to all the physical, chemical and biological processes which change the sediment profile after its initial deposition, such as redistribution of sediments. There are many arguments for and against diagenetic remobilization of mercury in the literature (Rasmussen, 1994; Fitzgerald et al. 1998; Johansson, 1985; Lockhart et al. 2000). However, it should be noted that interpretation of sediment records of Hg should consider the importance of diagenesis at a specific site.

### 1.6.2 Diffusion

Molecular diffusion is a net transport of molecules from a region of higher concentration to one with lower concentration by random molecular motion. Different techniques have been developed to obtain porewater samples such as dialysis, centrifugation (Berner, 1980) and squeezing of porewater (Patterson et al. 1978). While the Hg concentration in porewater is higher than the concentration in overlying water, it is necessary to assess whether sediments are a source of mercury to the overlying water, and consequently to the biota. Diffusive flux of Hg from the sediment- water interface to the overlying water can be calculated by applying Fick's first law of diffusion (Berner, 1980); and it is without considering the effect of bioirrigation and bioturbation of benthic infauna (Berelson et al. 2003). Bioturbation increases the flux of organic and inorganic complexes at the sediment-water interface by up to 2-10 times more than molecular diffusion (Rutgers van der Loeff et al. 1984). Some other factors such as macrophyte community, benthic macroalgae and resuspension of sediments (López, 2004) (Aller and Aller, 1998; López, 2004) might also affect the diffusion rate at the sediment-water interface. The benthic diffusion equation is as following:

$$J = - D \Phi (\delta C / \delta Z)$$

Where J is the diffusive flux (ng $cm^{-2}$ $yr^{-1}$), D is the molecular diffusion coefficient ($cm^2$ $yr^{-1}$), $\Phi$ is porosity and (($\delta$ C / $\delta$ Z) (ng $cm^{-4}$) is the concentration gradient with depth in the core. The sediment diffusion coefficient in most freshwater systems can be

easily calculated from the molecular diffusion coefficient at *in situ* temperature (Williams, 1969).

### *1.6.2.1 Pore-Water profiles using peepers*

Porewater profiles may provide an indirect measure of mercury dynamics from sediments, by applying Fick's First Law of diffusion to the vertical distribution of dissolved metals in porewaters (Boudreau, 1996). Porewater chemistry is usually different from the overlying water and it is of great interest to both ecotoxicologists and geochemists, because porewater represents an important source of bioavailable trace metals for biota and mediates the fluxes of metals between the sediment and water column (Teasdale et al. 1995). Peepers are *in situ* equilibrium dialysis samplers used for sampling sediment porewaters and for measuring trace metal depth profiles.

The peeper method relies on porewater equilibrium between porewater and de-ionized water trapped behind a membrane. Peepers were initially described and utilized by Hesslein et al. (1976).

### *1.6.2.2 In situ Benthic Chambers*

Benthic chambers provide a direct method of measuring exchanges at the sediment-water interface. This technique was first used by Rowe et al. (1975) and its use has become more frequent since then. Benthic chambers are made of plexiglass or plastic with different shapes and volumes, and they typically have a stirring device to mix the water inside the chamber. The volume of the benthic chamber ranges from a few litres to several dozen litres and depends on the expected flux (Gomez-para and Forja, 1993). Scuba divers are typically required for this *in situ* deployment (Hallberg et al, 1972). The

benthic chamber lies over an area of sediment, and diffusive flux is calculated by measuring the change in dissolved metal concentration over time (Hallberg et al. 1972). The benthic exchange rate of dissolved substances across the sediment-water interface is a key factor in modifying surface water and sediment chemistry (Berelson et al. 1990). At every sampling, the addition of equal amounts of ambient water compensates for the volume of the samples taken (Hallberg et al. 1972). Fluxes of dissolved substances across the sediment-water interface can be calculated using the following formula proposed by Santschi et al. (1990):

$$F = (\delta C / \delta t)^* (V / A)$$

Where F is the diffusive flux (ng $m^{-2}$ $yr^{-1}$), C is the concentration change with time (ng $m^{-3}$ $yr^{-1}$), A is the area of incubated sediment ($m^2$) and V is the volume of incubated water ($m^3$).

The volume of water can be determined from the area of incubated sediment and the average height of the benthic chamber (from the sediment surface to the top of the chamber). Diffusion flux rates of (ng $m^{-2}$ $yr^{-1}$), are converted to (ng $cm^{-2}$ $yr^{-1}$) by dividing the values by 10000.

## 1.7 Mercury Contamination in the St. Lawrence River Near Cornwall

In 1985, the Water Quality Board of the International Joint Commission (IJC), according to recommendations from the Great Lakes States and the Province of Ontario, identified 43 contaminated areas in the Great Lakes (Golder Associates, 2004). A

remedial plan was developed for each Area of Concern (AOC), to address environmental issues affecting the health of the St. Lawrence River. One such area is near Cornwall, Ontario because of its high concentrations of Hg along its northern coast and its high concentration of PCBs (polychlorinated biphenyls) on its southern coast. Sediments from this area have historically been contaminated with Hg because of local industries which were located in Cornwall at the time. The Hg concentration in sediments, water and fish along the Cornwall waterfront has been the principal reason for this designation (Environment Canada, 2004; Lepage et al. 2000). Local (and former) point sources of mercury to this river included ICI Forest, Domtar, Cornwall Chemicals, Courtalds, the City of Cornwall Water Pollution Control Plant, and Conpak (Stanchem), all of which were identified as the major sources of Hg to this river (Grapentine et al. 2003; Richman and Dreier, 2001).

ICI Forest products, a chlor alkali plant was in operation from 1935 to 1995. This plant used a mercury cell electrolytic process to convert salt to sodium hydroxide (caustic soda) and chlorine. ICI discharged Hg to the river through its liquid wastewater stream and from the ventilation air outlets in the Hg cell rooms. The release of Hg from the ventilation air outlets was eight times higher than the liquid discharge of Hg to the river (St. Lawrence River Institute, 2001). It is not known how much of the released Hg to air returned to the land or into the St. Lawrence River via wet or dry deposition. Domtar Fine Papers Ltd, a pulp and paper mill was in operation from 1881 to 2006. The mill used Hg compounds as slimicides to kill moulds on pulp fibers (St. Lawrence River RAP, 1997). Domtar discontinued using its mercurial slimicides in 1964 (MOE, 1979). Cornwall Chemicals is another industry in Cornwall that manufactured a variety of chemicals using

chlorine and sodium hydroxide which produced a relatively minor amount of Hg to the AOC (St. Lawrence River Institute, 2001). This plant closed its operations in 1995. Courtalds Fibers, a rayon fiber mill which was in operation from 1925 until 1992, discharged Hg to the river through the release of sodium hydroxide and sulfuric acid in its manufacturing processes. Although, both of these chemicals contained minute amounts of mercury, Courtalds is known as the largest polluter of Hg to the river (St. Lawrence River RAP, 1997). The city of Cornwall's water pollution control (the Cornwall wastewater treatment plant, WWTP) was another point source of mercury to the river which produced sewage sludge with high concentrations of mercury (St. Lawrence River RAP, 1997). Mercury loading from the Cornwall sewage treatment plant was measured at 7.7 g $day^{-1}$ by Schroeter and Associates, (1993). ICI Conpak (Stanchem) was another distributor of Hg to the St. Lawrence River that packaged inorganic chemicals for Stanchem. This plant used to release an average of 0.1 g $day^{-1}$ of mercury to the river in 1990. All of these point sources of mercury were closed at the time of this study, except the WWTP.

Some non- point sources of Hg to the river include upstream inputs from the Great Lakes basin and the upper St. Lawrence River, agriculture and municipal inputs, urban runoff form the city of Cornwall, atmospheric emissions from Cornwall and Massena industries as well as long range transport of airborne pollutants (St. Lawrence River RAP, 1992). The anthropogenic sources of mercury deposited about $170 \pm 85 \times 10^3$ kg of Hg to the entire lower St. Lawrence Estuary which is about six times higher than the natural Hg deposited during the same period (Gobeil and Cossa, 1993).

Since the concentrations of mercury in sediments were above the sediment quality guideline (SQG) of 170 ng $g^{-1}$, a limit set for the protection of biota by Environment Canada, some regulations were established in the1970s by the federal government to limit the discharge of mercury to the river in liquid effluent by local industries (Environment Canada, 1981, 2003). Consequently, mercury concentrations decreased in surface sediments (Golder Associates, 2004). The closure of the following plant Coutralds, ICI Forest and Cornwall Chemicals in the early 1990s caused another decrease in Hg discharge to this river which became obvious by $^{210}Pb$ dating in sediments and measuring Hg levels (Delongchamp, 2006; Richman and Dreier, 2001). Despite decreasing mercury concentrations in sediments since the 1970s (Kauss et al. 1988), Hg is still high in the sediments and this area is still listed as an area of concern (AOC) (Golder Associates, 2004). However, recent studies showed that sediments in the St. Lawrence River are not a major source of mercury to fish in this area through the food web (Environment Canada, 2005).

### 1.7.1 Hg Hotspots in the St. Lawrence River

Reduction of water flow causes particulate matter settling in the depositional zones along the Cornwall waterfront (Biberhofer and Rukavina, 2002). Three of these depositional zones in the St. Lawrence River were identified as Hg hotspots, including Zone 1which is located 1 km downstream from the discharge point used by both the pulp and paper mill and the chlor alkali plant; Zone 2 which is located 2 km downstream from the former location of the effluent outfall of the rayon fibers mill; and Zone 3 at Cornwall

Harbour between Zone 1 and Zone 2. The focus of this study is in Zone 1 which is along Cornwall waterfront in the St. Lawrence River.

#### *1.7.1.1 Characteristics of Zone 1*

Sediments in Zone 1 are characterized by high spatial heterogeneity (Biberhofer and Rukavina, 2002); hence, leading to a high variability in sediment Hg concentrations. Also, thick layers of wood fibers though to be deposited by the Domtar pulp and paper mill are observed in this zone. Deposited wood fibers are seen to decrease with increasing distance from the pulp and paper mill. In some cases these wood fibers are covered upto 10 cm of the fine grained sediments (Biberhofer and Rukavina, 2002). Decomposition of these wood fibers by microbial activities results in high gas production (Biberhofer and Rukavina, 2002).

Zone 1 is identified as a zone of high gas evolution in the St. Lawrence River (Biberhofer and Rukavina, 2002). The cycling of gases in the water column and in sediments are important processes in the aquatic environment (Huttunen et al. 2001). Typically gas bubbles from sediments consist of methane, nitrogen, carbon monoxide, carbon dioxide and hydrogen (Chau et al. 1977) which can be released from sediments to the water column and consequently to the atmosphere (Huttunen et al. 2001).

Bulk density is a factor affecting the movement of gas bubbles in sediment. Gases or dissolved gases move more easily and rapidly when sediments are less compacted at depths of less than 1 meter (Telmer et al. 2005). The movement of gas bubbles in sediments may destabilize the sediments and cause subsequent volatilization of contaminants from the sediment to water (Martens et al. 1980). Gas ebullition can also increase the release of solid particles from the sediments to the water. The higher the rate

of gas evolution, the stronger is the release and distribution of the solid particles into the water column. Typically heavier suspended particles brought to the water column by gas evolution fall back to the sediments and just the lighter particles remain suspended in the water column (Yuan et al. 2007). In general, gas evolution may cause sediment erodibility and resuspension and it is necessary to examine whether unique characteristics in this zone affects Hg bioavailability and distribution.

#### *1.7.1.2 HWF and LWF Sites in Zone 1*

In the present study two sites in Zone 1 were investigated in order to study Hg distribution. One site where high levels of deposited wood fibers had been observed (HWF), and an adjacent site that contained a lower level of wood fibers (LWF).

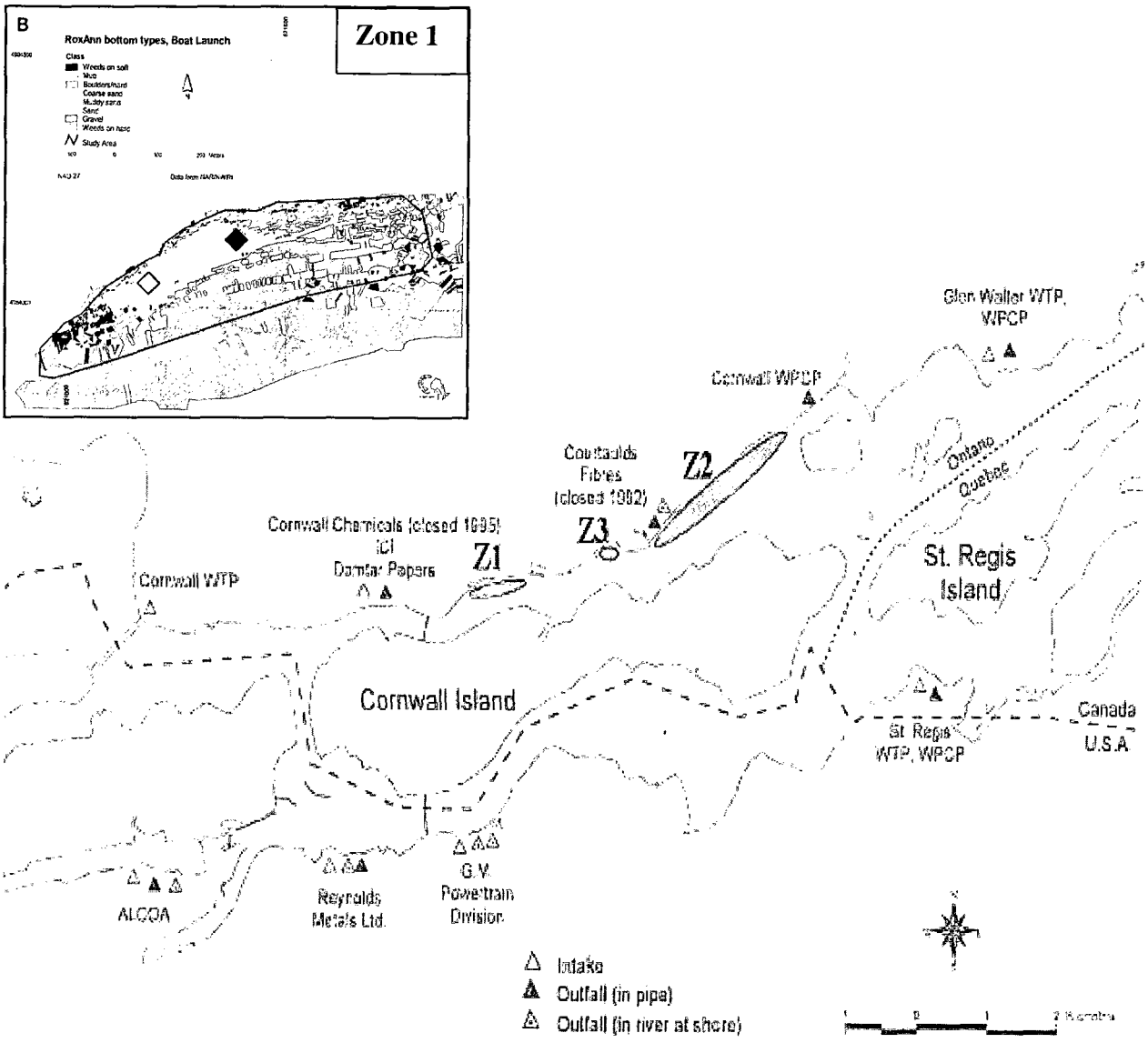


Figure 1-1. Location of mercury hotspots (Zone 1, Zone2, and Zone 3) in the St. Lawrence River near Cornwall, ON. High wood fiber site is indicated by ( ◆ ) and the Low wood fiber site by ( ◇ ).

## 1.8 Objectives:

The objectives of this study were to examine the spatial and temporal patterns of total and methyl mercury concentration gradients across the sediment-water interface in order to determine the direction and magnitude of diffusion in porewaters. Redox-dependent variables such as sulfate, sulfide and $Fe^{2+}$ in the porewater and overlying water were also measured in order to characterize the zones of MeHg production. Furthermore, the Hg accumulation rates were measured and compared with calculated Hg diffusion rates between sediments and water column to determine whether these sediments are source or sink for Hg.

The present study was structured to answer the following questions:

1. Does the presence of wood fibers in sediments from a nearby pulp and paper mill affect MeHg production and diffusion to overlying waters?
2. Do sediments of the St. Lawrence River act as a source or sink of Hg and MeHg?
3. Does the temporal trend in Hg concentrations and accumulation track the known pattern of anthropogenic Hg emissions in the St. Lawrence River near Cornwall?

In order to provide the critical information needed to answer these questions, four approaches were taken:

1. Sediment cores were collected from the HWF and LWF sites in order to examine the Hg distribution with depth in the sediments.

2. Sediment cores from the HWF and LWF sites were radiometrically dated to compare Hg accumulation rates and to assess whether Hg accumulation rate has changed over time.
3. Porewater sampling using peepers was performed in the HWF and LWF sites in June, July, and August 2007 to study the spatial and temporal patterns of THg, MeHg, and redox-dependent variables in porewater and overlying water. The measured values were used to calculate diffusion rates between sediments and overlying water.
4. Benthic chambers were deployed in the HWF and LWF sites in order to obtain mercury diffusion rates at the sediment-water interface that could be compared with those calculated from the porewater profiles (peepers).

We tested the following hypotheses:

1. Hg concentrations in sediments at the HWF site are higher due to higher levels of organic material deposited by nearby pulp and paper mill.
2. Depth profile of Hg concentrations in sediments will track the industrial history of Hg release in dated sediment cores.
3. The diffusion rate of THg and MeHg to the water column will be higher at the HWF site.
4. MeHg concentration in sediments will increase as the summer progresses, due to higher temperatures that stimulate higher microbial activities.

# 2 MATERIALS AND METHODS

## 2.1 Study Site

The Cornwall AOC includes an 80 km stretch of the St. Lawrence River, from the Moses-Saunders Power dam to the eastern outlet of Lake St. Francis in Quebec. This stretch of the river encompasses many jurisdictions, including the provinces of Ontario and Quebec, the state of New York, the federal governments of Canada and U.S.A, as well as the Mohawks of Akwesasne.

The St. Lawrence River, near Cornwall divides into two branches at Cornwall Island. The southern channel runs along the state of New York and the northern channel runs along the Cornwall waterfront (St. Lawrence River Rap, 1992). This study was done in Zone 1 of the St. Lawrence River, which is located along the Cornwall waterfront of the northern channel, approximately 1 km downstream from the discharge of two local industries, the Domtar pulp and paper mill (closed in 2006), and ICI Forest a chlor alkali plant, (closed in 1995) (Figure 1-1). Two sites were investigated in Zone 1, one site of high wood fiber accumulation had been observed (18° 521′298″ E, 49°84′ 357″ N) and an adjacent site that contained a low level of wood fiber accumulation (18°521′205″ E, 49° 84′295″ N). These wood fibers are believed to be deposited by the Domtar pulp and paper mill (St. Lawrence River Rap, 1992).

## 2.2 Sediment Sampling

Two sediment cores were collected from the HWF site and two cores from the LWF site in Zone 1, along the Cornwall waterfront of the St. Lawrence River in June and August 2007. Sediment cores were collected using a 1.5 m long Lexan (polycarbonate) coring tube with 7.5 cm inside diameter. The HWF cores were taken from a site with coordinates of 18° 521′351″ E, 49°84′ 373″ N and 18° 521′341″ E, 49°84′ 375″ N and the LWF cores were taken from a site with coordinates of 18° 521′207″ E, 49°84′ 297″ N and 18° 521′209″ E, 49°84′ 298″ N. Each sediment core was sectioned within one hour of its collection under nitrogen atmosphere. Cores were extruded on site into 1 cm thick slices for the first 10 top cm of the core and the remainder of the core was sectioned into 2-4 cm thick slices. The sediment samples were placed into air-tight centrifuge tubes and plastic bags, placed on ice, and transported in a dark cooler to the laboratory the same day. Sediments were then stored in a freezer for future analysis. The sediments were sub-sampled and freeze-dried for 2 to 3 days, and the dried sediments were ground by mortar and pestel. Freeze-dried samples were used for radiometric dating, THg and MeHg analysis. These samples were also used to determine the water content and loss on ignition (550°C, 950°C) to measure organic and carbonate content respectively following the method described by Heiri et al. (2001).

### 2.2.1 Sediment Appearance

The sediment cores were brown-black clayed mud with many wood fibers on the top layers. This was found especially in the cores from the HWF site. The cores contained

many gas pockets through their length. Traces of oil were seen in the cores from the HWF site. Benthic organisms were rarely seen in these cores.

## 2.2.2 Analytical Methods

### *2.2.2.1 Total Mercury in Sediments*

Homogenized freeze-dried sediment samples were analyzed for total mercury using an automatic mercury analyzer based on thermal decomposition, dual step gold amalgamation and detection via Cold-Vapor Atomic Absorption using a SP-3D mercury analyzer (Nippon Instrument Corp, Japon) with detection limit of 0.01ng per sample size. The accuracy of our analysis was estimated by running blanks and spikes as well as two Reference Materials during the analytical procedure. Spikes from a stock of Mercury Reference Solution (certified 1000 $\mu g\ g^{-1} \pm 1$ %; Fisher Scientific CSM114-100) were brought to a concentration of 50 $ng\ g^{-1}$ and were tested every 5 samples. The average recovery of the spikes was 102 % ± 5(SD), (n = 12). Procedural blanks showed no contamination during THg analysis. Reference Materials were tested every 4-5 samples and average percentage recovery for MESS-3 (Marine Sediment Certified Reference Materials from NRC with concentration of $91 \pm 9\ ng\ g^{-1}$ was 96 % ± 4 (SD), (n = 7). The average percentage recovery for CRM-580 (Commission of the European Communities Reference Material N° 580, Total and Methyl Mercury for Estuarine Sediments with total mercury concentration of $132 \pm 3\ mg\ kg^{-1}$) was 101 % ± 13 (SD), (n = 6). The first set of sediment samples (from the LWF core) which were ground manually, had a CV of 16%, (n = 17) which ranged between 0.02 and 40.7%. Given the high variance, sediments were thereafter ground mechanically, and CV improved to 3.6%, (n = 17) with a range

between 0.02 and 10.4% in the LWF core. Overall, both cores (the HWF and LWF) had a CV of 3.8 % with a range between 0.02 and 10.4 %.

#### *2.2.2.2 Methyl Mercury in Sediments*

The concentration of methyl mercury in sediments was determined by capillary gas chromatography coupled with atomic fluorescence spectrometry (GC-AFS) as described by Cai et al. (1997), with a detection limit of 0.02 ng per sample size. Sample mass ranged between 0.8 and 1.2 g.

The homogenized freeze-dried sediment samples were used for this analysis. Accuracy was ensured in sediment analysis by procedural blanks and spiked samples. The average recovery of spiked samples was 98.5 % ± 5 (SD), (n = 8) and analysis of procedural blanks revealed no contamination during MeHg analysis. The average recovery of Reference Material IAEA-405 (Trace and Major Elements in Estuarine Sediments from IAEA, Monaco with concentration of 5.49 ng $g^{-1}$ ) was 98 % ± 4 (SD), (n = 4).

#### *2.2.2.3 $^{210}$Pb Inventories and Sedimentation Rates*

Sediment cores were radiometrically dated using gamma ($\gamma$) spectrometry. Overall, four sediment cores (two cores from the HWF and two cores from the LWF site) were analyzed for the activity of $^{210}$Pb, $^{137}$Cs and $^{226}$Ra. Analysis of $^{210}$Pb was performed in selected depth intervals in the sediment cores to determine the sediment age, and the sediment accumulation rate. Homogenized (ground to fine powder), freeze-dried samples added to centrifuge tubes (8.4 cm high and 1.5 cm outer diameter) to a height of 2 cm. Sediment samples were settled for 2 to 3 days before sealing them with epoxy. After

being allowed to reach radioactive equilibrium for 3 weeks, samples were ready to be counted using a digital high purity germanium well detector (DSPec, Ortec), following the method described by Appleby, (2001). Samples were counted for 23 hours (82,800 seconds). The resulting spectrum files showed $^{210}$Pb activity with a peak at 46.5 keV, and $^{137}$Cs at 662 keV. $^{226}$Ra activity was determined by γ-ray emissions of its daughter isotope $^{214}$Pb, resulting in peaks at 295 and 352 keV.

In order to calculate the mean sedimentation rate, the slope calculated in profiles of the natural log of unsupported $^{210}$Pb against cumulative dry mass was divided by the $^{210}$Pb radioactive decay constant (0.03114 $yr^{-1}$) (Blais et al. 1998).

$$\text{Mean sedimentation rate} = \frac{\text{Radioactive decay constant}}{\text{Slope(a)*}}$$

* Slopes (a) were the slopes of the natural log of (unsupported $^{210}$Pb) and cumulative dry mass profiles.

The unsupported $^{210}$Pb fraction was calculated by subtracting the supported $^{210}$Pb, (which is determined by $^{226}$Ra activity) from total $^{210}$Pb activity to determine the sedimentation rate and sediment dating.

## 2.3 Porewater Peepers

Depth profiles for THg, MeHg, sulfate, sulfide, $Fe^{2+}$ and total Mn in both sediment porewater and overlying water in the St. Lawrence River were measured using *in situ* dialysis membrane device (Peepers) of the type described by Carignan et al. (1985) ; and

Carignan and Lean, (1991). Each peeper was comprised of polycarbonate (Lexan) plate (65× 20× 2.1 cm) which contains two rows of 38 cells with volume capacity of 4 mL. Peeper plates were immersed in a 10% nitric acid bath for 2 days, and then rinsed with de-ionized water (DIW) before assembling. Each peeper cell was filled with DIW and a sheet of 0.22 μm HT-200 membrane was placed on top of the rows covering the entire cells. Then a 0.5 cm plexiglass cover plate was screwed in place. Membranes were immersed in DIW 2 to 3 days prior to peeper assembling. The peeper method is based on the equilibrium between DIW trapped behind a 0.22 μm membrane and porewater. Peepers were placed into the plexiglass chambers and the chambers were purged with $O_2$ free nitrogen ($O_2$<0.5 mg $L^{-1}$) overnight and then for fifteen minutes a day for 12 days thereafter, taking care to ensure there were no air bubbles in the cells or any leakage. The presence of $O_2$ in the peeper cells can alter the shape of the redox-dependent profiles such as sulfate, sulfide, $Fe^{2+}$, and Mn (Mason et al. 1998). Peepers were transferred to the field in nitrogen purged chambers.

Once on site, the chambers containing peepers were immersed into water by divers and opened while immersed in the water in order to minimize exposure to $O_2$. Three peepers were deployed at each site (the HWF and the LWF) in June, July, and August 2007. Approximately, two thirds of the peepers were immersed into the sediments and approximately 10-15 peeper cells remained above the sediment-water interface. The sediment-water interface was identified by counting the number of peeper cells exposed to the water column. Peepers were placed about 50 cm to 75 cm apart and were removed within 14 to 15 days after their initial deployment. The peepers were quickly washed in the boat with river water to remove any caked sediments and were patted dry with clean

Kim-wipes and covered in plastic wrap to minimize air exposure. Then peepers were placed in a dark cooler and transferred to the laboratory. Redox values in porewater were measured using WEISS 6231N, Uster, Zurich, Switzerland redox meter.

## 2.3.1 Porewater Sampling and Analytical Methods

### *2.3.1.1 THg*

In order to retrieve an adequate volume of porewater, samples were pooled from two consecutive peeper cells to provide a depth resolution of 1 cm. 5 mL of samples were collected using a 5 mL calibrated Eppendorf pipette. Samples were transferred to 50mL polypropylene falcon tubes, where sample volume was brought to 40 mL by adding 35 mL of DIW and then acidifying with 300 µL of BrCl. Samples were kept in the dark at 4°C for future analysis.

THg samples in porewater were analyzed using pre-oxidation with BrCl and $SnCl_2$ reduction with pre-concentration by two-stage amalgamation, followed with detection using cold vapor atomic fluorescence spectroscopy (CV-AFS). This analysis was conducted using a Tekran 2600 system, following the modified US EPA method 1631 guideline for mercury analysis (US EPA, 2001). The method detection limit was estimated at 0.05 ng $L^{-1}$. To ensure the accuracy of the analysis, blanks and spikes were run throughout the whole procedure. Analysis of field and laboratory blanks showed no mercury contamination during THg analysis. The average recovery of the spikes was 102 % $\pm$ 13, (n = 42).

### *2.3.1.2 MeHg*

10 mL of sample were collected using a calibrated Eppendorf pipette. Samples were transferred to 50 mL polypropylene falcon tubes, and acidified with 50 μL of concentrated HCl. Samples were kept in the dark at 4°C for future analysis.

MeHg concentrations in porewater were determined using capillary gas chromatography coupled with atomic fluorescence spectrometry (GC-AFS) (Analytical Mercury System Model PSA 10.723) as described by Cai et al. (1996). The detection limit was estimated at 0.02 ng $L^{-1}$. Analysis of procedural blanks consisting of DIW revealed no mercury contamination during MeHg extraction and analysis. The average recovery of the spiked samples was 94 % $\pm$ 8, (n = 12).

### *2.3.1.3 Sulfide*

Porewater sample collection for sulfide analysis was completed in less than five minutes. 2 mL amber vials were filled with Cline reagents in an anaerobic chamber one day prior to sampling. For sulfide determination, 2 mL of porewater was collected from each peeper cell using 3 mL $N_2$ purged polypropylene syringes (Norm-Ject Syringes). 1.5 mL of the porewater was injected immediately into the 2 mL amber vials containing Cline reagents by piercing the Teflon septum. Each vial was shaken in order to mix the sample and the reagent and was kept at 4°C. Field blanks were prepared by injecting 1.5 mL of DIW into vials filled with Cline reagent under an anaerobic chamber. The MDL was estimated at 0.01 mg $L^{-1}$.

Sulfide analysis was conducted at a minimum of 2 to 3 hours after each sample collection. Sulfide concentration in porewater was measured using the method described

by Cline, (1969). The sulfide concentration and its absorbance at 670nm were read using a spectrophotometer (Hatch DR 2800 Loveland, Co, U.S.A).

#### *2.3.1.4 Sulfate*

Sulfate concentration in porewater was measured using the turbidity $SO_4$ assay method described by Rodier, (1975). Sample collections were performed from the bottom cells to the top and were completed in less than five minutes. Vials were labeled and filled with 25 µL of concentrated HCl one day before sampling.1 mL of the samples were collected from each peeper cells using 1 mL calibrated Eppendorf pipette by piercing the cell membrane. The collected samples were transferred to the 2 mL amber vials containing 25 µL of HCl. Samples were kept at 4°C. Sulfide analysis was conducted within one day after sampling (less than 24 hours). Each vial was vortexed for 30 seconds before analysis. The MDL was estimated at 0.1 mg $L^{-1}$. Sulfate concentration and its absorbance at 650nm were read using a, spectrophotometer (Hatch DR 2800 Loveland, Co, U.S.A).

#### *2.3.1.5 Ferrous Iron*

$Fe^{2+}$ concentration in porewater was measured using the method described by Viollier et al. (2000). A Ferrozin solution was prepared and added to the pre-labeled vials in an anaerobic chamber one day prior to sampling. 1 mL of porewater was collected from each peeper cell using 3 mL $N_2$ purged polypropylene syringes (Norm-Ject Syringes). 1 mL of porewater was injected immediately into the 2 mL amber vials containing Ferrozin solution by piercing the Teflon septum. Each vial was shaken in

order to mix the sample and reagent and was kept at 4°C. The MDL was estimated at 0.01 mg $L^{-1}$. $Fe^{2+}$ analysis was conducted at a maximum of 2 to 3 hours after sample collection. $Fe^{2+}$ concentration and its absorbance at 562 nm were read using a spectrophotometer (Hatch DR 2800 Loveland, Co, U.S.A).

#### *2.3.1.6 Manganese*

5 mL of porewaters was collected using a calibrated Eppendorf pipette. Samples were transferred to 15 mL polypropylene falcon tubes, and acidified with 50 µL of concentrated HCl. Samples were kept in the dark at 4°C for future analysis.

Total manganese concentration (Mn) was analyzed by an Inductively Coupled plasma-Atomic Emission Spectrometer (ICP-AES) by the University of Ottawa's geology department. Method detection limit (MDL) is estimated at 0.0004 mg $L^{-1}$.

#### *2.3.1.7 Diffusion*

Diffusive flux of the elements of interest at the sediment-water interface was determined using Fick's First Law of molecular diffusion.

A generally accepted form of the Fick's First Law in the absence of bioturbation and bioirrigation is:

$$F = - (\varphi D_w / \theta^2) (\delta C / \delta x)$$

Where F is the flux of solute with concentration C at depth x, $\theta$ is the tortuosity (dimensionless), $\varphi$ is the sediment porosity, $D_w$ is the diffusion coefficient of the solute of

interest in water without the presence of the sediment matrix, and ($\delta C$ / $\delta x$) calculated using the slope of the element of interest concentration profile.

Tortuosity is not readily measured but has been shown to be related to porosity and it was calculated using the following equation (Bourdreau, 1996) for all the flux calculations:

$$\theta^2 = 1 - \ln (\varphi^2)$$

Porosity was calculated using the following equation:

$$\varphi = 1 - (\text{bulk density / Particle density})$$

A particle density of 2.65 g cm $^{-3}$ was used (Brady and Weil, 2002).

In this study, we used the diffusion coefficient ($D_w$) for MeHgCl in water (25°C) of $1.3 \times 10^{-5}$ cm$^2$ s$^{-1}$ and a $D_w$ value for inorganic Hg in water of $9.5 \times 10^{-6}$ cm$^2$ s$^{-1}$ (Gill et al. 1999).

We adopted a $D_w$ value for sulfate of $0.3 \times 10^{-5}$ cm$^2$ s$^{-1}$ (Hordjik et al. 1985), $8.3 \times 10^{-6}$ cm$^2$ s$^{-1}$ for sulfide (Preisle et al. 2007; Li and Geregory, 1974) and $4.09 \times 10^{-6}$ cm$^2$ s$^{-1}$ for $Fe^{2+}$ (Peine et al. 2000; Li and Geregory, 1974).

## 2.4 Benthic Chamber Sampling

THg and MeHg concentrations were measured in the St. Lawrence River using benthic chambers to estimate the diffusion rates from sediments. Six benthic chambers were deployed in the HWF and six in the LWF sites during summer 2007 in order to quantify the benthic exchange at the sediment-water interface. Benthic chambers were constructed of square chambers (19 × 32 cm) with two valves, to allow water sample collection at timed intervals. A portion of the sediment surface was enclosed by the benthic chambers and the concentration of the constituents of interest was measured over time. Each benthic chamber had a stirring wheel used for mixing the water inside the chamber before sampling. The volume of the samples in the benthic chamber was compensated by the surrounding water which entered through the valves.

Benthic chambers were deployed by divers and samples were taken from the chambers using National Scientific Target* disposable syringes polypropylene/ poly ethylene by divers at timed intervals for the dissolved elements of interest. All the sub-sampling was performed in $N_2$ purged chambers. All the water samples were filtered in the $N_2$ purged chambers using VWR 25 mm GD/X sterile filter device with 0.45 μm pore size for THg and MeHg analysis.

THg and MeHg concentration determinations in benthic chambers samples were conducted using the same method as described above for THg and MeHg in porewater.

## 2.5 Statistical Analysis

The statistical analysis used both parametric and non-parametric analyses, including two-factor ANOVA and three-factor ANOVA, Spearman($r_s$) and Pearson (r) correlations, least-squares regressions and two-sample t-tests using SYSTAT ® 12 for windows and Minitab 15. Parametric tests were performed when both normality and homoscedasticity assumptions of residuals were achieved and non-parametric analysis otherwise.

We used two-factor ANOVA to determine the effect of site and month on MeHg concentrations. In order to determine the effect of site, month and depth on THg concentration, a three-factor ANOVA was applied.

Correlation analyses were performed to look for co-variation among all environmental variables. Kolmogorov-Smirnov test was applied to confirm the normality distribution of residuals and Levene's test to verify homoscedasticity of variances. Data were log or natural-log transformed, when possible, in order to reach normality and homoscedasticity.

# 3 RESULTS

In order to predict the transport rate of Hg to and from sediments, spatial and temporal patterns for THg and MeHg in both sediments and porewater are shown below, and have been compared with complimentary redox-dependent variables, including sulfate, sulfide, $Fe^{2+}$ and, Mn concentration in porewaters. These static measurements were then used to calculate flux rates using Fick's First Law of diffusion. $^{210}Pb$ dated sediment cores were used to calculate sediment accumulation rates which could then be related to Hg accumulation rates in these sediments. This information was then compared with diffusion rates of THg and MeHg from porewater profiles to obtain an overall measure of the net sediment transfers across the sediment-water interface.

## 3.1 Mercury in Solid Phase

### 3.1.1 Total Mercury

THg concentrations in the HWF and LWF cores ranged between 748 and 44800 ng $g^{-1}$ dw (Fig.3-1). In the HWF core, THg increased sharply to a depth of 42 cm (Fig.3-1.A). The highest concentration in the LWF core (Fig.3-1.B) was at 48.5cm, but this was the lowest interval from the core, so we do not know if the maximum Hg concentration was reached. Total mercury in surface sediments (0-5 top centimeter of the core) ranged between 1240 and 1740 ng $g^{-1}$ dw in the HWF core and from 766 and 1220 ng $g^{-1}$ dw in the LWF core. Total mercury concentrations in the HWF and LWF cores exceeded the background level of 20 to 175 ng $g^{-1}$ dw for uncontaminated sediments in freshwater

across Canada as estimated by Ramussen, (1994). A t-test analysis showed higher THg concentrations in the HWF than the LWF sediment core ($p = 0.008$).

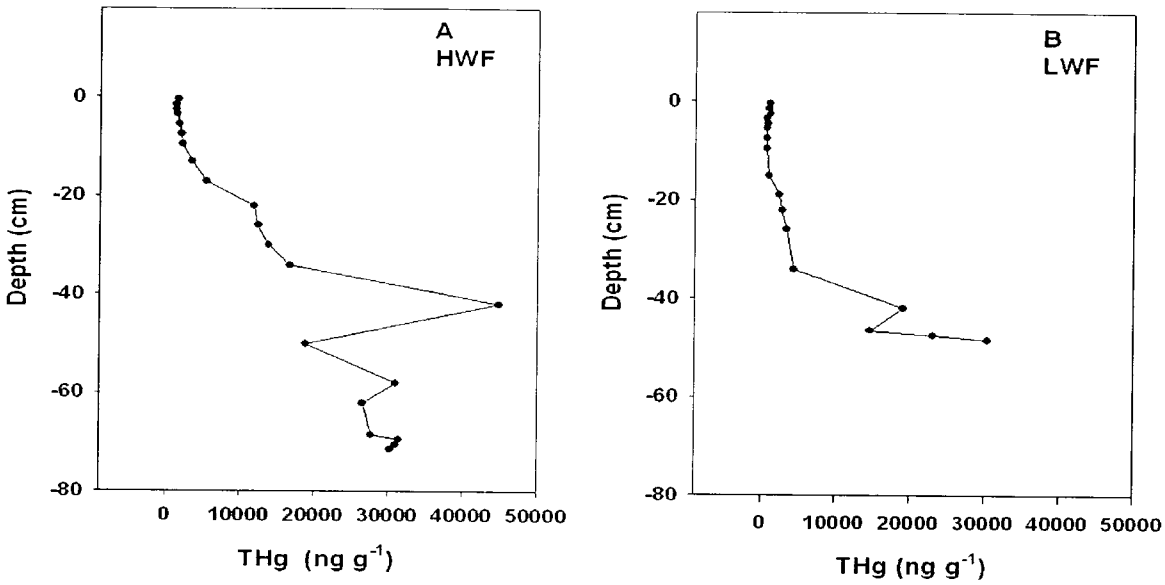


Figure 3-1. Depth profile of total mercury in sediment in the HWF (A) and LWF (B) cores.

Table 3-1. Mercury concentration range (mean ± (SD) if n>2) in surface sediments of Zone 1 of the St. Lawrence River from 1970 to 2007. The bold values in 1979 and 2003 are the median values since mean values were unavailable (modified from Richman and Dreier, 2001).

| Year | Hg (ng $g^{-1}$) dw | n | LEL/SEL | Present study Hg (ng $g^{-1}$) | |
|---|---|---|---|---|---|
| | | | | HWF* | LWF* |
| 1970[1] | 850-14500 (4700 ± 5370) | 6 | 200/2000 | 18850 | 3440 |
| 1975[1] | 850-18200 (6910 ± 7500) | 5 | | 30750 | 3125 |
| 1979[2] | 1500-19800 **(4500)** | 4 | | 12350 | 2810 |
| 1985[3] | 630-900 | 2 | | 11850 | 2410 |
| 1991[4] | 3260 | 1 | | 5465 | 1050 |
| 1997[5] | 790-1710 (1230 ± 460) | 3 | | 1970 | 7740 |
| 2003[6] | 378 -1646 **(576)** | — | | 1328 | 766 |
| 2005[7] | 553-806 (681± 94) | 6 | | 1435 | 1150 |
| 2007[8] | 766-1742 (1161 ± 264) | 9 | | | |

[1]MOE, 1979. (1970—7cm surficial grab, 1975—3 cm surficial grab sample)
[2]Kauss et al. 1988. (3 cm surficial grab sample)
[3]Anderson, 1990. (3 cm surficial grab sample)
[4]Richman, 1994. (3 cm surficial grab sample)
[5]Richman, 1999. (10 cm core sample)
[6]Grapentine et al. 2003. (10 cm core sample)
[7]Delongchamp, 2006. ( 2005— 3 cm core sample)
[8]Present study, 2009. ( 2007— 5 cm core sample)
* Hg concentrations in the HWF and LWF sites are at the exact depth intervals corresponding to the year. According to high variability of Hg concentration in Zone1, the increase in sediment Hg between 1985 and 1991, 1997 and 2003 and, 2005 and

2007and the difference between present study with previous studies was likely based on difference in sampling location between surveys.

### 3.1.2 Methyl Mercury

Methylmercury concentrations at both sites decreased slightly between the sediment-water interface and 5-10 cm of the cores (Fig.3-2), but otherwise showed a similar trend as THg profiles. MeHg ranged between ~1.9 and 38.4 ng $g^{-1}$ dw in both cores. MeHg concentration in surface sediments (0-5 top centimeter of the core) ranged between 2.0 and 9.5 ng $g^{-1}$ dw in the HWF and between 2.3 and 3.5 ng $g^{-1}$ dw in the LWF core. In the HWF core, the highest MeHg value was at 34 cm, and in the LWF site core it was at 48.5 cm (Fig.3-2), consistent with peaks of THg concentration in sediments of the same core (Fig.3-1).

A t-test analysis showed no significant difference between log of MeHg concentrations in sediments in the HWF and LWF sites ($t = 1.4$, $p = 0.17$, $df = 23$).

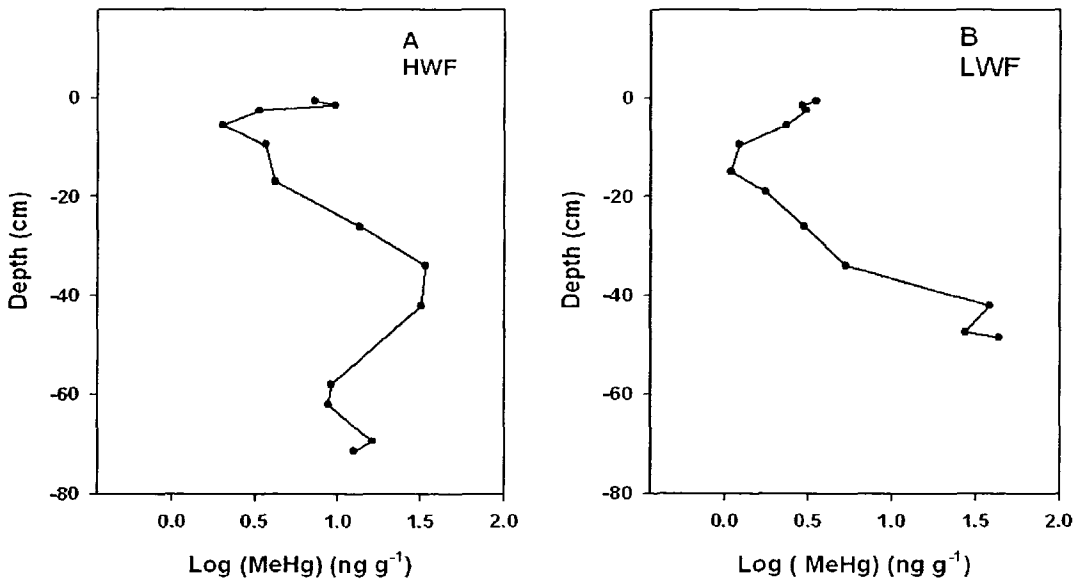

Figure 3-2. Depth profile of log of methylmercury in sediment in the HWF (A) and LWF (B) cores.

### 3.1.3 Methyl Mercury Distribution to Total Mercury in Sediment

The percent of MeHg/THg in surface sediments generally increased towards the sediment-water interface, and tended to be highest near the surface, with values reaching 0.7% in the HWF and 0.3% in the LWF core. There was an increase in % MeHg in both cores between 20-40 cm, and a decrease in deeper intervals (Fig.3-3). The MeHg/THg ratios ranged from 0.04 to 0.7 % in the HWF core and from 0.09 to 0.32% in the LWF core. In general, MeHg/THg ratios were less than 1% in sediments.

As THg increased in deeper sediments, so did the MeHg concentration, but the percent as MeHg was relatively constant between 0.03 and 0.2 % until near the surface where the percent as MeHg increased to 0.7% and 0.3% in the HWF and LWF cores respectively.

MeHg was positively correlated with THg in the sediment core from the HWF site (Fig.3-4.A), ($r_s$ = 0.67, p = 0.012), and in the LWF core (Fig.3-4.B), ($r_s$ = 0.81, p = 0.001).

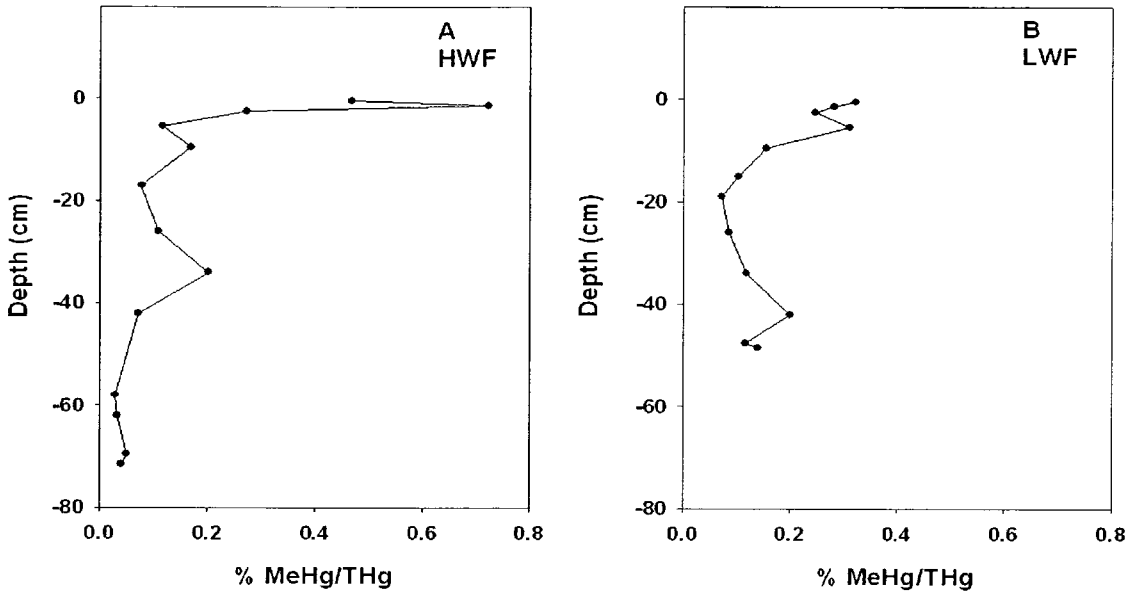


Figure 3-3. MeHg/THg ratio in sediment in the HWF (A) and LWF (B) cores.

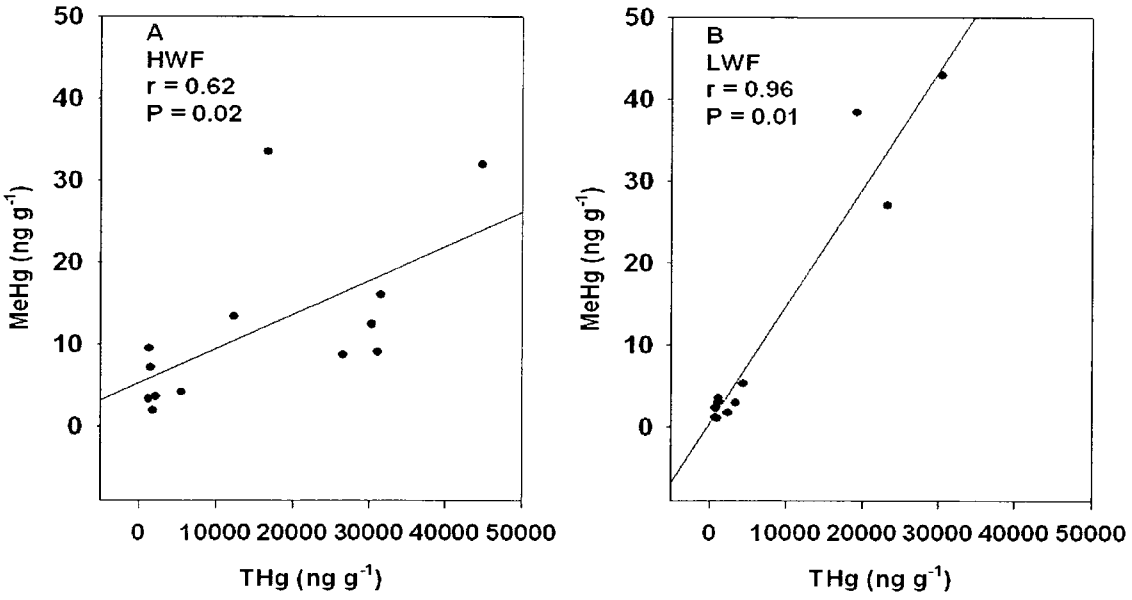


Figure 3-4. Correlation between MeHg and THg in the HWF (A) and LWF (B) sediment cores.

### 3.1.4 Organic Content

Organic content in the HWF core ranged between 5 and 55 %, whereas, it ranged from 7 to 15% in the LWF core (Fig. 3-5). In the HWF core organic content was low in surface sediments rising to a peak at 15 cm depth, and reaching the highest organic content at 65 to 70 cm. In the LWF site, organic content slightly decreased at 5 cm and it remained almost constant at ~ 10% until 20 cm, then increasing slightly between 20 and 45 cm. Overall, of organic content in the HWF core varied considerably and was much higher than the LWF core ($p = 0.001$).

There was a correlation between MeHg and organic content in the HWF core; however, this correlation was not significant since the p-value was exactly at the border line ($r_s = 0.53$, $p = 0.05$). Nevertheless, a significant correlation between MeHg and organic content in the LWF core was observed ($r_s = 0.89$, $p = 0.002$).

Significant correlations between THg and organic content in both the HWF core ($r_s = 0.49$, $p = 0.02$) and the LWF core ($r_s = 0.78$, $p = 0.003$) were observed.

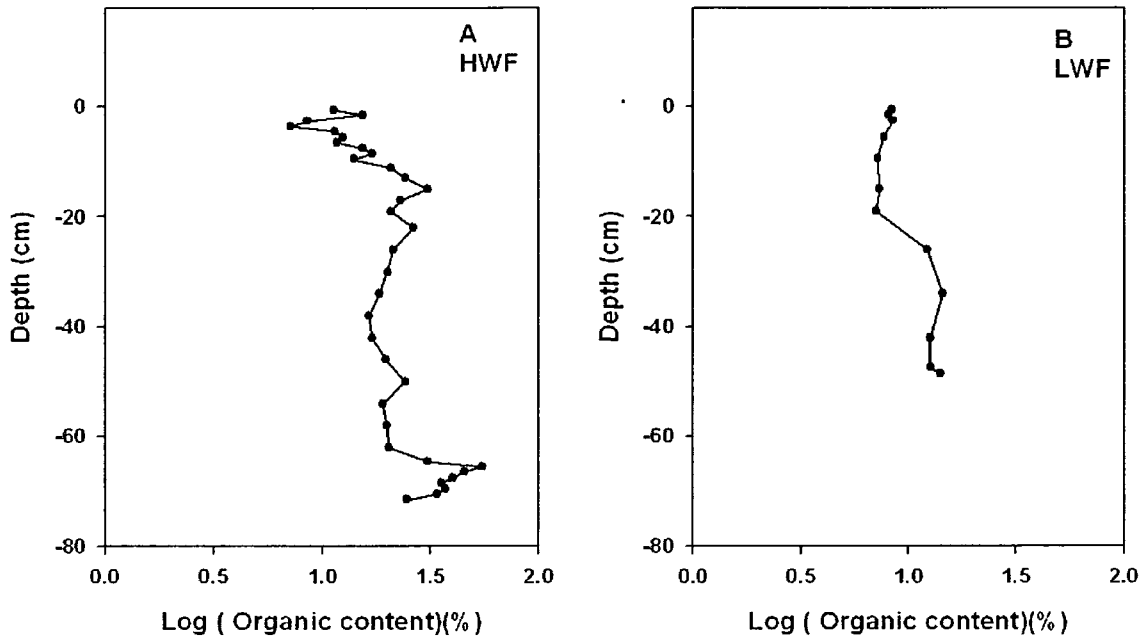


Figure 3-5. Depth profile of log of organic content in the HWF (A) and LWF (B) cores.

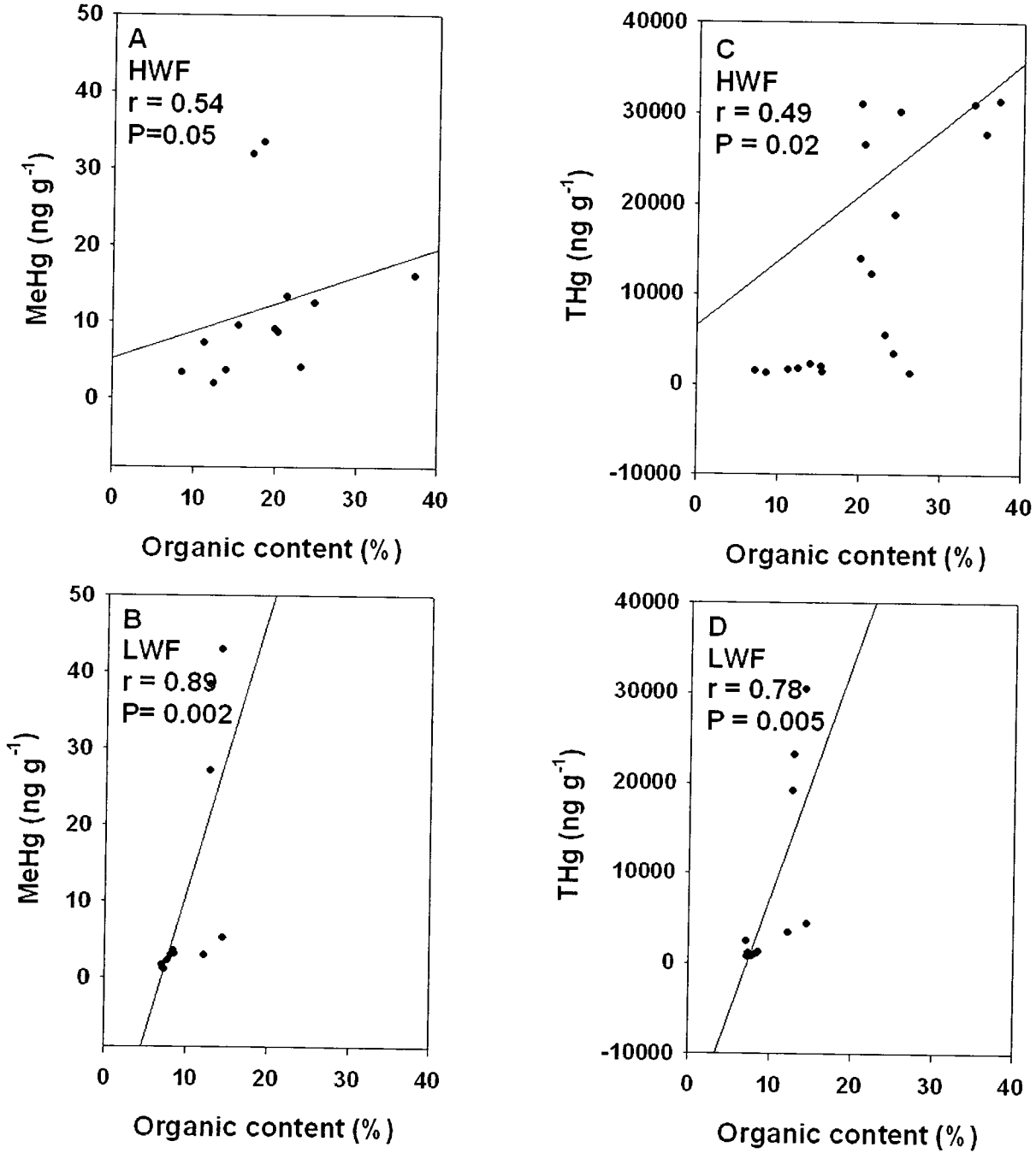


Figure 3-6. Correlation between mercury species and organic matter in the HWF (A, C), and LWF (B, D) cores.

### 3.1.5 Inventories of $^{210}Pb$, Sedimentation Rates and Mercury Accumulation Rates

Unsupported $^{210}Pb$ activities decreased exponentionally with sediment depth in the LWF cores, however, no such decrease was observed in either of the two HWF cores. Consequently, the HWF cores were not datable. The deepest sediment layer in the two LWF cores, at 59cm and at 48cm, were 96 and 63 years old, respectively based on applying $^{210}Pb$ activities to the CRS model. Both cores from the LWF site had similar unsupported $^{210}Pb$ inventories (Table 3-2).

The mean value of 16100 ± 1350 Bq $m^{-2}$ represents a $^{210}Pb$ supply rate of 502 ± 42 Bq $m^{-2}$ $yr^{-1}$, which showed how fast $^{210}Pb$ was accumulating at the LWF site. These fluxes of $^{210}Pb$, which were 3 times higher than atmospheric flux of 150 Bq $m^{-2}$ $yr^{-1}$ in northwestern Ontario (Omelchenko et al. 1995) indicating a high remobilization of sediment to these coring sites.

Mean sedimentation rates were calculated by dividing the $^{210}Pb$ radioactive decay constant (0.03114 $yr^{-1}$) by the slope(a) of the natural log of unsupported $^{210}Pb$ versus cumulative dry mass (Fig.3-7). Mean sedimentation rate in the LWF cores were 0.45 and 0.75 g $cm^{-2}$ $yr^{-1}$ and it was about 1.04 g $cm^{-2}$ $yr^{-1}$ in the HWF site.

$$\text{Mean sedimentation rate} = \frac{\text{Radioactive decay constant}}{\text{Slope(a)}*}$$

* Slopes (a) were the slopes of the Ln (unsupported $^{210}Pb$) and cumulative dry mass profiles (Fig. 3-7).

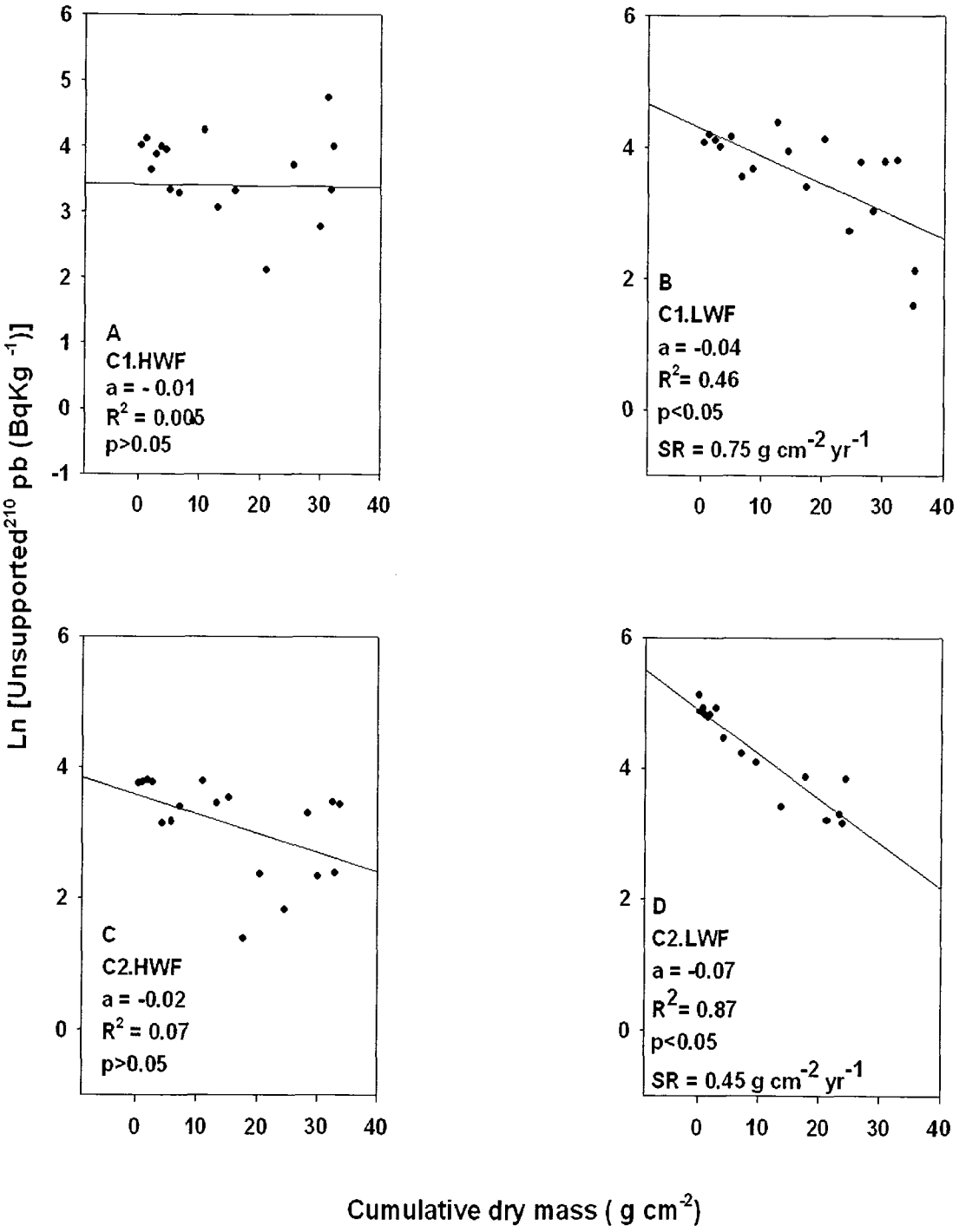


Figure 3-7. Profiles of the natural log of unsupported $^{210}$Pb activity versus cumulative dry mass. Mean sedimentation rate (g cm$^{-2}$ yr$^{-1}$) can be calculated by dividing $\lambda$ by the slope (a), where $\lambda$ is the $^{210}$Pb radioactive decay constant (0.03114 yr$^{-1}$).

Table 3-2. $^{210}Pb$ inventories, fluxes and focus factors in cores from the LWF site.

| Sample ID | $^{210}Pb$ Inventory Bq $m^{-2}$ | ± SE | $^{210}Pb$ Flux Bq $m^{-2}$ $yr^{-1}$ | ± SE | Focus Factor* |
|---|---|---|---|---|---|
| Core 1.LWF | 15400 | 1160 | 479 | 36 | 3.1 |
| Core 2.LWF | 16900 | 1540 | 525 | 48 | 3.5 |
| Mean | 16100 | 1350 | 502 | 42 | 3.3 |

* Calculated based on an estimated unsupported $^{210}Pb$ flux from the atmosphere of 150 Bq $m^{-2}$ $yr^{-1}$ (Omelchenko et al. 1995).

THg concentration in dated sediment cores from the LWF site (based on applying $^{210}Pb$ activities to the CRS model) was highest in sediment intervals corresponding to 1954. THg concentrations in the LWF site decreased in the 1970s, when regulations were established to limit the discharge of liquid Hg to the river. Another decrease in THg concentrations was also obvious after 1995 which corresponds to the closure of ICI Forest, Courtalds, and Domtar. However, THg concentrations rose slightly near the top of the core (Fig. 3-8).

In the HWF site THg concentration was highest in sediment intervals corresponding to 1974. THg in sediments of the HWF site decreased between 1995 and 2007, corresponding to the closure of ICI Forest Products, Courtalds, and Domtar. However no such decrease in THg concentrations were observed in 1970s (Fig. 3-8).

A non-parametric (Mann-Whitney U) test was applied to test the prediction that average THg concentrations in pre-1970 were higher than the average THg concentrations in sediments deposited from 1970-1995, and that the average THg concentrations in 1970-1995 were higher than the average THg concentrations in 1995-2006 in the HWF and LWF sites. Statistical analysis showed that THg concentrations decreased between 1995 and 2006 in both the HWF ($p = 0.004$) and the LWF sites ($p = 0.02$). Another decrease of THg concentrations was observed after 1970 in the LWF ($p = 0.02$); however, no such a deacrese was observed in the HWF site ($p = 0.06$).

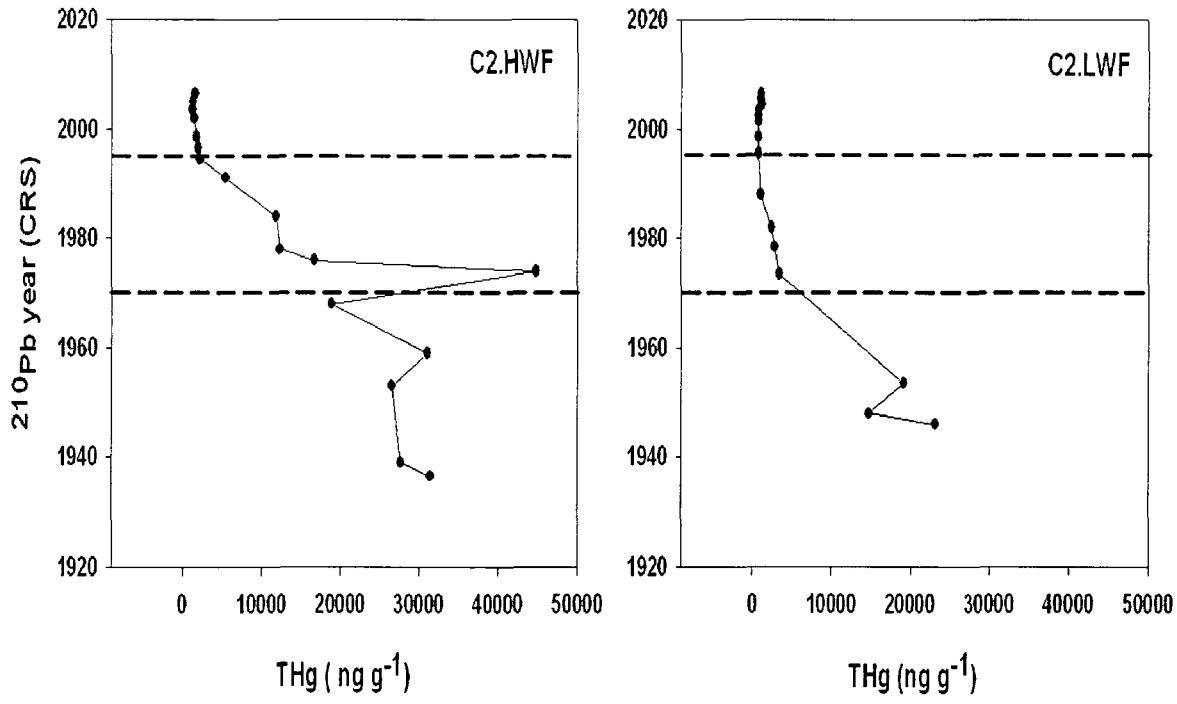


Figure 3-8. Total mercury concentration in cores from the HWF and LWF sites versus year. $^{210}$Pb year is based on the constant rate of supply (CRS) model.

THg accumulation rate in the LWF core was highest at 42 cm, which corresponds to 1953 (based on applying $^{210}Pb$ activities to the CRS model). There was a sharp decrease of THg accumulation rate from 1953 to about 1964. Another decrease in THg accumulation rate was obvious around 1974 and 1988 (between 15 and 25 cm). The top 15 cm of the core corresponds to the interval spanning from 1992 to 2007 (Fig. 3-9).

In the HWF site THg accumulation rate was highest at 42 cm of the core which corresponds to 1974 (based on applying 210Pb activities to the CRS model) (Fig. 3-9).

A non-parametric (Mann-Whitney U) test was applied to test the hypothesis that the average Hg accumulation rate in pre-1970 sediments was higher than the average accumulation rate in sediments dated to 1970-1995, and that the average Hg accumulation rate in 1970-1995 was higher than the average accumulation in 1995-2006 in the HWF and LWF sites. Results showed that there was no decrease in THg accumulation rates between pre-1970 and 1970-1995 in both the HWF ($p = 0.7$) and LWF sites ($p = 0.07$), but THg accumulation rate decreased significantly after 1995 in both the HWF ($p = 0.01$) and LWF sites ($p = 0.02$).

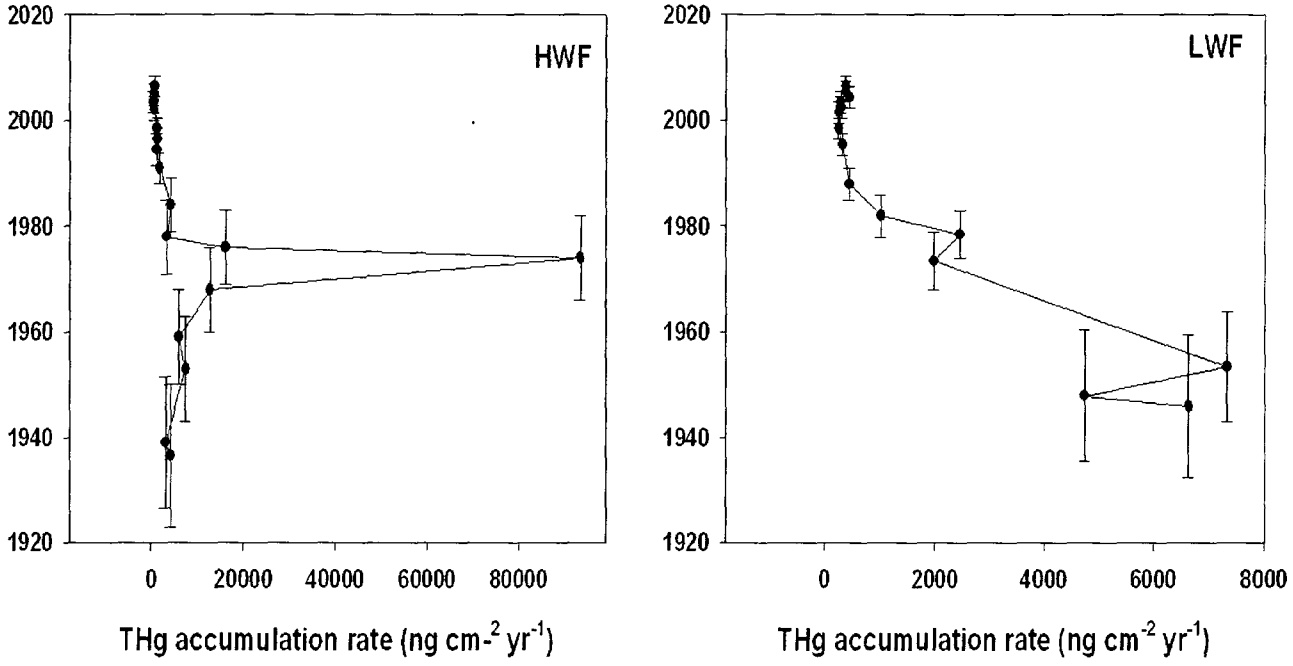


Figure 3-9. Total mercury accumulation rate versus year (determined by $^{210}$Pb activities and the CRS model) in the HWF and LWF sites.

## 3.2 Mercury and Complimentary Redox Profiles in Porewater and the Water Column

### 3.2.1 Total Mercury in Porewater

Total mercury mean concentration in the HWF site was 17.94 ± 0.97 (SE) ng $L^{-1}$, (n = 100) in the porewater and 12.79 ± 1.08 (SE) ng $L^{-1}$, (n = 57) in the overlying water, whereas in the LWF site it was 18.57 ± 1.18 (SE) ng $L^{-1}$, (n = 87) in the porewater and 15.92 ± 1.17(SE) ng $L^{-1}$, (n = 50) in the water column. The distribution of total mercury in porewater and overlying water was relatively homogenous across depths in these profiles (Fig.3-10, 3-11, 3-12), providing evidence that diffusion rates are likely to be small. In general total mercury concentration in porewater ranged between 3.1 and 58.6 ng $L^{-1}$ in the HWF site and from 4.5 to 76.9 ng $L^{-1}$ in the LWF site. THg concentration in overlying water ranged between 4.26 and 46 ng $L^{-1}$ in the HWF site and from 6.5 to 45.1 ng $L^{-1}$ in the LWF site. No correlation was observed between dissolved and solid phase THg in all the profiles in the HWF and LWF sites ($p > 0.05$) except for two porewater profiles in June, one in the HWF site ($r = 0.85$, $p < 0.05$) and the other in the LWF site ($r = 0.42$, $p < 0.05$). Percent dissolved to solid phase THg ranged between 0.0005 and 0.16 in the HWF site and from 0.0001 to 0.004 in the LWF site. A three-factor ANOVA analysis determined that there was no significant difference in THg concentrations between the sites ($p > 0.05$), and between porewater and overlying water. Additionally, no monthly THg concentration variation was observed ($p > 0.05$) during summer 2007 in the St. Lawrence River (See Appendix D).

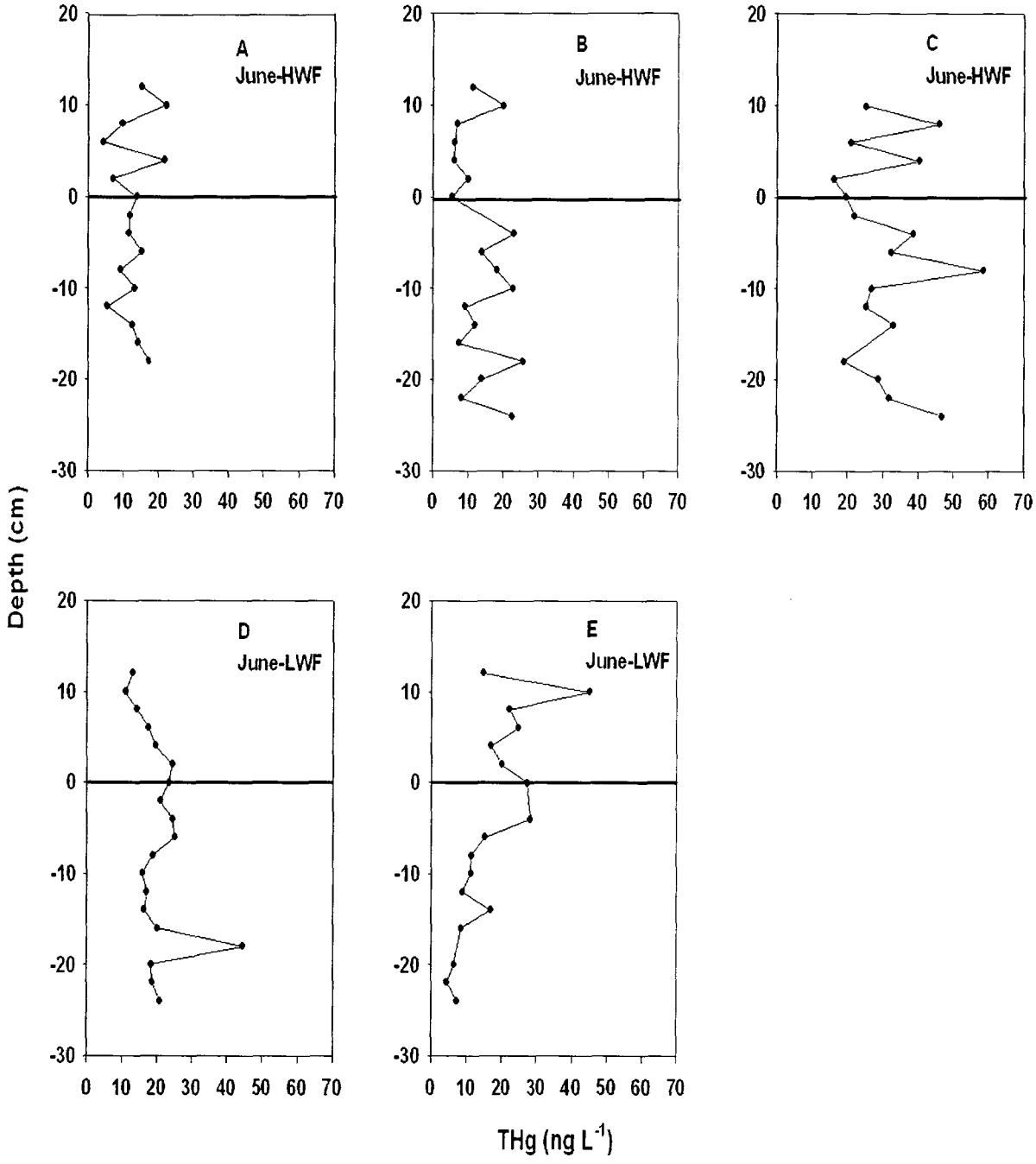


Figure 3-10. Vertical distribution of THg concentration in triplicate porewater profiles in the HWF (A, B, C) and LWF (D, E) sites. The black solid line shows the position of the sediment-water interface.

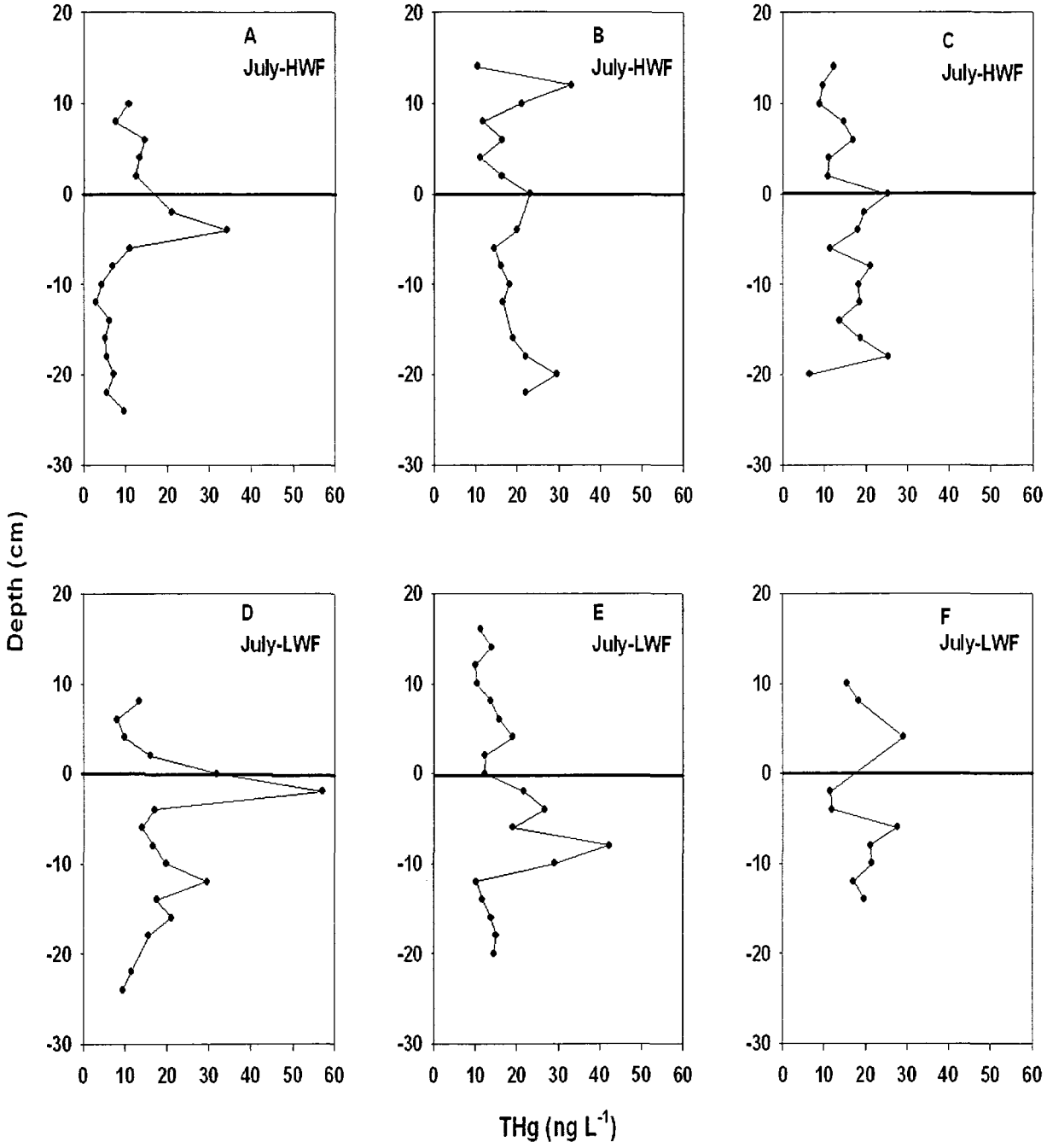


Figure 3-11. Vertical distribution of THg concentration in triplicate porewater profiles in the HWF (A, B, C) and LWF (D, E, F) sites. The black solid line shows the position of the sediment-water interface.

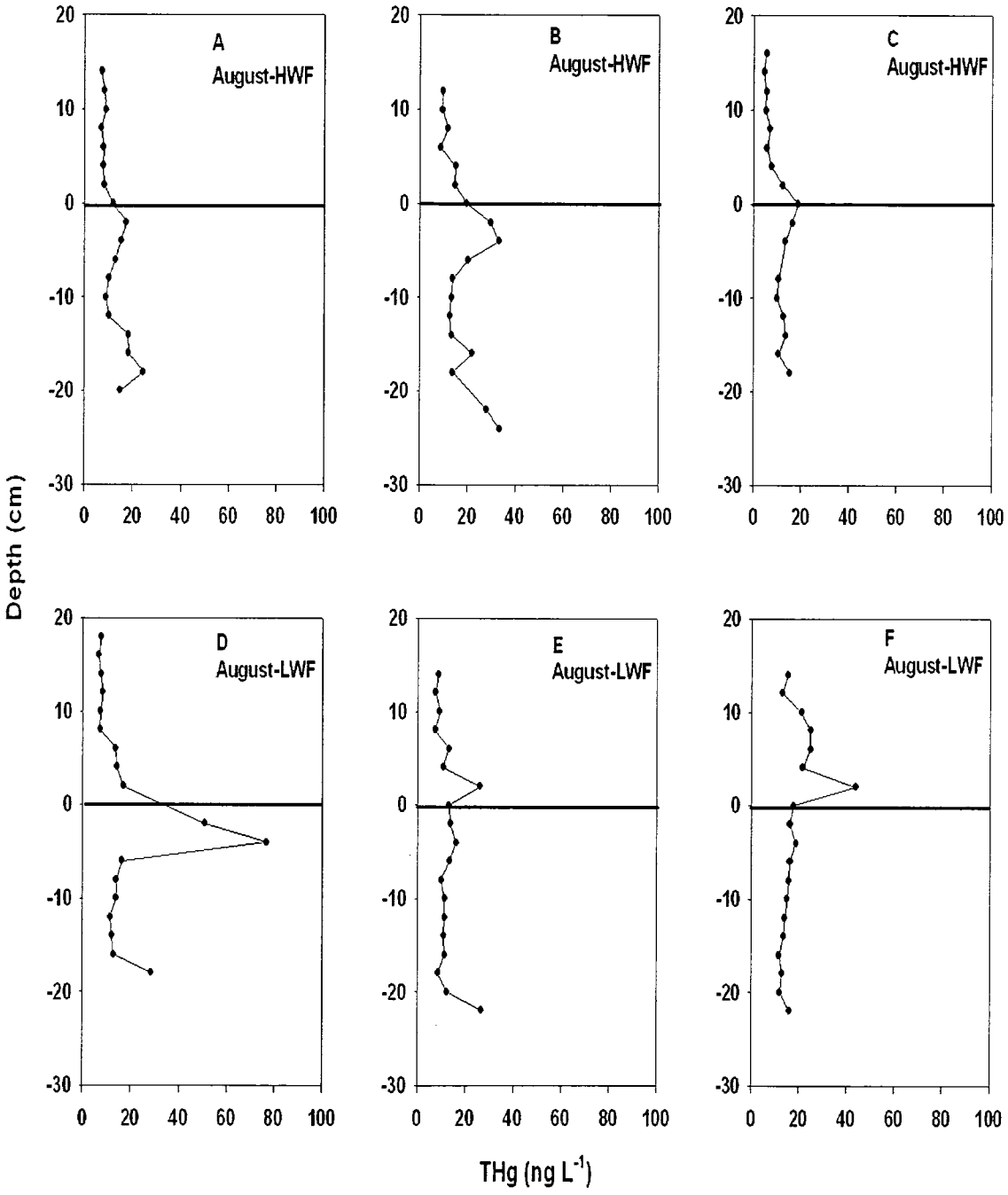


Figure 3-12. Vertical distribution of THg concentration in triplicate porewater profiles in the HWF (A, B, C) and LWF (D, E, F) sites. The black solid line shows the position of the sediment-water interface.

### 3.2.2 Methyl Mercury in Porewater

Mean MeHg concentration in the HWF site was 6.62 ± 0.62 (SE) ng $L^{-1}$, (n = 47) in porewater and 4.82 ± 1.14 (SE) ng $L^{-1,}$ (n = 26) in the water column, whereas in the LWF site it was 5.71 ± 0.44 (SE) ng $L^{-1}$, (n = 32) in the porewater and 3.45 ± 0.52 (SE) ng $L^{-1,}$ (n = 22) in the water column. Concentrations of MeHg in porewater ranged between 1.38 and 20.98 ng $L^{-1}$ in the HWF site and from 0.7 and 19.44 ng $L^{-1}$ in the LWF site, but generally showed no clear trend with depth. Concentrations of MeHg in the water column ranged between 1.66 and 27.87 ng $L^{-1}$ in the HWF site and from 1.4 and 11.29 ng $L^{-1}$ in the LWF site. MeHg concentrations were more variable in July and August (0.5 to 27.87 ng $L^{-1}$) than in June (1.71to 8.43 ng $L^{-1}$) (Fig.3-13). The percentage of MeHg to THg in porewater ranged from 4 to 100% in the HWF site and between 6 and 100% in the LWF sites. (Percent MeHg exceeded 100% in 5 cases in July and August, (n = 99)).

No correlation was observed between dissolved and particulate MeHg in all the profiles in both the HWF and LWF sites ($p > 0.05$) and percent dissolved to particulate MeHg ranged between 0.02 and 0.05 % in the HWF and from 0.16 to 1.31% in the LWF sites.

Despite 50% higher MeHg concentrations in the HWF site than the LWF, and 50% increase in MeHg concentrations between June and July in the HWF site, a two-factor ANOVA analysis determined that there was no significant difference in MeHg concentrations between the sites, and no monthly variation was observed in MeHg concentration during summer 2007 (See Appendix D).

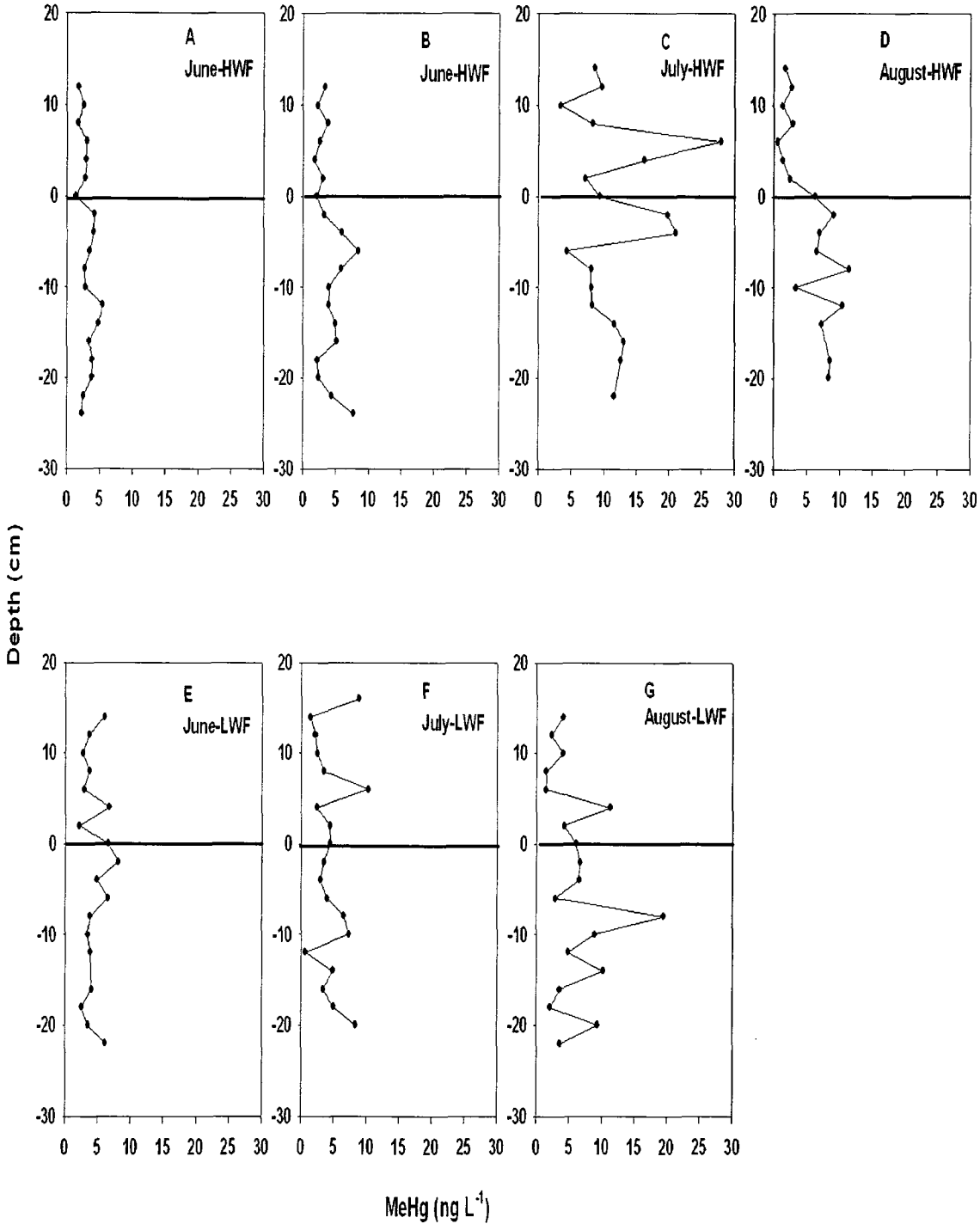


Figure 3-13. Vertical distribution of MeHg concentration in porewater profiles in June (A, B, E), July (C, F) and August (D, G) in the HWF and LWF sites. The black solid line shows the position of the sediment-water interface.

### 3.2.3 Hg Diffusion

Diffusive fluxes of mercury across the sediment-water interface were determined based on the concentration gradient between porewater and overlying water.

In the HWF site, there was no diffusion of THg in June and July, but all three THg profiles showed slight upward diffusion in August ranging between $2 \times 10^{-4}$ and $7.7 \times 10^{-5}$ ng $cm^{-2}$ $yr^{-1}$ (Table 3-3). In the LWF site, no diffusion of THg in August was observed, whereas THg diffusion from sediment to water varied between 0 and $2 \times 10^{-4}$ ng $cm^{-2}$ $yr^{-1}$ in June and July. Also there was an observation of diffusion from water to sediment of $2 \times 10^{-4}$ ng $cm^{-2}$ $yr^{-1}$ in June (Table 3-4).

MeHg diffusion rates ranged between 0 and $6 \times 10^{-5}$ ng $cm^{-2}$ $yr^{-1}$ in the HWF site whereas, no diffusion was observed in the LWF site (Table 3-5). It should be noted that, all the diffusion rates for THg and MeHg were calculated in the absence of bioturbation, bioirrigation, ebulition, and resuspension of the sediments.

Table 3-3. Sediment-water diffusion flux of THg in the HWF site. A positive value shows diffusion is from sediment to water.

| Site | Month | THg diffusion ($ng\ cm^{-2}\ yr^{-1}$) | Standard error ($ng\ cm^{-2}\ yr^{-1}$) |
|---|---|---|---|
| HWF | June | 0.0 | $\pm$ 0.0 |
| HWF | June | 0.0 | $\pm$ 0.0 |
| HWF | June | 0.0 | $\pm$ 0.0 |
| HWF | July | 0.0 | $\pm$ 0.0 |
| HWF | July | 0.0 | $\pm$ 0.0 |
| HWF | July | 0.0 | $\pm$ 0.0 |
| HWF | August | $+7.7\times10^{-5}$ | $\pm\ 2.7\times10^{-5}$ |
| HWF | August | $+2.0\times10^{-4}$ | $\pm\ 6.3\times10^{-5}$ |
| HWF | August | $+3.1\times10^{-5}$ | $\pm\ 8.5\times10^{-6}$ |

Table 3-4. Sediment-water diffusion flux of THg in the LWF site. A negative value shows diffusion is from water to sediment and a positive value shows diffusion is from sediment to water.

| Site | Month | THg diffusion ($ng\ cm^{-2}\ yr^{-1}$) | Standard error ($ng\ cm^{-2}\ yr^{-1}$) |
|---|---|---|---|
| LWF | June | $-2.0\times10^{-4}$ | $\pm 7.3\times10^{-5}$ |
| LWF | June | $+1.0\times10^{-4}$ | $\pm 3.7\times10^{-5}$ |
| LWF | July | 0.0 | $\pm 0.0$ |
| LWF | July | $+2.0\times10^{-4}$ | $\pm 6.0\times10^{-5}$ |
| LWF | July | 0.0 | $\pm 0.0$ |
| LWF | August | 0.0 | $\pm 0.0$ |
| LWF | August | 0.0 | $\pm 0.0$ |
| LWF | August | 0.0 | $\pm 0.0$ |

Table 3-5. Sediment-water diffusion flux of MeHg in the HWF site. A positive value shows diffusion is from sediment to water.

| Site | Month | MeHg diffusion (ng $cm^{-2}$ $yr^{-1}$) | Standard error (ng $cm^{-2}$ $yr^{-1}$) |
|---|---|---|---|
| HWF | June | $+3.0\times10^{-5}$ | $\pm 1.2\times10^{-5}$ |
| HWF | June | 0.0 | ± 0.0 |
| HWF | July | 0.0 | ± 0.0 |
| HWF | August | $+6.0\times10^{-5}$ | $\pm 2\times10^{-5}$ |
| LWF | June | 0.0 | ± 0.0 |
| LWF | July | 0.0 | ± 0.0 |
| LWF | August | 0.0 | ± 0.0 |

### 3.2.4 Sulfate in Porewater

Mean sulfate concentration in the HWF site was 5.31 ± 0.86 (SE) mg $L^{-1}$, (n = 74) in porewater and 20.70 ± 0.33 mg $L^{-1}$, (n = 38) in overlying water, whereas in the LWF site it was 2.77 ± 0.82 (SE) mg $L^{-1}$, (n = 70) in porewater and 22.31 ± 1.0 mg $L^{-1}$, (n = 36) in overlying water, indicating diffusive flux of sulfate was from water to sediment.

Sulfate reduction rates were calculated in both the HWF and LWF sites by summing sulfate inventories in the sediment porewater profiles from 0 (sediment-water interface) to 20 cm, each month, to quantify the rate of *in situ* sulfate reduction (Table 3-

6). Sulfate concentrations were higher in the water column but decreased sharply near the sediment water interface in all the profiles (Fig.3-14), indicating the activity of sulfate reducing bacteria near surface sediments.

Sulfate concentrations in the sediment phase decreased between sediment-water interface and depth of 10 cm and remained almost in constant range in the solid phase in all the profiles (Fig.3-14).

In the LWF site, there was very little production of sulfate from June to July, however from July to August, sulfate reduction rate was about 5 times higher than the HWF site (Table 3-6), which is consistent with a higher rate of sulfide production in this site (Table 3-8).

Sulfate diffusion rates ranged between $1.3\times10^{-3}$ and $2.4\times10^{-3}$ μmol $cm^{-2}$ $yr^{-1}$ in the HWF and from $0.3\times10^{-3}$ to $1.1\times10^{-3}$ μmol $cm^{-2}$ $yr^{-1}$ in the LWF site (Table 3-7). In general, the diffusion rates calculated in the HWF site were higher than the LWF site. Sulfate diffusion from water to sediment was likely mediated by SRB activities (sulfate reducing bacteria) in anaerobic sediments. However, sulfate diffusion was very low compared to the sulfate reduction rate (Table. 3.6, 3-7).

Table 3-6. Sulfate reduction rate in the HWF and LWF sites.

| Zone 1 | $SO_4$ reduction rate (μmol $SO_4$ $cm^{-2}$ $day^{-1}$) From June to July | $SO_4$ reduction rate (μmol $SO_4$ $cm^{-2}$ $day^{-1}$) From July to August |
|---|---|---|
| HWF | 0.034 | 0.025 |
| LWF | -0.006 | 0.118 |

Table 3-7. Sediment-water diffusion flux of sulfate in the HWF and LWF sites. A negative value shows diffusion is from water to sediments.

| Site | Month | Sulfate diffusion ($\mu mol\ cm^{-2}\ yr^{-1}$) | Standard error ($\mu mol\ cm^{-2}\ yr^{-1}$) |
|---|---|---|---|
| HWF | June | $-2.4\times10^{-3}$ | $\pm 0.9\times10^{-3}$ |
| HWF | July | $-1.3\times10^{-3}$ | $\pm 0.2\times10^{-3}$ |
| HWF | August | $-1.5\times10^{-3}$ | $\pm 0.3\times10^{-3}$ |
| LWF | June | $-0.3\times10^{-3}$ | $\pm 0.1\times10^{-3}$ |
| LWF | July | $-0.3\times10^{-3}$ | $\pm 0.1\times10^{-3}$ |
| LWF | August | $-1.1\times10^{-3}$ | $\pm 0.2\times10^{-3}$ |

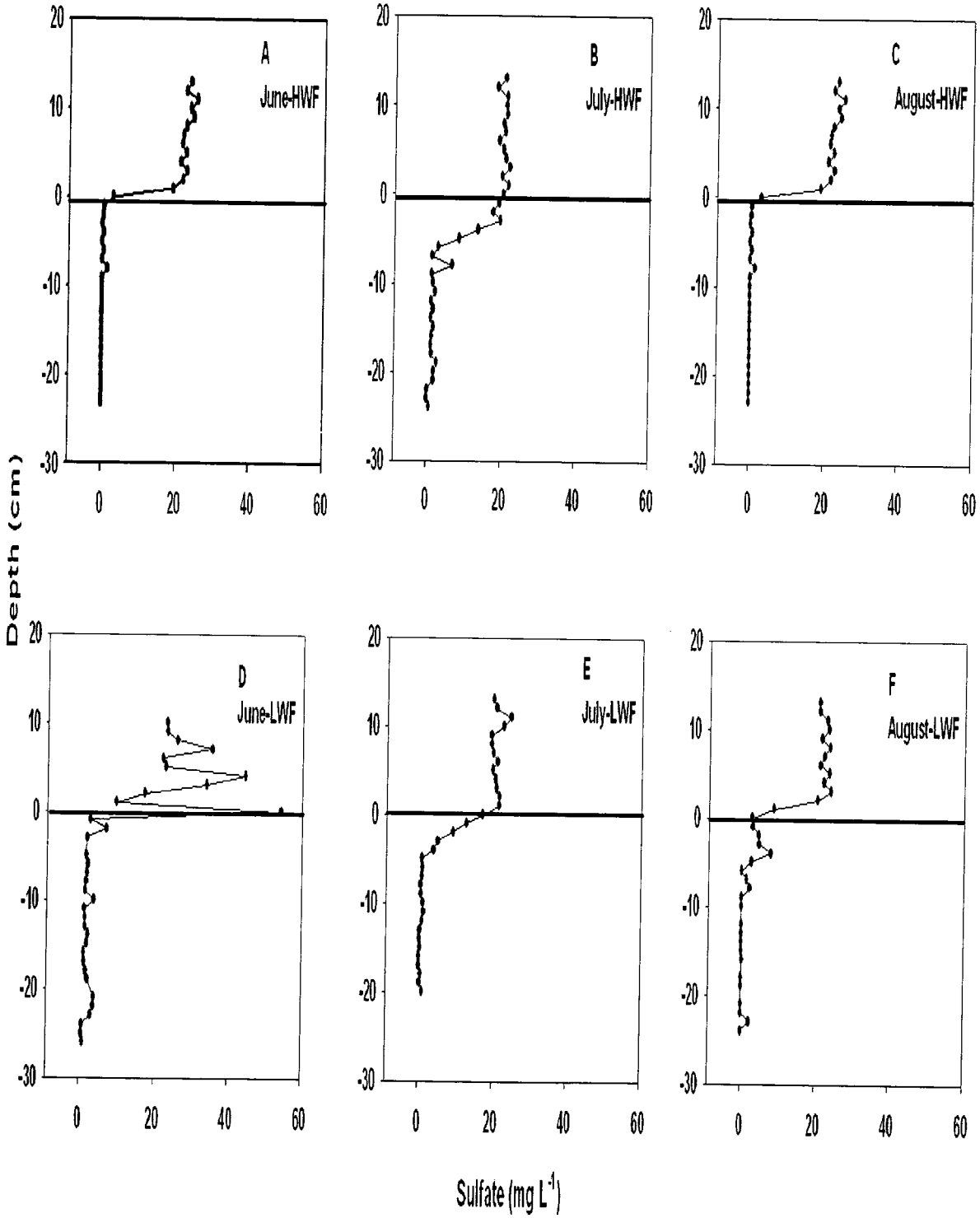


Figure 3-14. Vertical distribution of sulfate concentration in porewater profiles in the HWF and LWF sites. The black solid line shows the position of the sediment-water interface.

### 3.2.5 Sulfide in Porewater

Mean sulfide concentration in the HWF site was 0.30 ± 0.04 mg $L^{-1}$, (n = 72) in porewater and 0.03 ± 0.02 mg $L^{-1}$, (n = 37) in overlying water, whereas in the LWF site it was 0.58 ± 0.09 mg $L^{-1}$, (n = 72) in porewater and 0.03 ± 0.01 mg $L^{-1}$, (n = 40) in overlying water. Sulfide concentration ranged between 0 and 1.25 mg $L^{-1}$ in the HWF porewaters and from 0 to 2.98 mg $L^{-1}$ in the LWF site porewaters. Sulfide concentration in overlying water ranged between 0 and 0.48 mg $L^{-1}$ in the HWF site and from 0 to 0.22 mg $L^{-1}$ in the LWF site. In general, sulfide concentrations were near zero or very low in the overlying water but they increased in the sediment porewaters in all the profiles except for the June HWF and LWF sites where sulfide concentrations were very low in both the water column and the porewaters (Fig.3-15). There was a sharp increase in the concentration of sulfide between 0 and 15 cm in sediment in all the profiles in July and August. In July LWF profile (Fig.3-15.E), a bigger sulfide peak was observed deeper in intervals. Sulfide concentration in sediment porewaters increased over the season.

Sulfide production rates were calculated in both the HWF and LWF sites by summing sulfide inventories in the sediment porewater profiles from 0 (sediment-water interface) to 20 cm, each month, to quantify the rate of *in situ* sulfide production (Table 3-8). In the HWF site, production of sulfide was higher from June to July than from July to August, whereas in the LWF site sulfide production rate was highest from July to August. Overall, the sulfide production rate was higher in the LWF site, which was consistent with higher sulfate reduction rate from July to August in the LWF site.

Sulfide diffusion rates ranged between 0 and 4.7 $\times 10^{-4}$ μmol $cm^{-2}$ $yr^{-1}$ in the HWF site and from $0.2 \times 10^{-4}$ to $1.7 \times 10^{-4}$ μmol $cm^{-2}$ $yr^{-1}$ in the LWF site. Overall, sulfide diffusion was higher in the HWF site except in June when there was no diffusion from sediment to water (Table 3-9). In general the calculated diffusion rates of $S^{-2}$ were much lower than the *in situ* $S^{-2}$ production rates.

Table 3-8. Sulfide production rate in the HWF and LWF sites.

| Zone 1 | $S^{-2}$ production rate (μmol $S^{-2} cm^{-2}$ $day^{-1}$) | $S^{-2}$ production rate (μmol $S^{-2}$ $cm^{-2}$ $day^{-1}$) |
|---|---|---|
| | From June to July | From July to August |
| HWF | 0.005 | 0.001 |
| LWF | 0.009 | 0.011 |

Table 3-9. Sediment-water diffusion flux of sulfide in the HWF and LWF sites. A positive value shows diffusion is from sediment to water.

| Site | Month | Sulfide diffusion ($\mu mol\ cm^{-2}\ yr^{-1}$) | Standard error ($\mu mol\ cm^{-2}\ yr^{-1}$) |
|---|---|---|---|
| HWF | June | 0.0 | $\pm 0.0$ |
| HWF | July | $+4.7\times10^{-4}$ | $\pm 2.0\times10^{-4}$ |
| HWF | August | $+3.3\times10^{-4}$ | $\pm 3.8\times10^{-5}$ |
| LWF | June | $+0.2\times10^{-4}$ | $\pm 0.5\times10^{-5}$ |
| LWF | July | $+1.7\times10^{-4}$ | $\pm 7.3\times10^{-5}$ |
| LWF | August | $+0.5\times10^{-4}$ | $\pm 1.5\times10^{-5}$ |

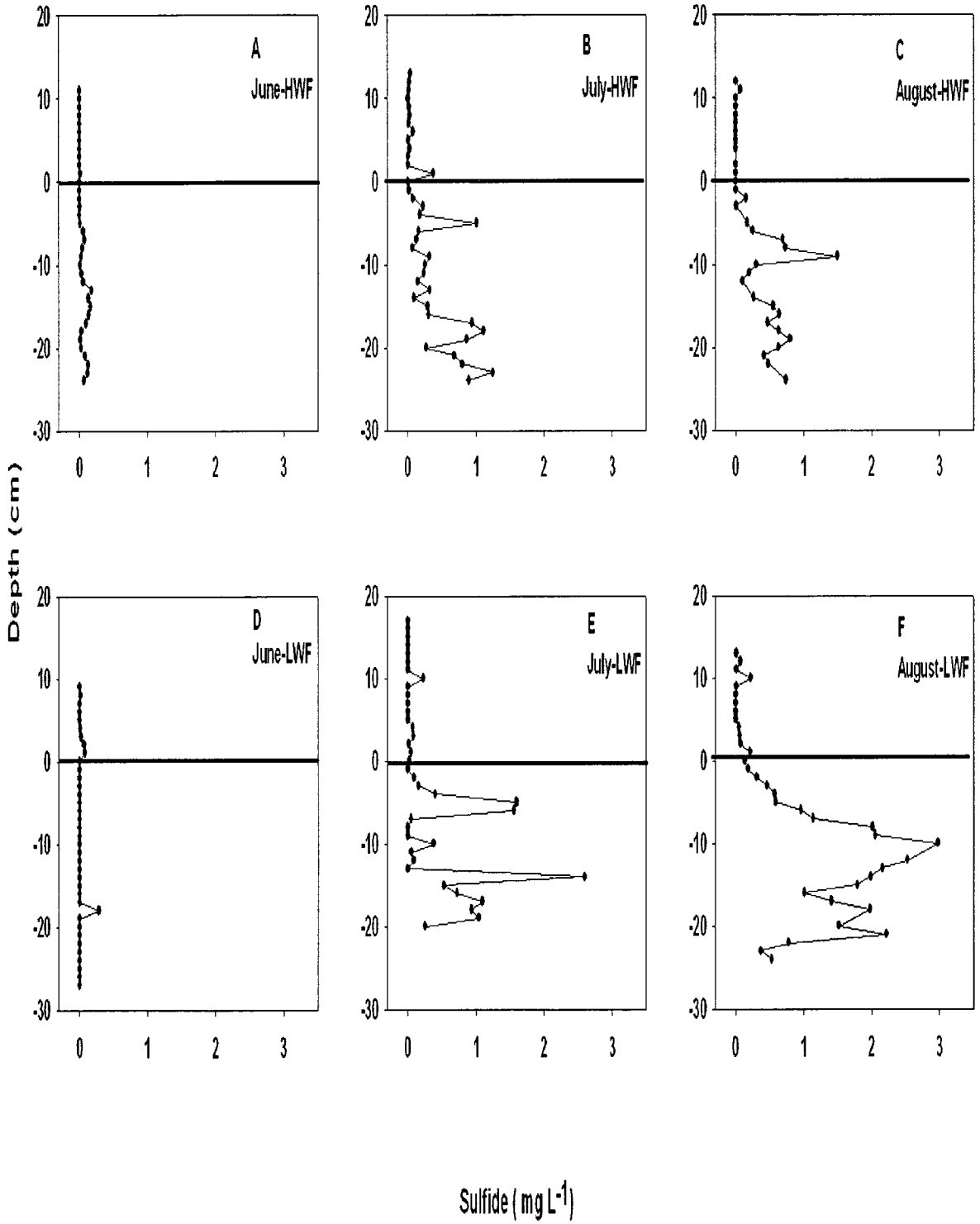


Figure 3-15. Vertical distribution of sulfide concentration in porewater profiles in the HWF and LWF sites. The black solid line shows the position of the sediment-water interface.

### 3.2.6 Ferrous Iron in Porewater

Mean $Fe^{2+}$ concentration was 3.25 ± 0. 34 (SE) mg $L^{-1}$, (n = 74) in porewater and 0.02 ± 0.016 mg $L^{-1}$, (n = 38) in overlying water, whereas in the LWF site it was 3.84 ± 0.29 (SE) mg $L^{-1}$, (n = 72) in porewater and 0.08 ± 0.03 mg $L^{-1}$, (n = 40) in overlying water indicating a net upward diffusive flux of $Fe^{2+}$. $Fe^{2+}$ concentrations ranged between 0 and 8.7 mg $L^{-1}$ in the HWF site and from 0 to 8.17 mg $L^{-1}$ in the LWF site (Fig.3-16). $Fe^{2+}$concentrations were zero or near zero in the water column of all profiles and near the sediment-water interface, there was an increase in $Fe^{2+}$ concentration with depth in all profiles (Fig.3-16).

$Fe^{2+}$ production rates were calculated in both the HWF and LWF sites by summing $Fe^{2+}$ inventories in the sediment porewater profiles from 0 (sediment-water interface) to 20 cm, each month, to quantify the rate of *in situ* $Fe^{2+}$ production (Table 3-10). In the HWF site, there was an increase in the production of $Fe^{2+}$ in late summer compared to early summer, whereas in the LWF site, $Fe^{2+}$ production rate was lower in late summer than in early summer (Table 3-10).

$Fe^{2+}$ diffusion ranged between $2 \times 10^{-4}$ and $5 \times 10^{-4}$ μmol $cm^{-2}$ $yr^{-1}$ in the HWF and from $0.1 \times 10^{-4}$ to $5 \times 10^{-4}$ μmol $cm^{-2}$ $yr^{-1}$ in the LWF site. These flux rates were all from sediments to water (Table 3-11). $Fe^{2+}$ diffusion rates were about one order of magnitude lower than $Fe^{2+}$ production rates (Table 3-11).

Table 3-10. $Fe^{2+}$ production rate in the HWF and LWF sites.

| Zone 1 | $Fe^{2+}$ production rate ($\mu$mol $Fe^{2+}cm^{-2}$ $day^{-1}$) From June to July | $Fe^{2+}$ production rate ($\mu$mol $Fe^{2+}$ $cm^{-2}$ $day^{-1}$) From July to August |
|---|---|---|
| HWF | 0.003 | 0.026 |
| LWF | 0.012 | 0.005 |

Table 3-11. Sediment-water diffusion flux of $Fe^{2+}$ in the HWF and LWF sites. A positive value shows diffusion is from sediment to water.

| Site | Month | $Fe^{2+}$diffusion ($\mu$mol $cm^{-2}$ $yr^{-1}$) | Standard error ($\mu$mol $cm^{-2}$ $yr^{-1}$) |
|---|---|---|---|
| HWF | June | $+5\times10^{-4}$ | $\pm 1.3\times10^{-5}$ |
| HWF | July | $+2\times10^{-4}$ | $\pm 4.3\times10^{-5}$ |
| HWF | August | $+2\times10^{-4}$ | $\pm 4.4\times10^{-5}$ |
| LWF | June | $+1\times10^{-4}$ | $\pm 3\times10^{-5}$ |
| LWF | July | $+0.1\times10^{-4}$ | $\pm 2.1\times10^{-6}$ |
| LWF | August | $+5\times10^{-4}$ | $\pm 8.6\times10^{-5}$ |

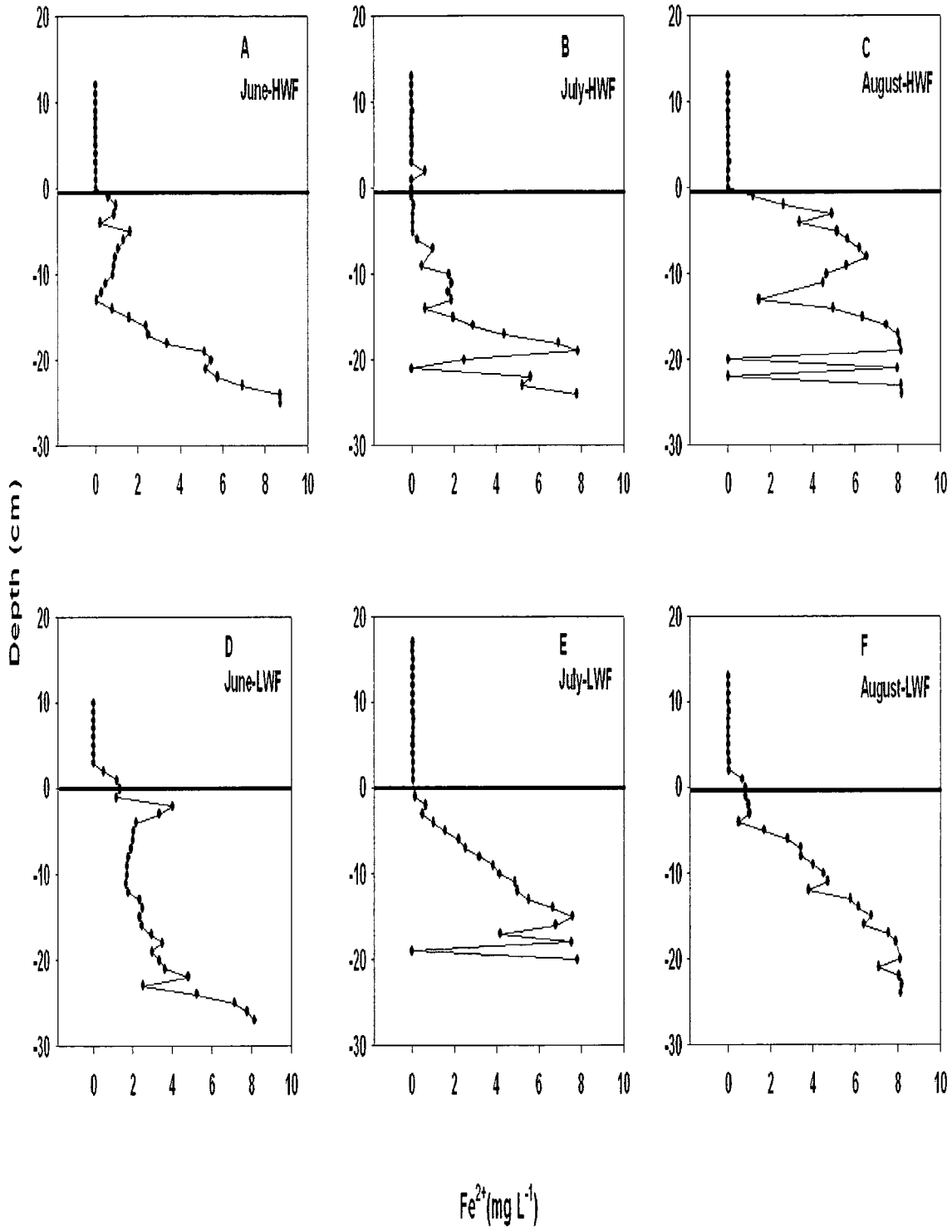


Figure 3-16. Vertical distribution of $Fe^{2+}$ concentration in porewater profiles in the HWF and LWF sites. The black solid line shows the position of the sediment-water interface.

### 3.2.7 Manganese in Porewater

Mean Mn concentration in the HWF site was 2.97 ± 0.67 (SE) mg $L^{-1}$ (n = 25) in porewater and 0.04 ± 0.01 (SE) mg $L^{-1}$ (n = 13) in overlying water, whereas in the LWF site it was 1.24 ± 0.27 (SE) mg $L^{-1}$ (n = 35) in porewater and 0.04 ± 0.02 (SE) mg $L^{-1}$ (n = 21) in overlying water, indicating upward Mn diffusive flux. Manganese concentrations ranged between 0.002 and 11.11 mg $L^{1}$ in the HWF site and from 0.0002 to 7.97 mg $L^{-1}$ in the LWF site. Concentration of Mn was constantly low in the water column but increased near the sediment-water interface (Fig.3-17).

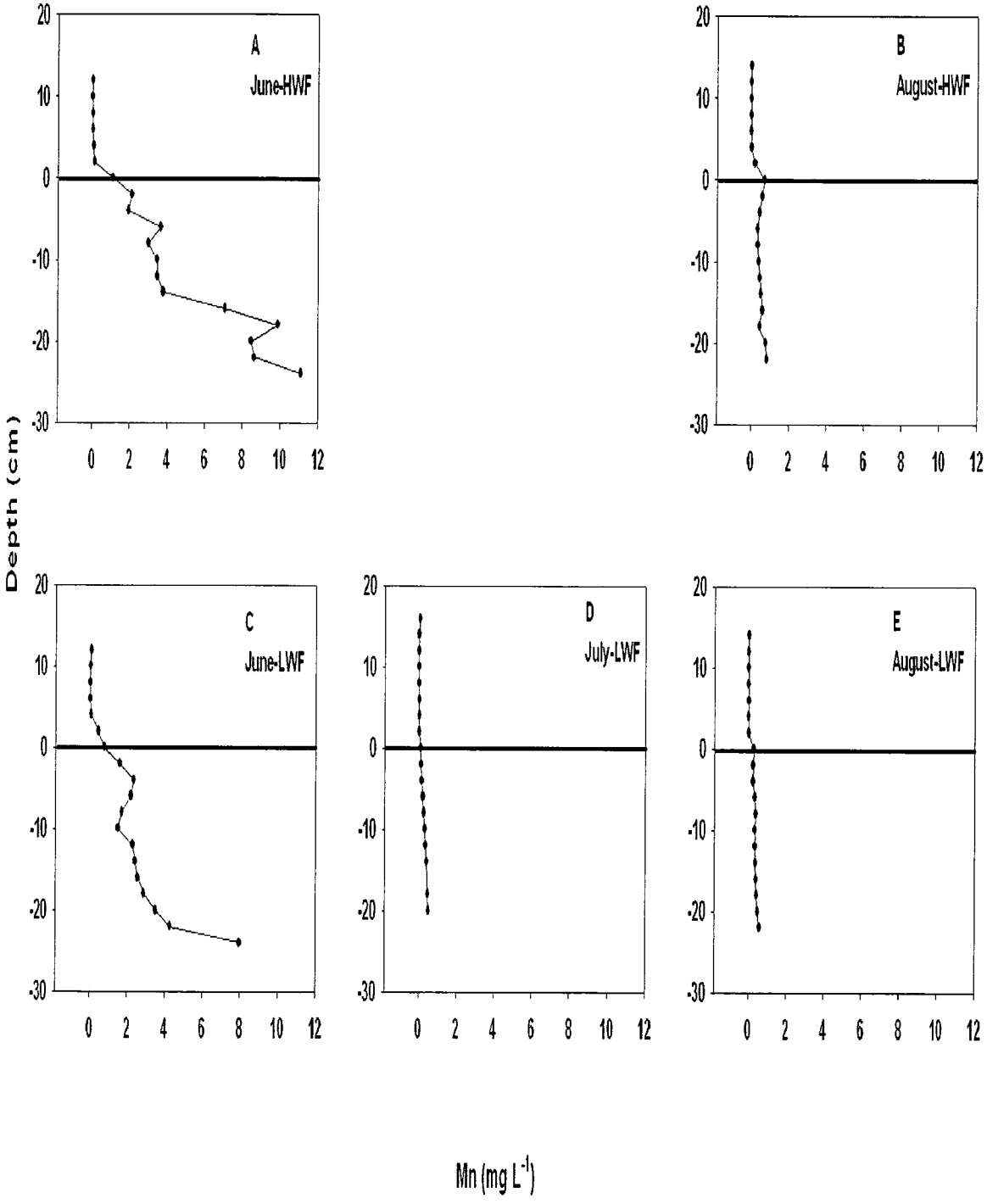


Figure 3-17. Vertical distribution of Mn concentration in porewater profiles in the HWF and LWF sites. The black solid line shows the position of the sediment-water interface.

### 3.2.8 Redox Measurement in Porewater

In the HWF site (Fig.3-18.A), Eh measurements were positive in the water column phase and decreased sharply near the sediment-water interface. In the LWF site (Fig.3-18.B), similar trends were observed. Although in the LWF site in June all the values were positive, there was a decrease in Eh values over the season in both sites.

In general, measured Eh values in the porewater and water column ranged between 173 and -71 mV. Observation of these values could be due to the analytical errors such as exposure of the porewater samples to air during sub-sampling and Eh measurements. However, in general Eh ranged between -87.7 and -259.5mV in Cornwall sediments which is a low-redox condition in the St. Lawrence River (Delongchamp, 2006).

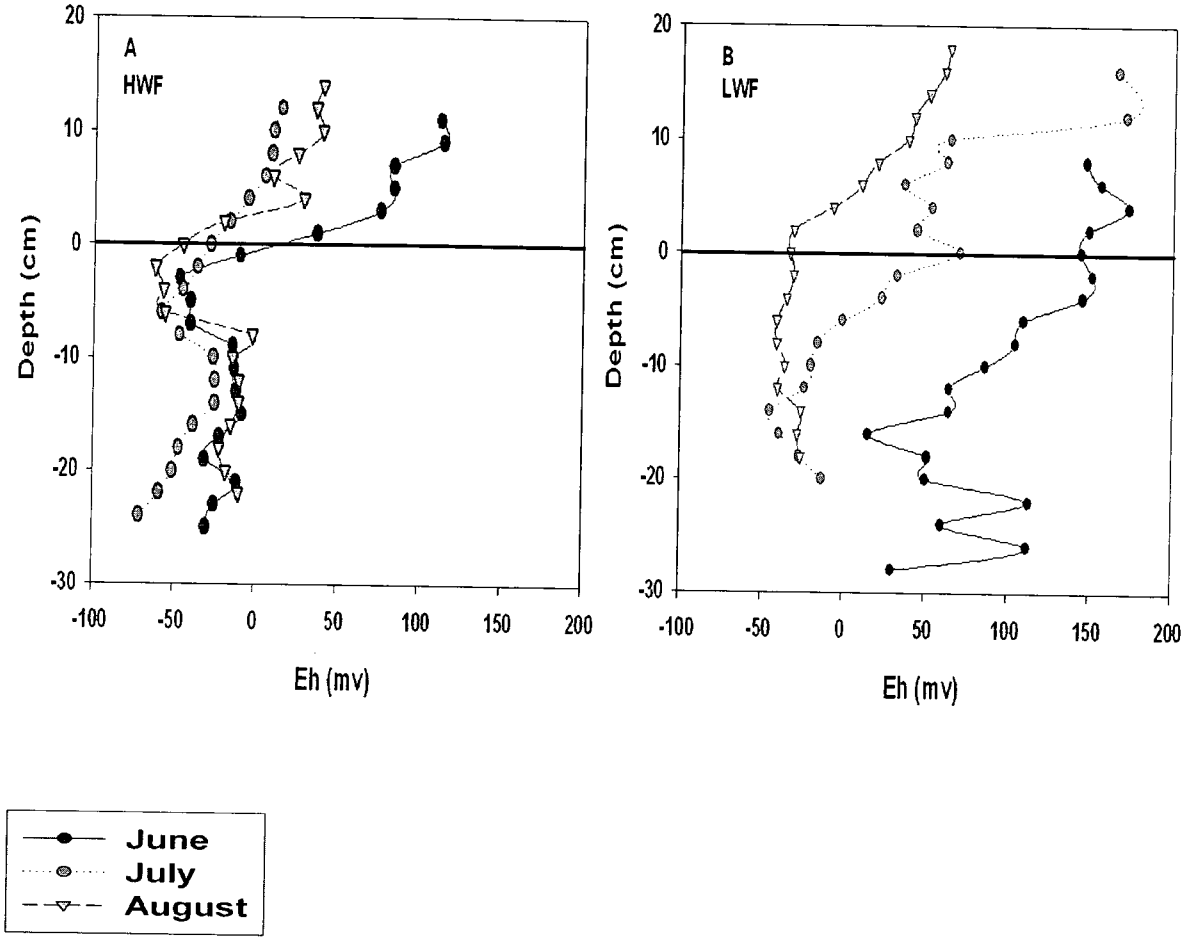


Figure 3-18. Redox (Eh) values with depth in the HWF (A) and LWF (B) sites. The black solid line shows the position of the sediment-water interface.

## 3.3 Benthic Chamber *In situ* Dialysis

Mean concentration of THg in benthic chambers ranged between 1.33 and 45.66 ng $L^{-1}$ in both the HWF and LWF sites. THg concentrations varied considerably and showed no gradual trend in THg concentrations over time for either site. Likewise, MeHg concentrations ranged considerably (between 0.6 and 2.67 ng $L^{-1}$ in the HWF and LWF sites) and showed no gradual trend in concentrations over time for either site (Fig. 3-19). Several redox-dependent variables, such as sulfate, sulfide, $Fe^{2+}$, and $Mn^{2+}$, were also measured in the benthic chambers; however no trends in concentration were observed. No measurable Hg diffusion rates were observed for either THg or MeHg in both the HWF and LWF sites, which was generally consistent with the very low calculated diffusion rates using the peeper method.

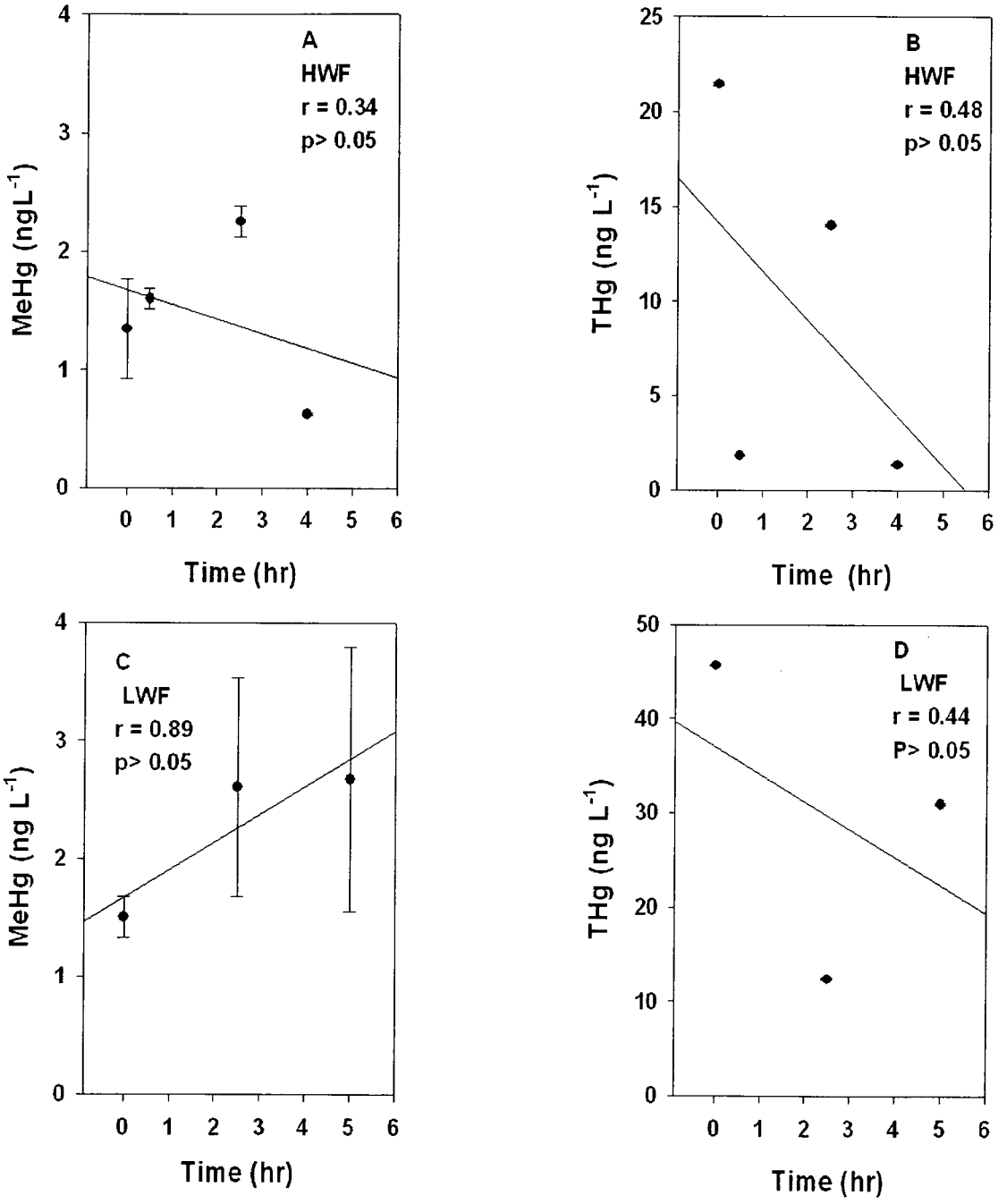


Figure 3-19. Concentration of THg (B, D) and MeHg (A, C) in benthic chambers over time in the HWF and LWF sites.

# 4 DISCUSSION

## 4.1 Mercury in the Solid Phase

### 4.1.1 Total Mercury

THg concentrations in the St. Lawrence River sediments near Cornwall ranged between 748 and 44800 ng $g^{-1}$ dw which were comparable to values previously reported in this stretch of river (326 to 43600 ng $g^{-1}$; Delongchamp, 2006; 284 to 5160 ng $g^{-1}$ (in the first 5 top centimeter of the sediments); Canàrio et al. 2008 and 768 to 17911 ng $g^{-1}$; (in the first 5 top centimeter of the sediments); Razavi, 2008). The total mercury concentrations measured here were much higher than those reported by Goulet et al. (2007) in the St. François Bay wetlands along the St. Lawrence River (24 and 54 ng $g^{-1}$) which suggests the effect of local industries near Cornwall on Hg discharge to the river. The range of Hg concentration reported by Goulet et al. (2007) was within the range of uncontaminated sediments in lakes (~50 ng $g^{-1}$; Hines et al. 2004; ~ 0.2 ng $g^{-1}$; Heit et al. 1981), and in San Francisco Bay (60 ± 10 ng $g^{-1}$; Hornberger et al. 1999).

THg profiles in sediment (Fig.3-1) in the LWF site generally followed the history of industrial release to the river with low mercury concentrations in sediments deposited after 1995, when the major plants (ICI Forest, a chlor alkali plant, Cornwall Chemical, Courtalds, and Domtar, a pulp and paper mill) stopped their operations and between 1970 and 1995, when government regulations limited the liquid discharge of Hg to the river (Delongchamp, 2006; Richman and Dreier, 2001). Much higher Hg concentrations were

found at deeper intervals in the cores, when major plants were in operation and released tonnes of Hg to the river (Richman and Dreier, 2001; Delongchamp, 2006).

In the HWF site THg concentration decreased after 1995 which corresponded to the closure of ICI Forest, Cortalds and Domtar. These decreases in THg concentrations in both sites confirmed the effect of industry closure to this river in the early 1990s. However no decrease of THg concentrations was observed between pre-1970 and 1970-1995. These results might be due to a big peak of THg corresponding to 1974. The resolution time for this sediment core (mixing depth / mass sedimentation rate) was about 6.5 years, which suggests the peak of THg in 1974 might have happened prior to 1970 when fewer controls on mercury emissions to the St. Lawrence River were in place.

The mean THg concentration in surface sediments (0.5-1cm) in both the HWF and LWF sites was 1320 ± 326 ng $g^{-1}$ dw, which was about 5 times higher than mercury concentrations of 246 ± 113 ng $g^{-1}$ dw in the surface sediments (0.5-1cm) of approximately 202 lakes in Ontario, Canada (Mills et al. 2008) indicating the severity of Hg contamination in the Cornwall AOC.

Concentrations of Hg in sediments of Zone 1 exceeded the sediment quality guideline of 170 ng $g^{-1}$, and the probable effect level of 486 ng $g^{-1}$, which are the limits set by Environment Canada for the protection of aquatic life (Richman and Dreier. 2001; Grapentine et al. 2003; Delongchamp, 2006; Razavi, 2008). Consequently, sediments of the St. Lawrence River remain as an area of concern.

### 4.1.2 Methyl Mercury

MeHg concentrations in the St. Lawrence River sediments ranged between 1.9 and 38.4 ng $g^{-1}$dw, which were fairly similar to those reported previously in the St. Lawrence River (0.8 to 134 ng $g^{-1}$; Delongchamp, 2006; 0.93-7.33 ng $g^{-1}$ (in surface sediments 0-5 cm); Canàrio et al. 2008), but higher than those reported in pond sediments from nearby the St. Lawrence River in the St. François Bay (0.21 to 1.72 ng $g^{-1}$; Goulet et al. 2007). These higher MeHg concentrations in the St. Lawrence AOC suggested high Hg methylation rates at this site and may explain the elevated mercury contamination along the Cornwall waterfront in the St. Lawrence River.

MeHg production usually occurs in moderately anaerobic surface sediments (Hintelmann and Wilken, 1995; Korthals and Winfrey, 1987; Bloom et al. 1999; Sunderland et al. 2004). In most of the aquatic environments, only a few millimeters of the top sediments are aerobic and the rest are anaerobic (Ullrich et al. 2001). Higher MeHg concentrations in the subsurface of both the HWF and LWF cores (Fig.3-2) may indicate zones of active Hg methylation in sediment. The highest MeHg concentrations were observed in both sites at deeper sediment intervals (34 and 42cm) (Fig.3-2), suggesting that MeHg production occurred not only in the subsurface zone, but also in deeper sediment intervals. Production of MeHg in deep sediments was also shown by He et al. (2007), who found a peak in MeHg at a depth of 14 cm in the sediments (2.03 ng $g^{-1}$) of the St. George Lake in Toronto, and Hines et al. (2004) who found peaks in MeHg at a depth of 19cm (~ 2.2 ng $L^{-1}$) and 31cm (~ 1.4 ng $L^{-1}$) in the sediment porewaters of Spring Lake in northern Minnesota, probably from Hg methylation by sulfate reducing bacteria (Hines et al. 2004). Jonson, (2004) showed activity of SRBs up to a depth of 23

cm in sediments of Spring Lake in northern Minnesota. Holems and Lean, (2006) also found a peak of MeHg at depth 12 cm in Stillwoods wetland's core which is located within the Marlbrough Forest Conservation Area.

Marvin-Dipasquale and Oremland, (1998) showed that demethylation rates decreased with increasing sediment depth, which may also explain the presence of MeHg in deeper sediment intervals. However, the presence of MeHg in deep sediments well below the disappearance of sulfate (Fig. 3-14) suggests that Hg methylation in deeper intervals is not by sulfate reducing bacteria (SRBs) or iron reducing bacteria. Other potential Hg methylators include methanogens (Ormeland et al. 1991; Wood et al. 1968; Pak and Bartha. 1998), may be resoponsible for this methylation in deep sediments. Methanogens methylate Hg using methylcobalamine as a methyl donor, producing methane gas as a metabolic by-product of anaerobic respiration (Wood et al. 1968).

Thermodynamic calculations showed that organic matter decomposition yields lower levels of energy using the following potential electron acceptors $FeOOH > SO_4^{2-} > CO_2$ (Claypool and Kaplan, 1974). Capone and Kiene, (1988) found that sulfate concentration may decrease with depth in sediments due to the consumption of sulfate by sulfate reducing bacteria, at which point methonogenesis becomes highly significant in carbon mineralization. In other words, methanogenesis occurs when there is not enough substrate for the activity of iron reducing bacteria and sulfate reducing bacteria; however, there is still enough labile organic matter available to support the methanogenesis in deep sediment intervals.

Another possibility for the large peaks of MeHg in deeper intervals is abiotic methylation. Chemical Hg methylation is possible in the presence of suitable methyl

donors. Hg (II) reduces to $Hg^0$ by reducing agents in the aquatic environment. $Hg^0$ (aq) may react with methyl iodide (a methyl donor) and may produce up to 1.1% MeHg, which is a relatively high yield for environmental reactions (Celo, 2004, Celo and secott, 2006), and is comparable to the MeHg/THg distribution observed in sediments here.

Large peaks of MeHg in both the HWF and LWF sites (Fig. 3-2) occurred where THg was elevated in deeper sediment horizons (Fig. 3-1). There is a strong correlation between THg and MeHg in sediment in both the HWF and LWF sites (Fig. 3-4). This correlation was also observed in a study by Razavi, (2008) in the same area of the St. Lawrence River, suggesting that *in situ* MeHg production was positively related to the THg concentration in the sediments. Han et al. (2008) found that the availability of Hg (II) may control Hg methylation rate. In other words, Hg methylation might be Hg limited.

The observed ratio of MeHg to THg of < 1% was comparable to other field studies, in surface sediments and in deeper intervals in the St. Lawrence River (~0.5 - 6%; Delongchamp, 2006; ~0.06 - 1.4%; Canàrio et al. 2008), in George lake and Philips lake in Toronto (~0.8 -1.8% ; He et al. 2007), and in Cooper's Marsh located on the Lake St. François along the St. Lawrence River (~0.1 -5.7%; Holmes and Lean, 2006). Distribution of MeHg to THg in sediments is typically ~ 1 to 1.5% (Olson and Copper, 1974; Bubb et al. 1993; Gobeil and Cossa, 1993; Cagnon et al. 1996).

In general, MeHg production occurs in a relatively narrow subsurface zone within the sediments (Benoit et al. 1998; Bloom et al. 1999). Sunderland et al. (2004) found the percent MeHg/THg is correlated with the Hg methylation rate in uncontaminated

sediments and two factors control this rate, (a) the availability of Hg (II) and (b) SRBs activity ( Han et al. 2008).

### 4.1.3 Organic Content

Organic content in the HWF sediment core was significantly higher than the LWF core, which corresponds to the presence of wood fibers deposited by the pulp and paper mill near this site. There were correlations between MeHg and organic matter as well as THg and organic matter in both the HWF and LWF sites, which suggest organic matter was a controlling factor for Hg distribution in both sites. (However, the correlation between MeHg and organic matter in the HWF site was not significant since the p-value was exactly at the border line, $p = 0.05$).

Hg methylation rates are usually much higher in high organic sediments (Jernelov, 1969; Jackson, 1986; Ullrich et al. 2001; Siciliano et al. 2004) presumably because organic matter stimulates the microbial methylation activities by serving as a nutrient substrate (Jackson, 1986; Falter, 1999; Siciliano et al, 2005).

### 4.1.4 $^{210}$Pb Inventories, Sedimentation Rates and Mercury Accumulation Rates

$^{210}$Pb activity profiles of the sediment cores were used to determine the chronological age of the sediment as well as the sedimentation rate. In the present study, sedimentation rates in Zone 1 (0.45 and 0.75 g cm$^{-2}$ yr$^{-1}$ in the LWF cores and 1.04 g cm$^{-2}$ yr$^{-1}$ in the HWF site) were similar to other values reported in the St. Lawrence River (0.11

and 1.78 g $cm^{-2}$ $yr^{-1}$; Carignan and Lorrain, 2000 ; 0.18 and 0.58 g $cm^{-2}$ $yr^{-1}$; Delongchamp, 2006).

One of the cores from the HWF site was not dated because there was no decrease in the unsupported $^{210}Pb$ activities with core depth. According to Appleby, (2001) dating models may occasionally be invalid due to mixing of the surface sediments by physical or biological processes or variations in the supply of $^{210}Pb$. In this study, mixing of the surficial sediments may have been caused by methane gas production from decomposing sediments, or it might be due to waterfront development construction (1997-1999), which may have disturbed the sediments at this site.

Mercury accumulation rates varied between 252 and 6161 ng $cm^{-2}$ $yr^{-1}$ in the LWF core, corresponding to 1998 and 1948, respectively (Figure 3-9) and in the HWF site, it ranged between 584 to 93000 ng cm-2 yr-1 corresponding to 2003 and 1974 repectively (Figure 3-9). Mercury accumulation rates in the present study were comparable to those reported by Delongchamp, (2006) (181 to 9340 ng $cm^{-2}$ $yr^{-1}$) in the St. Lawrence River. Statistical analysis showed that there was no decrease in THg accumulation rates in sediments from pre-1970 and 1970-1995 horizons (based on $^{210}Pb$ dating) in both sites. In the LWF site this result was partly attributed to higher sedimentation rates in 1970-1995, because THg concentrations decreased during this period and in HWF site it might be as a result of higher sedimentation rates as well as a big peak of THg concentration at depth 42cm which is corresponding to 1974. The resolution time for this sediment core (mixing depth / mass sedimentation rate) was about 6.5 years, which suggests the peak of THg in 1974 might have happened prior to 1970 when fewer controls on mercury emissions to the St. Lawrence River were in place.

However THg accumulation rates decreased after 1995 in both sites coinciding with the period of industrial closures in the Cornwall area, including ICI Forest products in 1995, Courtalds in 1992, Cornwall Chemical in 1995 , and Domtar pulp and paper mill in 2006.

## 4.2 Mercury and Complimentary Redox-dependent Variables in Porewater and Water Column

### 4.2.1 Total Mercury in Porewater

Total mercury concentrations in porewaters ranged between 3.1 and 76.9 ng $L^{-1}$ in Zone1 of the St. Lawrence River comparable to those reported by Delongchamp, (2006) (0.1 to 950 ng $L^{-1}$), and Razavi, (2008) (4.13 to 944 ng $L^{-1}$). These separate studies indicated a large heterogeneity of Hg concentrations in porewaters from the river bed at this site.

THg concentrations have been observed higher than those reported in other field studies; 2 to 8 ng $L^{-1}$ in the Patuxent River estuary , (Benoit et al. 1998) ; 2 to 10 ng $L^{-1}$ in the San Francisco Bay- Delta ,(Choe et al. 2004 ); 5 to 20 ng $L^{-1}$ in Lavaca Bay ; (Bloom et al. 1999); and from 2 to 15 ng $L^{-1}$ in the Everglades; (Gilmour et al. 1998) which shows severity of Hg contamination in the Cornwall AOC.

In some profiles THg concentrations decreased with depth which can be the consequence of insoluble mercury sulfide precipitation or iron sulfide co-precipitation (Gobeil and Cossa, 1999). Sulfide minerals have a high affinity for Hg and consequently may contribute to less availability of dissolved Hg by its precipitation (Stein et al. 1996).

Benoit et al. (1999) also indicated the importance of solid phase precipitation or sorption as a major control of dissolved Hg concentration. THg and MeHg may bind to dissolved organic matter with strong thiolic binding (Zhang et al. 2004). Rydberg et al. (2008) showed that Hg is mainly bound to reduced sulfur groups attached to refractory organic matter in sediments in Lake Nylandssjön's sediments in northern Sweden. Between 30 and 60% of the sulfur in sediments of the Lake Nylandssjön is in the form of thiols, which are known as the most important form of sulfur for binding Hg to organic matter (Shchukarev et al. 2008).

Precipitation of iron sulfides also limits the availability of dissolved Hg and consequently inhibits the MeHg production rate where Fe is abundant, which could be caused by sulfide removal since there is no production of $S^0$ and polysulfide that forms Hg-polysulfide complexes (Han et al. 2008).

### 4.2.2 Methyl Mercury in Porewater

MeHg concentrations were relatively homogeneous between porewater and overlying water, and generally showed no clear trend, indicating (a) that there is very little net diffusion of MeHg and (b) that redox-dependent processes such as sulfate reduction and Fe reduction have little effect on the distribution of dissolved MeHg on these sediment porewaters.

The percentage of MeHg to THg in porewater (4 to~ 100%) (the measured MeHg/ THg actually exceeded 100% in 5 cases in July and August, (n = 99)), indicating that the majority of Hg in the porewater were in methylated form (MeHg), especially in July and August. These results were slightly higher than those reported elsewhere (4-76%)

(Covelli et al. 1999; He et al. 2007), but within the same range as those reported in the St. Lawrence River, (2 to 97%; Delongchamp, 2006). MeHg/THg ratios above 100% (5 cases in 99 samples) can be due to uncertainty of the analysis. Another possibility for these observations might be the presence of sediment particles in porewater samples, which could increase the THg concentration.

### 4.2.3 Hg Deposition and Diffusion

There was little evidence for diffusion of MeHg and THg from sediments to water. Large variations for MeHg and THg flux rates have been observed in different studies. THg diffusion rates in present study (0 to 2.0 $\times 10^{-4}$ ng $cm^{-2}$ $yr^{-1}$) were lower than those reported in Saguenay Fjord in Canada (3.8 to 36 ng $cm^{-2}$ $yr^{-1}$; Gagnon et al. 1997), and in heavily contaminated sediments of the Gulf of Trieste in northern Adriatic Sea (0.99 to 236 ng $cm^{-2}$ $yr^{-1}$; Covelli et al. 1999). MeHg flux from sediment to water in present study (0 to 6.0$\times$ $10^{-5}$ ng $cm^{-2}$ $yr^{-1}$) were also lower than those reported in Spring Lake in northern Minnesota (6.0$\times$ $10^{-4}$ ng $cm^{-2}$ $yr^{-1}$; Hines et al. 2004); and in St. François Bay (0.02 to 0.2 ng $cm^{-2}$ $yr^{-1}$; Goulet et al. 2007); on the continental shelf of southern New England (0.05 and 0.09 ng $cm^{-2}$ $yr^{-1}$; Hammerschmidt and Fitzgerald, 2006); and in Barn Island salt marsh (1.14 and 16.1 ng $cm^{-2}$ $yr^{-1}$; Langer et al. 2001).

The distribution coefficient of MeHg ($K_D^{MeHg}$) (0.2 to 5.95 L $g^{-1}$) was higher than those reported in the St. François Bay (0.004 to 2.6 L $g^{-1}$; Goulet et al. 2007). In addition, the distribution coefficient of THg ($K_D^{THg}$) (39 to 750 L $g^{-1}$) were considerably higher than those reported by Goulet et al. 2007 (6 to 34 L $g^{-1}$) in the St. François Bay. High distribution coefficients in both MeHg and THg revealed that a higher proportion of Hg

was bound to particles in the St. Lawrence River which was in line with percent dissolved to particulate THg (0.0005 and 0.04%) and percent dissolved to particulate MeHg (0.02 and 1.3%); thus, a very low proportion of these metal forms (< 1.5%) was available for diffusion from sediments to water.

In general, sediments in Zone 1 had low redox potential and consequently the reduction of Fe and Mn oxides and their dissolution may remobilize Hg to the porewater (Froelich et al. 1977; Murray, 1975; Gobeil et al. 1999).

The diffusion rates did not include the influence of ebullition, bioturbation, bioirrigation, and resuspension of the sediments. Bioturbation can increase the flux of organic and inorganic complexes up to 2 to 10 times at the sediment-water interface (Rutgers van der Loeff et al. 1984). Ebullition disturbs the sediments and contributes to the suspended load in the water column (Yuan et al. 2007). Sediment resuspension enhances the flux of trace metals including Hg, iron, manganese, zinc and copper at the sediment-water interface (Peterson et al. 1997).

The mean THg concentration (14.26 ± 0.8 ng $L^{-1}$) and mean MeHg concentration (4.59 ± 0.65 ng $L^{-1}$) in the overlying water in the present study were higher than mean THg and MeHg concentrations measured previously in surface water (up to 1 m below surface) of 1.15 ± 0.09 ng $L^{-1}$, (n = 12) and 0.07 ± 0.04 ng $L^{-1}$, (n= 12) respectively. Also, Hg concentrations just above the sediments were about 10 times higher than the samples above 50 cm of the bottom sediment which suggests Hg diffusion from overlying water (immediately above the sediments) to the water column. However no such diffusion has been observed. This might be due to the presence of a nepheloid layer (a layer of water immidiately above the sediment surface). The presence of a nepheloid

layer has been reported in the oceans (Churchill et al. 1988) and in all of the Great Lakes (Bell et al. 1983). Nepheloid layers develop each summer (during the stratification season in lakes) and disappear in early fall (Urban et al. 2004; Hickes et al. 2004) and are characterized by high suspended solid particles (Urban et al. 2004; Hicks et al. 2004; Schneider et al. 2002) and low water transparency (Chambers and Eadie, 1981). These layers may maintain the Hg concentration by particle resuspension or stratification, so diffusion is not the only possible scenario between a nepheloid layer and water column. Some factors such as temperature, $O_2$ and conductivity indicate if stratification is a factor in maintaining Hg concentration gradients in the water column near the bottom sediments. Another possibility for higher Hg concentration just above the sediments could be the discharge of Hg in the vicinity of the sampling site.

Mortimer, (1971) showed that within the nepheloid layer, upwelling events are common during the stratification season in Lake Michigan which may explain the presence of the same concentration of dissolved THg and MeHg in porewater and overlying water and consequently no or very low diffusion rates.

THg diffusion rates (ranged between 0 and $2\times10^{-4}$ ng $cm^{-2}$ $yr^{-1}$) were determined to be very low compared to the recent Hg sedimentation rate (0.45 and 0.75 g $cm^{-2}$ $yr^{-1}$ in the LWF site and 1.04 g $cm^{-2}$ $yr^{-1}$ in the HWF site). Observations of no or very little diffusion of THg and MeHg from sediment to water support the hypothesis that sediments in the St. Lawrence River were a major sink for Hg.

### 4.2.4 Redox-dependent Variables in Porewater

Sulfate profiles (Fig 3-14) showed constant concentrations in the water column with sharply decreasing concentrations in porewater. These observations indicate that sulfate was reduced below the sediment-water interface by sulfate reducing bacteria (SRBs) which are believed to be the primary methylators of Hg in anoxic sediments (Compeau and Bartha, 1985; Celo et al. 2006). Increases in sulfide concentration below the sediment-water interface (Figure 3-15) were also consistent with this scenario.

The mean sulfate concentration (4.1 ± 0.6 mg $L^{-1}$) in the porewaters was similar to those reported in the St. François Bay 0.1 and 5.67 mg $L^{-1}$; (Goulet et al. 2007; 6.2) and 7.7 mg $L^{-1}$; (Holmes, 2005). Likewise, mean sulfide concentration (0.44 ± 0.05 mg $L^{-1}$) in porewaters was higher than those reported elsewhere in the St. Lawrence River 0 and 0.05 mg $L^{-1}$; (Delongchamp, 2006); and in the St. François Bay 0 to 0.09 mg $L^{-1}$ and 0 to 0.14 mg $L^{-1}$; (Goulet et al. 2007), which may suggest higher sulfate reduction or resuspension of sediments by gas evolution in this site.

Interestingly, sulfate reduction rates ranged from 0.02 to 0.1 µmol $cm^{-2}$ $yr^{-1}$, but sulfide production rates (0.001and 0.01 µmol $cm^{-2}$ $yr^{-1}$) were about one order of magnitude lower. These observations suggest that sulfide might be co-precipitated with other metals, such as $Fe^{2+}$. Co-precipitation of sulfide and $Fe^{2+}$has been observed in many studies (Gobeil and Cossa, 1999; Drobner et al. 1990; Han et al. 2008). The most common sulfide minerals are Fe sulfides such as $FeS_2$ (pyrite) or FeS (Bower et al. 2008). In general, production of pyrite in sediments is limited by the supply of organic matter, availability of dissolved sulfate and iron mineral (Bower et al. 2008). Pyrite is the major metal sulfide in nature which is capable of adsorbing toxic elements such as Hg (Doyle et

al. 2004; Ozvedi and Erdem, 2006) and consequently affecting subsurface transport of Hg (II) and its sorption and immobilization in sediments (Brown et al. 1979; Stein et al. 1996; Bower et al. 2008). Saturation index calculations indicated that the sulfides formed from the activity of SRBs were sequestered as metal sulfide phases such as FeS (0.46 to 3.13) and mackanwite (0.40 to 3.87) as well as cinnabar (3.08 to 5.76). This evidence was in line with the difference between the rate of aqueous sulfate reduction and sulfide production and also observations of zero or very low net diffusion of Hg from sediments to water, since according to Benoit et al. (1999), total dissolved Hg concentrations are mainly controlled by solid phase precipitation. In other words, precipitations of Hg and sulfide minerals reduce the availability of Hg in dissolved form.

Production of $Fe^{2+}$ in the anoxic sediments indicates the activity of iron reducing bacteria which are also thought to be responsible for Hg methylation (Chapelle and Lovley, 1992; Lonergan et al. 1996). The mean $Fe^{2+}$ concentration in the present study was $0.05 \pm 0.02$ mg $L^{-1}$, (n=78) in the overlying water which was one order of magnitude higher than those reported in surface water in the St. Lawrence River ($0.004 \pm 0.002$ mg $L^{-1,}$ (n= 39); Quémerais et al. 1998). In general, $Fe^{2+}$ production rates were higher than $Fe^{2+}$ diffusion rates from sediments to water, though $Fe^{2+}$ quickly transforms to $Fe^{3+}$ in presence of $O_2$.

The mean Mn concentration was $1.96 \pm 0.34$ mg $L^{-1}$, (n = 60) in porewater, (0.12 to 11.11 mg $L^{-1}$) similar to those reported in the St. François Bay (0 and 7.5 mg $L^{-1}$; Goulet et al. 2007); in the Gulf of Finland (1.1 and 3.3 mg $L^{-1}$; Pakhornova et al. 2007); in Kalix River in the Gulf of Bothnia, northern Sweden ( 5.9 and 20.2 mg $L^{-1}$; and 19.8 and 30.7

mg $L^{-1}$; Widerlund and Ingri, 1996); and in the Laurentian Trough ( 0.14 and 13.7 mg $L^{-1}$; Gobeil and Cossa, 1993).

There were no correlations between MeHg and Mn concentration suggesting Mn oxy-hydroxides are not a controlling factor for Hg distributions in these sediments. It is well known that Fe and/or Mn oxi-hydroxides are scavengers of trace metals in the aquatic environment (Lockwood and Chen, 1973; Loring, 1975). Reduction of Fe and Mn oxides and their dissolution as a consequence of the microbial degradation of organic matter, may remobilize Hg to the porewater (Froelich et al. 1977). In the present study, due to low-redox conditions, these oxides might be absent (Froelich et al. 1979). In general, redox-dependent processes such as sulfate reduction and Fe reduction as well as Mn oxyhydroxides appears to have little effect on the distribution of dissolved MeHg and THg on the sediment porewaters.

# 5 CONCLUSIONS

## 5.1 General Conclusion

Sediments are recognized as a sink for mercury in the aquatic ecosystem but their role as a source of mercury continues to be debated. The potential of Hg diffusion from sediment to water was investigated here for highly contaminated sediments in the St. Lawrence River to determine whether they are a potential source to aquatic biota. If indeed the sediments act as a source of Hg to water and consequently contribute to the contamination in the aquatic food web, it is critical to develop remedial strategies.

Zone 1 of the St. Lawrence River is not only highly contaminated with mercury but also has other complicating factors such as a large physical heterogeneity of sediments , high methane gas production (Biberhofer and Rukavina, 2002) and the presence of wood fibers which are thought to be deposited from the nearby pulp and paper mill. Elevated gas evolution in this zone is believed to be the result of microbial degradation of these wood fibers (Biberhofer and Rukavina, 2002). This zone supports the most Hg contaminated fish and invertebrates within the AOC, despite having lower Hg concentrations in sediment than Zone 2 (Yanch, 2007; Fowlie et al. 2008). These results suggest Hg availability might be higher in Zone 1, (Delongchamp, 2006; Yanch, 2007) perhaps due to higher Hg methylation rates as a result of high organic matter (wood fibers) in this zone or disturbance of sediments by methane gas release (Golder Associates, 2004; Biberhofer and Rukavina, 2002). These observations motivated this study on Hg distributions in sediments and its diffusion between sediment and water to

identify whether sediments in Zone 1 of the St. Lawrence River act as a source or sink for Hg.

Despite 50% higher MeHg concentrations in sediments of the HWF site than the LWF site, statistical analysis showed no significant difference in MeHg concentrations in sediments between the two sites; whereas, higher concentrations of THg were observed in the HWF site than the LWF site. Strong correlation between THg and MeHg in sediments which also have been observed in a study by Razavi, (2008) in the same area of the St. Lawrence River, suggests that *in situ* MeHg production was positively related to the THg concentration in the sediments. In other words, Hg methylation might be Hg limited.

There were correlations between MeHg and organic matter as well as THg and organic matter in both the HWF and LWF sites, which suggest organic matter was a controlling factor for Hg distribution in both sites.

There was no relationship between MeHg and Mn porewater profiles which suggests that Mn oxy-hydroxides are not a controlling factor in the distribution and partitioning of Hg in these sediments. These findings support the claim that dated sediment cores accurately track the history of Hg accumulation in these sediments, which has also been observed in other recent studies (Rydberg et al. 2008; Engstrom et al. 2007; Lindberg et al. 2007).

Dated sediment profiles revealed that THg concentration decreased significantly after 1970, when federal regulations and plant modifications limited the amount of Hg discharge by the chlor alkali plant, the pulp and paper mill, and Courtalds and again after 1995, when the major Hg releasing industries in the area closed their operations. Although contaminated sediments are being buried by a layer of cleaner sediments, THg

concentrations in surface sediments are still above the SQG of 170 ng $g^{-1}$ and the PEL of 486 ng $g^{-1}$ set by Environment Canada for the protection of aquatic biota.

A 50 % increase in MeHg concentration in porewater profiles was observed from June to July in the HWF site. However, this variation was not statistically significant. Increased temperature attributed to higher microbial activities and may control the Hg methylation and demethylation rates in the aquatic environment as long as there is available Hg (II). However, with increased sulfide formation as a by-product of SRBs activity, Hg (II) becomes less available to bacteria; hence, MeHg rates decrease (Ullrich et al. 2001).

MeHg and THg concentrations were relatively homogenous in both the porewater and overlying water, and generally showed no clear gradient, indicating that there was very little net diffusion of MeHg and THg in sediments. The diffusion coefficients of THg and MeHg and observation of less than 0.16 % of dissolved to particulate THg and dissolved to particulate MeHg showed that just a minor fraction of THg and MeHg were in dissolved form and the majority of THg and MeHg were precipitated in sediments, which indicate very little net diffusion of THg and MeHg from sediments to water. These observations support the hypothesis that sediments in the St. Lawrence River were a major sink for Hg.

Sulfate reduction rates were about one order of magnitude higher than sulfide production rates. These observations suggest that sulfide might be co-precipitated with other metals, such as $Fe^{2+}$, and $Mn^{2+}$, and $Hg^{2+}$. Saturation index calculations indicated that the sulfide formed from the activity of SRBs were sequestered as metal sulfide phase such as FeS (0.46 to 3.13) and mackanwite (0.40 to 3.87) as well as cinnabar (3.08 to

5.76) which may explain the observation of higher sulfate reduction than sulfide production as well as no or very little diffusion of Hg from sediments.

In general, porewater profiles of THg, MeHg, sulfate, sulfide and $Fe^{2+}$ in summer 2007 revealed that areas of redox-dependent processes in sediment such as sulfate reduction and Fe reduction as well as Mn oxyhydroxides appear to have little effect on the distribution of dissolved MeHg and THg on the sediment porewaters.

Statistical analyses in porewater profiles revealed that there was no significant difference in Hg distribution between the HWF and LWF sites in Cornwall AOC.

## 5.2 Future Recommendations

Further improvements are still needed in Zone 1 of the St. Lawrence River, prior to delisting this area as an area of concern. According to Razavi, (2008) variability in gas ebullition rate was high in Zone 1 due to the heterogeneity of the sediments, grain size, the amount of wood fibers and current direction. Therefore, several measurements of gas production rates in the HWF and LWF sites in Zone 1 are highly recommended to ensure higher gas production in the HWF site due to decomposition of higher amount of wood fibers. The effect of seasonal changes on Hg concentration and its bioavailability in this zone also needs more attention.

Measuring sulfide concentration and acid volatile sulfides (AVS) in the sediments would be beneficial and may be of great value for determining the stability of Hg in sediment and hence the overall fate of Hg within the river system. Measurements of $O_2$, temperature and conductivity at the sediment-water interface may provide considerable insight to ensure the existence of a dense layer of water above the sediment (nepheloid layer). Temperature, $O_2$ and conductivity would tell us if stratification is a factor in

maintaining a mercury concentration gradient in the water column near the bottom sediments. The higher mercury concentration in the water near the sediments may be maintained by stratification, so diffusion is not the only possible scenario.

For the future redox measurements, it is highly recommended to use Advanced Micro Oxidation-Reduction system as an alternative method in order to measure redox values especially in the peeper. The system includes a micro electrode that fits directly inside peeper's cells and it has a rapid response. As a result the exposure time of the sample to the oxygen is considerably reduced. Moreover, this instrument works with small volume of sample (10 μL, less than volume of a single drop of liquid).

## 5.3 Significance of Findings

Most of the mercury in the St. Lawrence River sediment near Cornwall is associated with particulate material, and is not diffusing to water to any significant extent. We see the clear horizon of Hg in the sediment profile which corresponds to when the highest Hg releases were occurring. Many studies have shown that Hg mainly binds to organic matter, a tiny fraction is recycled with Fe and/or Mn oxides and some is adsorbed or co-precipitate with acid volatile sulfides (AVS) (Morse and Luther, 1999; Drobner et al. 1990). It is likely that in the present study most of the mercury in the sediment cores was also associated with the organic material in the sediments and/or as sulfides, which was shown in many other studies as well (Zhang et al. 2004; Rydberg et al. 2008; Stein et al. 1996).

There is a controversy whether to remove the sediments or leave them in place. I would argue for the latter. If they were transferred to a landfill site, the sulfides would be oxidized and removed with runoff as sulfate. The mercury which is tightly bound as

mercury sulfide would then be available for methylation and transport, probably associated with organic material. It is suffice to mention that we would also be disturbing the sediments which in turn is another major problem. By removing the sediments, we would be amplifying a problem that we know is slowly disappearing.

# 6 REFERENCES


Aller RC, Aller JY: The effect of biogenic irrigation intensity and solute exchange on diagenetic reaction rates in marine sediments. *Journal of Marine Research* 1998, 56(4):905-936.

Amyot M, Lean DRS, Poissant L, Doyon MR: Distribution and transformation of elemental mercury in the St. Lawrence River and Lake Ontario. *Canadian Journal of Fisheries and Aquatic Sciences* 2000, 57:155-163.

Anderson J: St. Lawrence River Environment Investigation. Volume 4. Assessment of water and sediment quality in the Cornwall area of the St. Lawrence River, 1985. Technical report, Great Lakes Section. *Water Resources Branch.* Ontario Ministry of the Environment. 1990.

Appleby PG, Oldfield F, Thompson R, Huttunen P, Tolonen K: Pb-210 Dating of Annually Laminated Lake-Sediments from Finland. *Nature* 1979, 280(5717):53-55.

Appleby PG, Oldfield F: The calculation of lead-210 dates assuming a constant rate of supply of unsupported 210Pb to the sediment. *Catena* 1978, 5, 1-8.

Appleby PG: Chronostratigraphic techniques in recent sediments. 2001. In Last WM, Smol JP, editors, *Tracking environmentalchange using lake sediments volume 1: basin analysis, coring, and chronological techniques. Kluwer Academic.* 171-203.

Appleby PG: Three decades of dating recent sediments by fallout radionuclides: a review. *Holocene* 2008, 18(1):83-93.

Barkay T, Gillman M, Turner RR: Effects of dissolved organic carbon and salinity on bioavailability of mercury. *Applied and Environmental Microbiology* 1997, 63(11):4267-4271.

Bell GL, Eadie BJ: Variations in the distribution of suspended particles during an upwelling event in Lake Michigan in 1980. *Journal of Great Lakes Research* 1983, 9(4):559-567.

Benoit JM, Gilmour CC, Mason RP, Heyes A: Sulfide controls on mercury speciation and bioavailability to methylating bacteria in sediment pore waters (vol 33, pg 951, 1999). *Environmental Science & Technology* 1999, 33(10):1780-1780.

Benoit JM, Gilmour CC, Mason RP, Riedel GS, Riedel GF: Behavior of mercury in the Patuxent River estuary. *Biogeochemistry* 1998, 40(2-3):249-265.

Benoit JM, Gilmour CC, Mason RP: The influence of sulfide on solid phase mercury bioavailability for methylation by pure cultures of Desulfobulbus propionicus (1pr3). *Environmental Science & Technology* 2001, 35(1):127-132.

Berelson W, McManus J, Coale K, Johnson K, Burdige D, Kilgore T, Colodner D, Chavez F, Kudela R, Boucher J: A time series of benthic flux measurements from Monterey Bay, CA. *Continental Shelf Research* 2003, 23(5):457-481.

Berelson WM, Hammond, D.E, O'Neill,D, XU, X.-M., Chin,C., and Zukin, J: Benthic fluxes and pore water studies from sediments of the central equatorial north Pacific: Nutrient diagenesis. *Geochimica Et Cosmochimica Acta* 1990, 54(11):3001-3012.

Berner RA: Early diagenesis: A theoretical approach. Princeton University Press: New Jersey; 1980, 241 pp.

Biberhofer J, Rukavina NA: Data on the distribution and stability of St. Lawrence River sediments at Cornwall, ON. Technical Report Contribution number 02-195, *National Water Research Institute,* Environment Canada 2002.

Bisogni JJ, Lawrence AW: Kinetics of Mercury Methylation in Aerobic and Anaerobic Aquatic Environments. *Journal Water Pollution Control Federation* 1975, 47(1):135-152.

Blais JM, Kalff J, Cornett RJ, Evans RD: Evaluation of Pb-210 Dating in Lake-Sediments Using Stable Pb, Ambrosia Pollen, and Cs-137. *Journal of Paleolimnology* 1995, 13(2):169-178.

Blais JM, France RL, Kimpe LE, Cornett RJ: Climatic changes in northwestern Ontario have had a greater effect on erosion and sediment accumulation than logging and fire: Evidence from Pb-210 chronology in lake sediments. *Biogeochemistry* 1998, 43(3):235-252.

Bloom NS, Gill GA, Cappellino S, Dobbs C, McShea L, Driscoll C, Mason R, Rudd J: Speciation and cycling of mercury in Lavaca Bay, Texas, sediments. *Environmental Science & Technology* 1999, 33(1):7-13.

Boudreau BP: The diffusive tortuosity of fine-grained unlithified sediments. *Geochimica Et Cosmochimica Acta* 1996, 60(16):3139-3142.

Bower J, Savage KS, Weinman B, Barnett MO, Hamilton WP, Harper WF: Immobilization of mercury by pyrite (FeS2). *Environmental Pollution* 2008, 156(2):504-514.

Brady NC, Weil RR: The Nature and Properties of Soils (13th Ed.). Prentice Hall, New York, 2002, 960 pp.

Brown JR, Bancroft GM, Fyfe WS, McLean RAN: Mercury Removal from Water by Iron Sulfide Minerals - Electron-Spectroscopy for Chemical-Analysis (Esca) Study. *Environmental Science & Technology* 1979, 13(9):1142-1144.

Bubb JM, Williams TP, Lester JN: The Behavior of Mercury within a Contaminated Tidal River System. *Water Science and Technology* 1993, 28(8-9):329-338.

Bunce NJ: Environmental Chemistry, Winnipeg: *Wuerz Publishing Ltd.* 1991, ISBN 0-920063-46-2.

Bunce NJ: Environmental Chemistry, Winnipeg: *Wuerz Publishing Ltd.* 1994, 2nd Ed. ISBN 0-920063-65-9.

Cai Y, Jaffe R, Alli A, Jones RD: Determination of organomercury compounds in aqueous samples by capillary gas chromatography atomic fluorescence spectrometry following solid-phase extraction. *Analytica Chimica Acta* 1996, 334(3):251-259.

Cai Y, Tang G, Jaffe R, Jones R: Evaluation of some isolation methods for organomercury determination in soil and fish samples by capillary gas chromatography - Atomic fluorescence spectrometry. *International Journal of Environmental Analytical Chemistry* 1997, 68(3):331-345.

Canadian Council of Ministers of the Environment (CCME). Protocol for the derivation of Canadian sediment quality guidelines for the protection of aquatic life: Summary Tables - Update 2002. CCME EPC-98E; Prepared by Environment Canada, Guidelines Division, Technical Secretariat of the CCME Task Group on Water Quality Guidelines, Ottawa, 2005.

Canário J, Poissant L, O'Driscoll N, Pilote M, Constant P, Blais J, Lean D: Mercury partitioning in surface sediments of the upper st. Lawrence river (Canada): Evidence of the importance of the sulphur chemistry. *Water Air and Soil Pollution* 2008, 187(1-4):219-231.

Capone DG, Kiene RP: Comparison of Microbial Dynamics in Marine and Fresh-Water Sediments - Contrasts in Anaerobic Carbon Catabolism. *Limnology and Oceanography* 1988, 33(4):725-749.

Carignan R, Lean DRS: Regeneration of Dissolved Substances in a Seasonally Anoxic Lake - the Relative Importance of Processes Occurring in the Water Column and in the Sediments. *Limnology and Oceanography* 1991, 36(4):683-707.

Carignan R, Lorrain S: Sediment dynamics in the fluvial lakes of the St. Lawrence River: accumulation rates and characterization of the mixed sediment layer. *Canadian Journal of Fisheries and Aquatic Sciences* 2000, 57:63-77.

Carignan R, Lorrain S: Sediment dynamics in the fluvial lakes of the St. Lawrence River: accumulation rates and characterization of the mixed sediment layer. *Canadian Journal of Fisheries and Aquatic Sciences* 2000, 57:63-77.

Carignan R, Rapin F, Tessier A: Sediment Porewater Sampling for Metal Analysis - a Comparison of Techniques. *Geochimica Et Cosmochimica Acta* 1985, 49(11):2493-2497.

Celo V LD, Scott SL: Abiotic methylation of mercury in the aquatic environment. *Science of the Total Environment* 2006, 368(1):126-137.

Celo V, Ananth RV, Scott SL, Lean DRS: Methylmercury artifact formation during solid-phase extraction of water samples using sulfhydryl cotton fiber adsorbent. *Analytica Chimica Acta* 2004, 516(1-2):171-177.

Chambers RL, Eadie BJ: Nepheloid and Suspended Particulate Matter in Southeastern Lake-Michigan. *Sedimentology* 1981, 28(3):439-447.

Chapelle FH, Lovley DR: Competitive-Exclusion of Sulfate Reduction by Fe(Iii)-Reducing Bacteria - a Mechanism for Producing Discrete Zones of High-Iron Ground-Water. *Ground Water* 1992, 30(1):29-36.

Chapman PM, Wang FY, Adams WL, Green A: Appropriate applications of sediment quality values for metals and metalloids. *Environmental Science & Technology* 1999, 33(22):3937-3941.

Chau YK, Snodgrass WJ, Wong PTS: Sampler for Collecting Evolved Gases from Sediment. *Water Research* 1977, 11(9):807-809.

Choe KY, Gill GA, Lehman RD, Han S, Heim WA, Coale KH: Sediment-water exchange of total mercury and monomethyl mercury in the San Francisco Bay-Delta. *Limnology and Oceanography* 2004, 49(5):1512-1527.

Churchill JH, Biscaye PE, Aikman F: The Character and Motion of Suspended Particulate Matter over the Shelf Edge and Upper Slope Off Cape-Cod. *Continental Shelf Research* 1988, 8(5-7):789-809.

Claypool GE, Kaplan IR: The origin and distribution of methane in marine sediments.1974, 99-139. In.I.R. Kaplan [ed.] Natural gases in marine sediments.Plenum.

Cline JD: Spectrophotometric determination of hydrogen sulfide in natural waters. *Limnol. Oceanogr* 1969. 14: 454-458.

Compeau GC, Bartha R: Effects of Sea Salt Anions on the Formation and Stability of Methylmercury. *Bulletin of Environmental Contamination and Toxicology* 1983, 31(4):486-493.

Compeau GC, Bartha R: Sulfate-Reducing Bacteria - Principal Methylators of Mercury in Anoxic Estuarine Sediment. *Applied and Environmental Microbiology* 1985, 50(2):498-502.

Covelli S, Faganeli J, Horvat M, Brambati A: Porewater distribution and benthic flux measurements of mercury and methylmercury in the Gulf of Trieste (northern Adriatic Sea). *Estuarine Coastal and Shelf Science* 1999, 48(4):415-428.

Craig PJ, Moreton PA: Total Mercury, Methyl Mercury and Sulfide in River Carron Sediments. *Marine Pollution Bulletin* 1983, 14(11):408-411.

Craig PJ: Organometallic compounds in the environment. London7, *Longman*; 1986.

Davidson PW, Myers GJ, Weiss B: Mercury exposure and child development outcomes. Pediatrics 2004, 113(4):1023-1029.

Delongchamp TM: Mercury dynamics in sediments of the St. Lawrence River near Cornwall, Ontario. 2006. M.Sc. thesis, University of Ottawa.

Di Toro DM: Sediment flux modeling. *John Wiley & sons Inc.* 2001 ISBN_10: 0-471-13535-6.

Doyle CS, Kendelewicz T, Bostick BC, Brown GE: Soft X-ray spectroscopic studies of the reaction of fractured pyrite surfaces with Cr(Vl)-containing aqueous solutions. *Geochimica Et Cosmochimica Acta* 2004, 68(21):4287-4299.

Drobner E, Huber H, Wachtershauser G, Rose D, Stetter KO: Pyrite Formation Linked with Hydrogen Evolution under Anaerobic Conditions. *Nature* 1990, 346(6286):742-744.

Drott A, Lambertsson L, Bjorn E, Skyllberg U: Importance of dissolved neutral mercury sulfides for methyl mercury production in contaminated sediments. *Environmental Science & Technology* 2007, 41(7):2270-2276.

EC, MENVIQ (Environment Canada and Ministere de l'Envionnement du Quebec). Interim criteria for quality assessment of St.Lawrence River sediment, 1992. Environment Canada, Ottawa.

Engstrom DR, Balogh SJ, Swain EB: History of mercury inputs to Minnesota lakes: Influences of watershed disturbance and localized atmospheric deposition. *Limnology and Oceanography* 2007, 52(6):2467-2483.

Environment Canada 1981. Status report on compliance with the chlor-alkali mercury regulations. Abatement and Compliance Branch, Water Pollution Control Directorate, Environmental Protection Service, Environment Canada.

Environment Canada Last updated June 11 2005. Cornwall Sediment Strategy. http://www.ec.gc.ca/media archive/press/2005/050611 b e.htm.

Environment Canada Last updated March 1 2004. Factsheet 1: Basic concepts and program highlights. Sediments: sink and source-putting the problem in perspective. http://www.ec.gc.ca/ceqg-rcqe/English/Html/SAS/factsheet 1.cfm.

Fagerstrom.T, Jernelov A: Formation of Methyl Mercury from Pure Mercuric Sulphide in Aerobic Organic Sediment. *Water Research* 1971, 5(3):121-&.

Falter R: Experimental study on the unintentional abiotic methylation of inorganic mercury during analysis: Part 1: Localisation of the compounds effecting the abiotic mercury methylation. *Chemosphere* 1999, 39(7):1051-1073.

Fitzgerald WF, Engstrom DR, Mason RP, Nater EA: The case for atmospheric mercury contamination in remote areas. *Environmental Science & Technology* 1998, 32(1):1-7.

Fitzgerald WF: Is Mercury Increasing in the Atmosphere - the Need for an Atmospheric Mercury Network (Amnet). *Water Air and Soil Pollution* 1995,245-254.

Fleming JE, Nelson Dc: Contribution of Iron-Reducing Bacteria to Mercury Methylation in Marine Sediments 2006. University of California.

Fowlie AR, Hodson PV, Hickey MBC: Spatial and seasonal patterns of mercury concentrations in fish from the St. Lawrence River at Cornwall, Ontario: Implications for monitoring. *Journal of Great Lakes Research* 2008, 34(1):72-85.

Froelich PN, Klinkhammer GP, Bender ML, Fanning KA: Pore Water Nutrient and Metal Profiles During Organic-Matter Regeneration in Pelagic Sediments of Eastern Equatorial Atlantic. *Transactions-American Geophysical Union* 1977, 58(12):1154-1154.

Froelich PN, Klinkhammer GP, Bender ML, Luedtke NA, Heath GR, Cullen D, Dauphin P, Hammond D, Hartman B, Maynard V: Early Oxidation of Organic-Matter in Pelagic Sediments of the Eastern Equatorial Atlantic - Suboxic Diagenesis. *Geochimica Et Cosmochimica Acta* 1979, 43(7):1075-1090.

Furutani A, Rudd JWM: Measurement of Mercury Methylation in Lake Water and Sediment Samples. *Applied and Environmental Microbiology* 1980, 40(4):770-776.

Gagnon C, Pelletier E, Mucci A, Fitzgerald WF: Diagenetic behavior of methylmercury in organic-rich coastal sediments. *Limnology and Oceanography* 1996, 41(3):428-434.

Gagnon C, Pelletier E, Mucci A: Behaviour of anthropogenic mercury in coastal marine sediments. *Marine Chemistry* 1997, 59(1-2):159-176.

Gilbert SG, Grantwebster KS: Neurobehavioral Effects of Developmental Methylmercury Exposure. *Environmental Health Perspectives* 1995, 103:135-142.

Gill GA, Bloom NS, Cappellino S, Driscoll CT, Dobbs C, McShea L, Mason R, Rudd JWM: Sediment-water fluxes of mercury in Lavaca Bay, Texas. *Environmental Science & Technology* 1999, 33(5):663-669.

Gilmour CC, Henry EA, Mitchell R: Sulfate Stimulation of Mercury Methylation in Fresh-Water Sediments. *Environmental Science & Technology* 1992, 26(11):2281-2287.

Gilmour CC, Henry EA: Mercury Methylation in Aquatic Systems Affected by Acid Deposition. *Environmental Pollution* 1991, 71(2-4):131-169.

Gilmour CC, Riedel GS, Ederington MC, Bell JT, Benoit JM, Gill GA, Stordal MC: Methylmercury concentrations and production rates across a trophic gradient in the northern Everglades. *Biogeochemistry* 1998, 40(2-3):327-345.

Gobeil C, Cossa D: Mercury in Sediments and Sediment Pore-Water in the Laurentian Trough. *Canadian Journal of Fisheries and Aquatic Sciences* 1993, 50(8):1794-1800.

Gobeil C, Macdonald RW, Smith JN: Mercury profiles in sediments of the Arctic Ocean basins. *Environmental Science & Technology* 1999, 33(23):4194-4198.

Golder Associates Ltd. Evaluation of Sediment Management Options for the St. Lawrence River (Cornwall) Area of Concern. Report submitted to: Ontario Ministry of the Environment, Kingston, Ontario, Canada 2004, 107, ISBN 04-1112-017.

Gomezparra A, Forja JM: Benthic Nutrient Fluxes in Cadiz Bay (Sw Spain). *Hydrobiologia* 1993, 252(1):23-34.

Goulet RR, Holmes J, Page B, Poissant L, Siciliano SD, Lean DRS, Wang F, Amyot M, Tessier A: Mercury transformations and fluxes in sediments of a riverine wetland. *Geochimica Et Cosmochimica Acta* 2007, 71(14):3393-3406.

Grapentine L, Milani D, Mackay S: Assessment of the potential for mercury biomagnification from sediment in the St. Lawrence River (Cornwall) Area of Concern. *Environment Canada Publication, Canada*, 2003.

Hallberg RO, Bagander LE, Engvall AG, Schippel FA: Method for studying geochemistry of sediment-water interface. *Ambio* 1972. 1(2): 71-72.

Hammerschmidt CR, Fitzgerald WF: Methylmercury cycling in sediments on the continental shelf of southern New England. *Geochimica Et Cosmochimica Acta* 2006, 70, 918-930.

Hammerschmidt CR, Sandheinrich MB, Wiener JG, Rada RG: Effects of dietary methylmercury on reproduction of fathead minnows. *Environmental Science & Technology* 2002, 36(5):877-883.

Han S, Obraztsova A, Pretto P, Deheyn DD, Gieskes J, Tebo BM: Sulfide and iron control on mercury speciation in anoxic estuarine sediment slurries. *Marine Chemistry* 2008, 111(3-4):214-220.

Harada M: Minamata Disease - Methylmercury Poisoning in Japan Caused by Environmental-Pollution. Critical Reviews in Toxicology 1995, 25(1):1-24.

He TR, Lu J, Yang F, Feng XB: Horizontal and vertical variability of mercury species in pore water and sediments in small lakes in Ontario. *Science of the Total Environment* 2007, 386(1-3):53-64.

Heiri O, Lotter AF, Lemcke G: Loss on ignition as a method for estimating organic and carbonate content in sediments: reproducibility and comparability of results. *Journal of Paleolimnology* 2001, 25(1):101-110.

Hesslein RH: Insitu Sampler for Close Interval Pore Water Studies. *Limnology and Oceanography* 1976, 21(6):912-914.

Heit M, Tan Y, Klusek C, Burke JC: Anthropogenic Trace-Elements and Polycyclic Aromatic Hydrocarbon Levels in Sediment Cores from two Lakes in the Adirondack Acid Lake Region. *Water Air and Soil Pollution* 1981, 15(4):441-464.

Hicks RE, Aas P, Jankovich C: Annual and offshore changes in bacterioplankton communities in the western arm of Lake Superior during 1989 and 1990. *Journal of Great Lakes Research* 2004, 30:196-213.

Hines NA, Brezonik PL, Engstrom DR: Sediment and porewater profiles and fluxes of mercury and methylmercury in a small seepage lake in northern Minnesota. *Environmental Science & Technology* 2004, 38(24):6610-6617.

Hintelmann H, Welbourn PM, Evans RD: Binding of Methylmercury Compounds by Humic and Fulvic-Acids. *Water Air and Soil Pollution* 1995, 80(1-4):1031-1034.

Hintelmann H, Wilken RD: Levels of Total Mercury and Methylmercury Compounds in Sediments of the Polluted Elbe River - Influence of Seasonally and Spatially Varying Environmental-Factors. *Science of the Total Environment* 1995, 166(1-3):1-10.

Holmes JB, Lean D: Factors that influence methylmercury flux rates from wetland sediments. *Science of the Total Environment* 2006, 368(1):306-319.

Holmes JB: Factors affecting methylmercury levels in water, sediment and fish of temperate wetlands, 2005. Ph.D. thesis, University of Ottwa.

Hordijk KA, Hagenaars C, Cappenberg TE: Kinetic-Studies of Bacterial Sulfate Reduction in Fresh-Water Sediments by High-Pressure Liquid-Chromatography and Microdistillation. *Applied and Environmental Microbiology* 1985, 49(2):434-440.

Hornberger MI, Luoma SN, van Geen A, Fuller C, Anima R: Historical trends of metals in the sediments of San Francisco Bay, California. *Marine Chemistry* 1999, 64(1-2):39-55.

Hurley JP, Krabbenhoft DP, Babiarz CL, Andren AW: Cycling of Mercury across the Sediment-Water Interface in Seepage Lakes. *Environmental Chemistry of Lakes and Reservoirs* 1994, 237:425-449.

Huttunen JT, Lappalainen KM, Saarijarvi E, Vaisanen T, Martikainen PJ: A novel sediment gas sampler and a subsurface gas collector used for measurement of the ebullition of methane and carbon dioxide from a eutrophied lake. *Science of the Total Environment* 2001, 266(1-3):153-158.

Iverfeldt A: Mercury in Forest Canopy Throughfall Water and Its Relation to Atmospheric Deposition. *Water Air and Soil Pollution* 1991, 56:553-564.

Jackson TA: Biological and Environmental-Control of Mercury Accumulation by Fish in Lakes and Reservoirs of Northern Manitoba, Canada. *Canadian Journal of Fisheries and Aquatic Sciences* 1991, 48(12):2449-2470.

Jackson TA: Methyl Mercury Levels in a Polluted Prairie River Lake System - Seasonal and Site-Specific Variations, and the Dominant Influence of Trophic Conditions. *Canadian Journal of Fisheries and Aquatic Sciences* 1986, 43(10):1873-1887.

Jenne EA: Trace element sorption by sediments and soils-sites and processes. In: Chapell, WR (Ed.), Molybdenum in the Environment. Marcel Dekker, New York, NY, 1977, 425-552.

Jensen S, Jernelov A: Biological Methylation of Mercury in Aquatic Organisms. *Nature* 1969, 223(5207):753-&.

JernelövA: Conversion of mercury compounds, in: Chemical fallout, Miller MW, Berg GG, Eds. Thomas CC, Springfield, Illinois, USA, 1969, 68-73.

Johansson K: Mercury in sediment in Swedish forest lakes. Verh. Int. Ver. Theor. Angew. *Limnol* 1985, 22, 2359-2363.

Johnson BM: Sulfate reducing bacteria and the role of nutrients in mercury methylation in Spring Lake, Minnesota M.Sc. Thesis, University of Minnesota, 2004.

Kauss P, Hamdy YS, Hamma BS ; St. Lawrence River Investigations Volume 1. Background Assessment of water, sediment and biota in the Cornwall, Ontario and Massena, New York section of the St. Lawrence River 1979-1982. 1988.Technical report, Water Resources Branch Ontario Ministry of the Environment.

King JK, Kostka JE, Frischer ME, Saunders FM, Jahnke RA: A quantitative relationship that demonstrates mercury methylation rates in marine sediments are based on the community composition and activity of sulfate-reducing bacteria. *Environmental Science & Technology* 2001, 35(12):2491-2496.

Korthals ET, Winfrey MR: Seasonal and Spatial Variations in Mercury Methylation and Demethylation in an Oligotrophic Lake. *Applied and Environmental Microbiology* 1987, 53(10):2397-2404.

Kroenke AE: Atmospheric mercury deposition to sediments of New Jersey and Southern New York State: interpretations from dated sediment cores. Ph.D. Thesis: Rensselaer Polytechnic Institute, New York; 2003, 283 pp.

Lambertsson L, Nilsson M: Organic material: The primary control on mercury methylation and ambient methyl mercury concentrations in estuarine sediments. *Environmental Science & Technology* 2006, 40(6):1822-1829.

Langer CS, Fitzgerald WF, Visscher PT, Vandal GM: Biogeochemical cycling of methylmercury at Barn Island Salt Marsh, Stonington, CT, USA. Wetland Ecol. *Manag* 2001, 9, 295-310.

Lee YH, Bishop KH, Munthe J: Do concepts about catchment cycling of methylmercury and mercury in boreal catchments stand the test of time? Six years of atmospheric inputs and runoff export at Svartberget, northern Sweden. *Science of the Total Environment* 2000, 260(1-3):11-20.

Lepage S, Biberhofer J, Lorrain S: Sediment dynamics and the transport of suspended matter in the upstream area of Lake St. Francis. *Canadian Journal of Fisheries and Aquatic Sciences* 2000, 57:52-62.

Li YH, Gregory S: Diffusion of Ions in Sea-Water and in Deep-Sea Sediments. *Geochimica Et Cosmochimica Acta* 1974, 38(5):703-714.

Lindberg S, Bullock R, Ebinghaus R, Engstrom D, Feng XB, Fitzgerald W, Pirrone N, Prestbo E, Seigneur C: A synthesis of progress and uncertainties in attributing the sources of mercury in deposition. *Ambio* 2007, 36(1):19-32.

Lindqvist O, Johansson K, Aastrup M, Andersson A, Bringmark L, Hovsenius G, Hakanson L, Iverfeldt A, Meili M, Timm B: Mercury in the Swedish Environment - Recent Research on Causes, Consequences and Corrective Methods. *Water Air and Soil Pollution* 1991, 55(1-2):R11-&.

Lockhart WL, Macdonald RW, Outridge PM, Wilkinson P, DeLaronde JB, Rudd JWM: Tests of the fidelity of lake sediment core records of mercury deposition to known histories of mercury contamination. *Science of the Total Environment* 2000, 260(1-3):171-180.

Lockhart WL, Wilkinson P, Billeck BN, Danell RA, Hunt RV, Brunskill GJ, Delaronde J, St Louis V: Fluxes of mercury to lake sediments in central and northern Canada inferred from dated sediment cores. *Biogeochemistry* 1998, 40(2-3):163-173.

Lockwood RA, Chen KY: Adsorption of Hg (II) by Hydrous Manganese Oxides. *Environmental Science & Technology* 1973, 7(11):1028-1034.

Lonergan DJ, Jenter HL, Coates JD, Phillips EJP, Schmidt TM, Lovley DR: Phylogenetic analysis of dissimilatory Fe(III)-reducing bacteria. *Journal of Bacteriology* 1996, 178(8):2402-2408.

Long ER, Morgan LG: The potential for biological effects of sediment sorbed contaminants tested in the National Status and Trends Program. NOAA Technical Memorandum NOS OMA 52, National Oceanic and Atmospheric Administration, Seattle, WA, 1991 ,175 pp 1 appendices.

Lopez P: Composition of porewater and benthic fluxes in the mesohaline Es Grau lagoon (Minorca, Spain) during spring and early summer. *Wetlands* 2004, 24(4):796-810.

Loring DH: Mercury in Sediments of Gulf of St-Lawrence. *Canadian Journal of Earth Sciences* 1975, 12(7):1219-1237.

Lucotte M, Mucci A, Hillairemarcel C, Pichet P, Grondin A: Anthropogenic Mercury Enrichment in Remote Lakes of Northern Quebec (Canada). *Water Air and Soil Pollution* 1995, 80(1-4):467-476.

MacDonald DD, Ingersoll CG, Berger TA: Development and evaluation of consensus-based sediment quality guidelines for freshwater ecosystems. *Archives of Environmental Contamination and Toxicology* 2000, 39(1):20-31.

Mahaffey KR: Biomarkers of mercury exposure: Differences between children and adult women in the distribution of blood and hair mercury concentrations among the 1999/2000 NHANES examinees. *Neurotoxicology* 2004, 25(4):677-678.

Martens CS, Valklump J: Biogeochemical Cycling in an Organic-Rich Coastal Marine Basin .1. Methane Sediment-Water Exchange Processes. *Geochimica Et Cosmochimica Acta* 1980, 44(3):471-490.

Marvin-Dipasquale MC, Oremland RS: Bacterial methylmercury degradation in Florida Everglades peat sediment. *Environmental Science & Technology* 1998, 32(17):2556-2563.

Mason R, Bloom N, Cappellino S, Gill G, Benoit J, Dobbs C: Investigation of porewater sampling methods for mercury and methylmercury. *Environmental Science & Technology* 1998, 32(24):4031-4040.

Mason RP, Fitzgerald WF, Morel FMM: The Biogeochemical Cycling of Elemental Mercury - Anthropogenic Influences. *Geochimica Et Cosmochimica Acta* 1994, 58(15):3191-3198.

Mason RP, Reinfelder JR, Morel FMM: Uptake, toxicity, and trophic transfer of mercury in a coastal diatom. *Environmental Science & Technology* 1996, 30(6):1835-1845.

Meili M: Mercury in lakes and rivers. In: Metal Ions in Biological Systems, Vol 34. vol. 34; 1997: 21-51.

Mills BR, Paterson AM, Lean DRS, Smol JP, Mierle G, Blais JM: Dissecting the spatial scales of mercury accumulation in Ontario lake sediment. *Environmental Pollution.* In Press.

Miskimmin BM, Rudd JWM, Kelly CA: Influence of Dissolved Organic-Carbon, Ph, and Microbial Respiration Rates on Mercury Methylation and Demethylation in Lake Water. *Canadian Journal of Fisheries and Aquatic Sciences* 1992, 49(1):17-22.

Miskimmin BM: Effect of Natural Levels of Dissolved Organic-Carbon (Doc) on Methyl Mercury Formation and Sediment Water Partitioning. *Bulletin of Environmental Contamination and Toxicology* 1991, 47(5):743-750.

Morel FMM, Kraepiel AML, Amyot M: The chemical cycle and bioaccumulation of mercury. Annual Review of Ecology and Systematics 1998, 29:543-566.

Morse JW, Luther GW: Chemical influences on trace metal-sulfide interactions in anoxic sediments. *Geochimica Et Cosmochimica Acta* 1999, 63(19-20):3373-3378.

Mortimer CH: Large-scale oscillatory motions and seasonal temperature changes in Lake Michigan and Lake Ontario. 1971. Center for Great Lakes Studies Special Report NO. 12, prepared under U.S. Army Corps of Engineers Contract NO. DACW-35-68-C-0072, University of Wisconsin, Milwaukee,Wisconsin.

Muir DB, Braune B, Demarch R, Norstrom R, Wagemann L, Lockhart B, Hargrave D, Bright R, Addison J, Payne K Reimer: Spatial and Temporal Trends and Effects of Contaminants in the Canadian Arctic Marine Ecosystem: a Review. *Science of the Total Environment* 1999. 83-144.

Munthe J, McElroy WJ: Some Aqueous Reactions of Potential Importance in the Atmospheric Chemistry of Mercury. Atmospheric Environment Part a-General Topics 1992, 26(4):553-557.

Murray JW: Interaction of Metal-Ions at Manganese Dioxide Solution Interface. *Geochimica Et Cosmochimica Acta* 1975, 39(4):505-519.

Nriagu JO: A Global Assessment of Natural Sources of Atmospheric Trace-Metals. *Nature* 1989, 338(6210):47-49.

Nriagu JO: Mechanistic Steps in the Photoreduction of Mercury in Natural-Waters. *Science of the Total Environment* 1994, 154(1):1-8.

Oldfield F, Appleby PG: Empirical testing of 210pb-dating models for lake sediments. In Haworth EY, Lund JWG editors, Lake Sediments and Environmental History, *Leicester University Press* 1984, 93-124.

Oldfield F, Appleby PG: Alternative Approach to Pb-210 Based Sediment Dating. *Geophysical Journal of the Royal Astronomical Society* 1978, 53(1):177-177.

Olson BH, Cooper RC: Comparison of Aerobic and Anaerobic Methylation of Mercuric-Chloride by San-Francisco Bay Sediments. *Water Research* 1976, 10(2):113-116.

Olson BH, Cooper RC: Insitu Methylation of Mercury in Estuarine Sediment. *Nature* 1974, 252(5485):682-683.

Omelchenko A, Lockhart WL, Wilkinson : Study the Depositional Characteristic of the Lake Sediments Across Canada with Pb-210 and Cs-137. Fresh water Institute, Department of Fisheries and Oceans, Winnipeg, Manitoba, Canada, R3T 2N6.Unpublished report.

Ontario Ministry of the Environment. Concentrations of mercury in sediments and fish in the St. Lawrence River. 1979. 2nd Ed.

Oremland RS, Culbertson CW, Winfrey MR: Methylmercury Decomposition in Sediments and Bacterial Cultures - Involvement of Methanogens and Sulfate Reducers in Oxidative Demethylation. *Applied and Environmental Microbiology* 1991, 57(1):130-137.

Ozverdi A, Erdem M: Cu2+, Cd2+ and Pb2+ adsorption from aqueous solutions by pyrite and synthetic iron sulphide. Journal of Hazardous Materials 2006, 137(1):626-632.

Pacyna EG, Pacyna JM, Steenhuisen F, Wilson S: Global anthropogenic mercury emission inventory for 2000. *Atmospheric Environment* 2006, 40(22):4048-4063.

Pacyna JM, Pacyna EG, Steenhuisen F, Wilson S: Mapping 1995 global anthropogenic emissions of mercury. *Atmospheric Environment* 2003, 37:S109-S117.

Pak KR, Bartha R: Mercury methylation and demethylation in anoxic lake sediments and by strictly anaerobic bacteria. *Applied and Environmental Microbiology* 1998, 64(3):1013-1017.

Pakhornova SV, Hall POJ, Kononets MY, Rozanov AG, Tengberg A, Vershinin AV: Fluxes of iron and manganese across the sediment-water interface under various redox conditions. *Marine Chemistry* 2007, 107(3):319-331.

Parsons MB, Percival JB: Mercury: Sources, Measurements and Cycles and Effects. 2005, 34.

Patterson RJ, Frape SK, Dykes LS, McLeod RA: Coring and Squeezing Technique for Detailed Study of Subsurface Water Chemistry. *Canadian Journal of Earth Sciences* 1978, 15(1):162-169.

Peine A, Tritschler A, Kusel K, Peiffer S: Electron flow in an iron-rich acidic sediment - evidence for an acidity-driven iron cycle. *Limnology and Oceanography* 2000, 5(5):1077-1087.

Perry E, Norton SA, Kamman NC, Lorey PM, Driscoll CT: Deconstruction of historic mercury accumulation in lake sediments, northeastern United States. *Ecotoxicology* 2005, 14(1-2):85-99.

Persaud D, Jaagumagi R, Hayton A: Guidelines for the protection and management of aquatic sediment quality in Ontario. Ontario Ministry of the Environment and Energy, Ontario, Canada, 1993.

Petersen W, Willer E, Willamowski C: Remobilization of trace elements from polluted anoxic sediments after resuspension in oxic water. *Water Air and Soil Pollution* 1997, 99(1-4):515-522.

Pirrone N, Costa P, Pacyna JM, Ferrara R: Mercury emissions to the atmosphere from natural and anthropogenic sources in the Mediterranean region. *Atmospheric Environment* 2001, 35(17):2997-3006.

Preisler A, de Beer D, Lichtschlag A, Lavik G, Boetius A, Jorgensen BB: Biological and chemical sulfide oxidation in a Beggiatoa inhabited marine sediment. *Isme Journal* 2007, 1(4):341-353.

Quemerais B, Cossa D, Rondeau B, Pham TT, Fortin B: Mercury distribution in relation to iron and manganese in the waters of the St. Lawrence river. *Science of the Total Environment* 1998, 213(1-3):193-201.

Ramalhosa E, Monterroso P, Abreu S, Pereira E, Vale C, Duarte A: Storage and export of mercury from a contaminated bay (Ria de Aveiro, Portugal). *Wetl. Ecol. Manage* 2001, 9, 311-316.

Rasmussen PE: Current Methods of Estimating Atmospheric Mercury Fluxes in Remote Areas. *Environmental Science & Technology* 1994, 28(13):2233-2241.

Ravichandran M: Interactions between mercury and dissolved organic matter - a review. *Chemosphere* 2004, 55(3):319-331.

Razavi NR: Role of bubbling from aquatic sediments in mercury transfer to a benthic invertebrate in the St. Lawrence River, Cornwall, ON. 2008. M.Sc. thesis, Queen's University.

Richman L: St. Lawrence River Sediment Chemical Assessment 1997, Cornwall, Ontario. Technical Report ISBN 0-778-9064-X, Ontario Ministry of the Environment and Energy. 1999.

Richman LA, Dreier SI: Sediment contamination in the St. Lawrence River along the Cornwall, Ontario waterfront. *Journal of Great Lakes Research* 2001, 27(1):60-83.

Richman LA: St. Lawrence River sediment and biological assessment 1991. Technical Report ISBN 0-7778-2743-3, Ontario Ministry of Environment and Energy. 1994.

Rodier J: L'analysis de l'eau. 5em ed., Paris, Dunod 1975, 176-177.

Rowe GT, Clifford CH, Smith KL: Benthic Nutrient Regeneration and Its Coupling to Primary Productivity in Coastal Waters. *Nature* 1975, 255(5505):215-217.

Rutgers van der loeff MR, Anderson LG, Hall POJ, Iverfeldt A, Josefson AB, Sundby B, Westerlund SFG: The Asphyxiation Technique - an Approach to Distinguishing between Molecular-Diffusion and Biologically Mediated Transport at the Sediment Water Interface. *Limnology and Oceanography* 1984, 29(4):675-686.

Rydberg J, Galman V, Renberg I, Bindler R, Lambertsson L, Martinez-Cortizas A: Assessing the stability of mercury and methylmercury in a varved lake sediment deposit. *Environmental Science & Technology* 2008, 42(12):4391-4396.

Santschi P, Hohener P, Benoit G, Buchholztenbrink M: Chemical Processes at the Sediment Water Interface. *Marine Chemistry* 1990, 30(1-3):269-315.

Scheulhammer AM, Meyer MW, Sandheinrich MB, Murray MW: Effects of environmental methylmercury on the health of wild birds, mammals, and fish. *Ambio* 2007, 36(1):12-18.

Schneider AR, Eadie BJ, Baker JE: Episodic particle transport events controlling PAH and PCB cycling in Grand Traverse Bay, Lake Michigan. *Environmental Science & Technology* 2002, 36(6):1181-1190.

Schroeder WH, Munther J: Atmospheric mercury, an overview. *Atmos. Environ* 1998, 32, 809-822.

Schroeter and Associates: Toxic contaminants loading from municipal sources in Ontario RAP sites. Final report submitted to Wastewater Technology Centre, Canada Centre for Inland Waters, Burlington, Ontario. Contract No. KA168-2-2215. 1993.

Sellers P, Kelly CA, Rudd JWM, MacHutchon AR: Photodegradation of methylmercury in lakes. *Nature* 1996, 380(6576):694-697.

Shchukarev A, Galman V, Rydberg J, Sjoberg S, Renberg I: Speciation of iron and sulphur in seasonal layers of varved lake sediment: an XPS study. Surface and Interface Analysis 2008, 40(3-4):354-357.

Siciliano SD, O'Driscoll NJ, Lean DRS: Microbial reduction and oxidation of mercury in freshwater lakes. *Environmental Science & Technology* 2002, 36(14):3064-3068.

Siciliano SD, O'Driscoll NJ, Tordon R, Hill J, Beauchamp S, Lean DRS: Abiotic production of methylmercury by solar radiation. *Environmental Science & Technology* 2005, 39(4):1071-1077.

Smith SL, MacDonald DD, Keenleyside KA, Ingersoll CG, Field LJ: A preliminary evaluation of sediment quality assessment values for freshwater ecosystems. *Journal of Great Lakes Research* 1996, 22(3):624-638.

St. Lawrence River Institute of Environmental Sciences: Movement of persistent toxic contaminants through the aquatic food chain, 2001.

http://www.ontarioenvirothon.on.ca/pdf/Aquatics/aquaticspartone3.pdf.

St.Lawrence River RAP Team..Remedial Action Plan for the Lake St. Francis River (Cornwall) Area of Concern. Stage 1 Report: Environmental Conditions and Problem Defenitions. Environment Canada & Environment Ontario 1992, ISBN 0-662-19958-8.

St.Lawrence River Rap Team. Remedial action plan for the St.Lawrence River (Cornwall) Area of Concern. Stage 2 Report: The recommended Plan. Environment Canada & Environment Ontario 1997, ISBN 0-7778-6881-4.

Stein ED, Cohen Y, Winer AM: Environmental distribution and transformation of mercury compounds. Critical Reviews in *Environmental Science and Technology* 1996, 26(1):1-43.

Sunderland EM, Gobas F, Heyes A, Branfireun BA, Bayer AK, Cranston RE, Parsons MB: Speciation and bioavailability of mercury in well-mixed estuarine sediments. *Marine Chemistry* 2004, 90(1-4):91-105.

Teasdale PR, Batley GE, Apte SC, Webster IT: Pore-Water Sampling with Sediment Peepers. Trac-Trends in *Analytical Chemistry* 1995, 14(6):250-256.

Telmer KH, Desjardins MJ, Ferguson P: Mercury cycling in lake sediments and porewaters on modern to Holocene time scales In Mercury Cycling in a Wetland-Dominated Ecosystem: Multidisciplinary Study, *SETAC Press* 2005, 69-114.

Ullrich SM, Tanton TW, Abdrashitova SA: Mercury in the aquatic environment: A review of factors affecting methylation. Critical Reviews in *Environmental Science and Technology* 2001, 31(3):241-293.

Urban NR, Jeong J, Chai YT: The benthic nepheloid layer (BNL) north of the Keweenaw Peninsula in Lake Superior: Composition, dynamics, and role in sediment transport. *Journal of Great Lakes Research* 2004, 30:133-146.

Viollier E, Inglett PW, Hunter K, Roychoudhury AN, Van Cappellen P: The ferrozine method revisited: Fe(II)/Fe(III) determination in natural waters. *Applied Geochemistry* 2000, 15(6):785-790.

Warner KA, Bonzongo JC: Microbial mercury transformation in anoxic freshwater sediments under iron-reducing and other electron-accepting conditions. *Environmental Science & Technology* 2003, 37(10):2159-2165.

Weber JH: Review of possible paths for abiotic methylation of mercury (II) in the aquatic environment. *Chemospher* 1993, 26(11):2063-2077.

Widerlund A, Ingri J: Redox Cycling of Iron and Manganese in Sediments of the Kalix River Estuary, Northern Sweden. *Aquatic Geochemistry* 1996, 2(2): 185-201.

Williams GP: Water temperature during the melting of lake ice WaterResour 1969, Res.5:1134-1138.

Wolfe MF, Schwarzbach S, Sulaiman RA: Effects of mercury on wildlife: A comprehensive review. *Environmental Toxicology and Chemistry* 1998, 17(2):146-160.

Wood JM, Kennedy FS, Rosen CG: Synthesis of Methyl-Mercury Compounds by Extracts of a Methanogenic Bacterium. *Nature* 1968, 220(5163):173-&.

Yamashita N, Kannan K, Imagawa T, Villeneuve DL, Hashimoto S, Miyazaki A, Giesy JP: Vertical profile of polychlorinated dibenzo-p-dioxins, dibenzofurans, naphthalenes, biphenyls, polycyclic aromatic hydrocarbons, and alkylphenols in a sediment core from Tokyo Bay, Japan. *Environmental Science & Technology* 2000, 34(17):3560-3567.

Yanch LE: Assessing the spatial and temporal patterns of total mercury, δ15N and δ 13C in yellow perch and their prey items from a contaminated site, St. Lawrence River, Cornwall, ON. 2007. M.Sc. thesis, Queen's University.

Yuan QZ, Valsaraj KT, Reible DD, Willson CS: A laboratory study of sediment and contaminant release during gas ebullition. *Journal of the Air & Waste Management Association* 2007, 57(9):1103-1111.

Zhang JZ, Wang FY, House JD, Page B: Thiols in wetland interstitial waters and their role in mercury and methylmercury speciation. *Limnology and Oceanography* 2004, 49(6):2276-2286.

# APPENDIX A

# Mercury in Sediment

# &

# Water Content Data

Table A-1. Sediment weight and water content in the HWF core.

| Intervals (cm) | wet weight (g) | Freeze-dried weight (g) | % water |
|---|---|---|---|
| 0-1 | 15.4891 | 6.8707 | 56 |
| 1-2 | 17.574 | 8.8497 | 50 |
| 2-3 | 25.2341 | 14.822 | 41 |
| 3-4 | 20.6105 | 11.2959 | 45 |
| 4-5 | 21.5089 | 11.9149 | 45 |
| 5-6 | 18.3333 | 9.9712 | 46 |
| 6-7 | 16.5888 | 8.6811 | 48 |
| 7-8 | 15.1245 | 7.6523 | 49 |
| 8-9 | 10.353 | 5.3557 | 48 |
| 9-10 | 13.2772 | 5.6322 | 58 |
| 12-14 | 14.7036 | 5.3523 | 64 |
| 16-18 | 13.7813 | 5.1971 | 62 |
| 20-24 | 15.0862 | 5.3325 | 65 |
| 24-28 | 16.7956 | 6.5952 | 61 |
| 32-36 | 10.5797 | 4.2475 | 60 |
| 40-44 | 15.6085 | 6.3081 | 60 |
| 48-52 | 18.8659 | 7.3034 | 61 |
| 56-60 | 20.7693 | 6.8947 | 67 |
| 60-64 | 15.8935 | 5.6512 | 64 |
| 66-67 | 10.9795 | 2.9131 | 73 |
| 68-69 | 11.6659 | 3.1157 | 73 |
| 69-70 | 13.6033 | 3.7504 | 72 |
| 70-71 | 14.8934 | 4.5035 | 70 |
| 71-72 | 15.591 | 5.1151 | 67 |

Table A-2. Sediment weight and water content in the LWF core.

| Intervals (cm) | wet weight (g) | Freeze-dried weight (g) | % water |
|---|---|---|---|
| 0-1 | 16.3465 | 2.9149 | 82 |
| 1-2 | 40.7419 | 11.9979 | 71 |
| 2-3 | 39.8306 | 11.7348 | 71 |
| 3-4 | 21.046 | 6.7808 | 68 |
| 4-5 | 26.3186 | 9.1355 | 65 |
| 5-6 | 30.7341 | 10.9955 | 64 |
| 6-7 | 34.5699 | 13.3738 | 61 |
| 7-8 | 38.4302 | 15.5173 | 60 |
| 8-9 | 42.061 | 17.1658 | 59 |
| 9-10 | 24.9484 | 10.3046 | 59 |
| 10-12 | 32.2289 | 14.0949 | 56 |
| 12-14 | 32.2994 | 13.9245 | 57 |
| 14-16 | 33.5875 | 14.0957 | 58 |
| 16-18 | 33.9751 | 15.2073 | 55 |
| 18-20 | 19.5655 | 8.978 | 54 |
| 20-24 | 21.4056 | 10.6578 | 50 |
| 24-28 | 20.2005 | 8.3643 | 59 |
| 28-32 | 20.9606 | 6.7212 | 68 |
| 32-36 | 18.7539 | 6.4507 | 66 |
| 36-40 | 16.179 | 5.379 | 67 |
| 40-44 | 18.1373 | 6.4828 | 64 |
| 44-45 | 11.6811 | 4.1884 | 64 |
| 45-46 | 12.6527 | 4.6044 | 64 |
| 46-47 | 13.7316 | 4.9483 | 64 |
| 47-48 | 11.0146 | 4.0721 | 63 |
| 48-49 | 12.2525 | 4.6628 | 62 |

Table A-3. THg concentration in sediment in the HWF core.

| Intervals (cm) | THg ($ng\ g^{-1}$) | THg ($ng\ g^{-1}$) | Ave THg ($ng\ g^{-1}$) | SD | CV |
|---|---|---|---|---|---|
| 0-1 | 1500 | 1600 | 1550 | 71 | 4.6 |
| 1-2 | 1300 | 1340 | 1320 | 28 | 2.1 |
| 2-3 | 1200 | 1260 | 1240 | 42 | 3.4 |
| 3-4 | 1450 | 1400 | 1420 | 35 | 2.5 |
| 5-6 | 1770 | 1720 | 1740 | 35 | 2.0 |
| 7-8 | 1870 | 2070 | 1970 | 141 | 7.2 |
| 9-10 | 2210 | 2110 | 2160 | 71 | 3.3 |
| 12-14 | 3600 | 3330 | 3460 | 191 | 5.5 |
| 16-18 | 5200 | 5730 | 5460 | 375 | 6.9 |
| 20-24 | 11800 | 11900 | 1180 | 71 | 6.0 |
| 24-28 | 11900 | 12800 | 12300 | 636 | 5.2 |
| 28-32 | 14300 | 13500 | 13900 | 566 | 4.1 |
| 32-36 | 16200 | 17200 | 160700 | 707 | 0.4 |
| 40-44 | 44000 | 45600 | 44800 | 1131 | 2.5 |
| 48-52 | 17500 | 20200 | 18800 | 1909 | 10.2 |
| 56-60 | 31500 | 30600 | 31000 | 636 | 2.1 |
| 60-64 | 26400 | 26700 | 26500 | 212 | 0.8 |
| 68-69 | 28700 | 26700 | 27700 | 1414 | 5.1 |
| 69-70 | 30500 | 32400 | 31400 | 1344 | 4.3 |
| 70-71 | 32000 | 30100 | 31000 | 1344 | 4.3 |
| 71-72 | 29900 | 30600 | 30200 | 495 | 1.6 |

Table A-4. THg concentration in sediment in the LWF core.

| Intervals (cm) | THg ($ng\ g^{-1}$) | THg ($ng\ g^{-1}$) | Ave THg ($ng\ g^{-1}$) | SD | CV |
|---|---|---|---|---|---|
| 0-1 | 1070 | 1100 | 1080 | 21 | 1.9 |
| 1-2 | 954 | 1100 | 1030 | 103 | 10.0 |
| 2-3 | 1250 | 1200 | 1220 | 35 | 2.9 |
| 3-4 | 785 | 747 | 766 | 27 | 3.5 |
| 4-5 | 803 | 810 | 8060 | 5 | 0.1 |
| 5-6 | 775 | 721 | 748 | 38 | 5.1 |
| 7-8 | 812 | 737 | 7740 | 53 | 0.7 |
| 9-10 | 798 | 751 | 7740 | 33 | 0.4 |
| 14-16 | 1050 | 1050 | 1050 | 0 | 0.0 |
| 18-20 | 2270 | 2560 | 2410 | 205 | 8.5 |
| 20-24 | 2810 | 2810 | 2810 | 0 | 0.0 |
| 24-28 | 3440 | 3440 | 3440 | 0 | 0.0 |
| 32-36 | 4440 | 4360 | 4400 | 57 | 1.3 |
| 40-44 | 18700 | 19600 | 19100 | 636 | 3.3 |
| 46-47 | 15000 | 14600 | 14800 | 283 | 1.9 |
| 47-48 | 23600 | 22800 | 23200 | 566 | 2.4 |
| 48-49 | 28800 | 32100 | 30400 | 2330 | 7.7 |

Table A-5. MeHg concentration in sediment in the HWF core.

| Intervals (cm) | MeHg ($ng\ g^{-1}$) | MeHg ($ng\ g^{-1}$) | Ave MeHg ($ng\ g^{-1}$) | SD |
|---|---|---|---|---|
| 0-1 | 7.2 | 7.3 | 7.2 | 0.1 |
| 1-2 | 10.0 | 9.1 | 9.5 | 0.8 |
| 2-3 | 4.1 | 2.7 | 3.4 | 1.0 |
| 5-6 | 2.0 | 2.0 | 2.0 | 0.2 |
| 9-10 | 4.6 | 2.7 | 3.6 | 1.3 |
| 16-18 | 4.4 | 4.0 | 4.2 | 0.3 |
| 24-28 | 12.2 | 14.7 | 13.4 | 1.5 |
| 32-36 | 32.4 | 34.7 | 33.6 | 1.6 |
| 40-44 | 37.6 | 26.2 | 32.0 | 6.8 |
| 56-60 | 8.8 | 9.4 | 9.1 | 0.8 |
| 60-64 | 8.8 | 8.6 | 8.7 | 0.2 |
| 69-70 | 16.1 | 0.0 | 8.0 | 11.4 |
| 71-72 | 9.4 | 15.5 | 12.5 | 4.3 |

Table A-6. MeHg concentration in sediment in the LWF core.

| Intervals (cm) | MeHg ($ng\ g^{-1}$) | MeHg ($ng\ g^{-1}$) | Ave MeHg ($ng\ g^{-1}$) | SD |
|---|---|---|---|---|
| 0-1 | 3.2 | 3.8 | 3.5 | 0.4 |
| 1-2 | 2.2 | 3.6 | 2.9 | 0.9 |
| 2-3 | 1.9 | 4.2 | 3.0 | 1.4 |
| 5-6 | 2.2 | 2.5 | 2.3 | 0.2 |
| 9-10 | 0.9 | 1.6 | 1.2 | 0.5 |
| 14-16 | 1.1 | 1.1 | 1.1 | 0.1 |
| 18-20 | 1.5 | 2.0 | 1.7 | 0.5 |
| 24-28 | 2.7 | 3.2 | 3.0 | 0.3 |
| 32-36 | 5.6 | 4.9 | 5.3 | 0.5 |
| 40-44 | 38.1 | 38.7 | 38.4 | 0.4 |
| 47-48 | 23.0 | 31.2 | 27.1 | 5.8 |
| 48-49 | 43.3 | 42.6 | 43.0 | 0.5 |

# APPENDIX B

# Mercury in Porewater

# Profiles

Table B-1. Depth profile of THg concentration in porewater and water column.

| Site | Month | Depth (cm) | THg ($ng\ L^{-1}$) |
|---|---|---|---|
| HWF | June | -22 | 48.00 |
| HWF | June | -18 | 17.36 |
| HWF | June | -16 | 14.28 |
| HWF | June | -14 | 12.46 |
| HWF | June | -12 | 5.50 |
| HWF | June | -10 | 13.31 |
| HWF | June | -8 | 9.25 |
| HWF | June | -6 | 15.21 |
| HWF | June | -4 | 11.65 |
| HWF | June | -2 | 11.85 |
| HWF | June | 0 | 13.67 |
| HWF | June | 2 | 7.17 |
| HWF | June | 4 | 21.83 |
| HWF | June | 6 | 4.26 |
| HWF | June | 8 | 9.82 |
| HWF | June | 10 | 22.19 |
| HWF | June | 12 | 15.10 |

Table B-2. Depth profile of THg concentration in porewater and water column.

| Site | Month | Depth (cm) | THg ($ng\ L^{-1}$) |
|---|---|---|---|
| HWF | June | -24 | 22.8 |
| HWF | June | -22 | 8.3 |
| HWF | June | -20 | 13.9 |
| HWF | June | -18 | 25.8 |
| HWF | June | -16 | 7.5 |
| HWF | June | -14 | 12.1 |
| HWF | June | -12 | 9.2 |
| HWF | June | -10 | 22.9 |
| HWF | June | -8 | 18.1 |
| HWF | June | -6 | 13.8 |
| HWF | June | -4 | 23.1 |
| HWF | June | 0 | 5.4 |
| HWF | June | 2 | 10.0 |
| HWF | June | 4 | 6.0 |
| HWF | June | 6 | 6.2 |
| HWF | June | 8 | 7.0 |
| HWF | June | 10 | 20.1 |
| HWF | June | 12 | 11.4 |

Table B-3. Depth profile of THg concentration in porewater and water column.

| Site | Month | Depth (cm) | THg (ng $L^{-1}$) |
|---|---|---|---|
| HWF | June | -24 | 46.9 |
| HWF | June | -22 | 31.9 |
| HWF | June | -20 | 28.7 |
| HWF | June | -18 | 19.0 |
| HWF | June | -14 | 33.1 |
| HWF | June | -12 | 25.2 |
| HWF | June | -10 | 26.8 |
| HWF | June | -8 | 58.6 |
| HWF | June | -6 | 32.4 |
| HWF | June | -4 | 38.7 |
| HWF | June | -2 | 22.0 |
| HWF | June | 0 | 19.6 |
| HWF | June | 2 | 16.1 |
| HWF | June | 4 | 40.4 |
| HWF | June | 6 | 20.8 |
| HWF | June | 8 | 46.0 |
| HWF | June | 10 | 25.2 |

Table B-4. Depth profile of THg concentration in porewater and water column.

| Site | Month | Depth (cm) | THg ($ng\ L^{-1}$) |
|---|---|---|---|
| LWF | June | -24 | 7.3 |
| LWF | June | -22 | 4.5 |
| LWF | June | -20 | 6.6 |
| LWF | June | -18 | 171.2 |
| LWF | June | -16 | 8.4 |
| LWF | June | -14 | 16.9 |
| LWF | June | -12 | 8.8 |
| LWF | June | -10 | 11.2 |
| LWF | June | -8 | 11.5 |
| LWF | June | -6 | 15.2 |
| LWF | June | -4 | 28.2 |
| LWF | June | 0 | 27.4 |
| LWF | June | 2 | 20.0 |
| LWF | June | 4 | 17.0 |
| LWF | June | 6 | 24.9 |
| LWF | June | 8 | 22.2 |
| LWF | June | 10 | 45.1 |
| LWF | June | 12 | 14.9 |

Table B-5. Depth profile of THg concentration in porewater and water column.

| Site | Month | Depth (cm) | THg ($ng\ L^{-1}$) |
|---|---|---|---|
| LWF | June | -24 | 20.9 |
| LWF | June | -22 | 18.7 |
| LWF | June | -20 | 18.4 |
| LWF | June | -18 | 44.6 |
| LWF | June | -16 | 20.1 |
| LWF | June | -14 | 16.4 |
| LWF | June | -12 | 17.1 |
| LWF | June | -10 | 15.9 |
| LWF | June | -8 | 18.8 |
| LWF | June | -6 | 25.0 |
| LWF | June | -4 | 24.4 |
| LWF | June | -2 | 21.0 |
| LWF | June | 0 | 23.5 |
| LWF | June | 2 | 24.4 |
| LWF | June | 4 | 19.6 |
| LWF | June | 6 | 17.6 |
| LWF | June | 8 | 14.2 |
| LWF | June | 10 | 11.0 |
| LWF | June | 12 | 12.9 |

Table B-6. Depth profile of THg concentration in porewater and water column.

| Site | Month | Depth (cm) | THg ($ng\ L^{-1}$) |
|---|---|---|---|
| HWF | July | -24 | 9.8 |
| HWF | July | -22 | 5.7 |
| HWF | July | -20 | 7.3 |
| HWF | July | -18 | 5.6 |
| HWF | July | -16 | 5.3 |
| HWF | July | -14 | 6.4 |
| HWF | July | -12 | 3.1 |
| HWF | July | -10 | 4.3 |
| HWF | July | -8 | 7.1 |
| HWF | July | -6 | 11.2 |
| HWF | July | -4 | 34.3 |
| HWF | July | -2 | 21.0 |
| HWF | July | 2 | 12.6 |
| HWF | July | 4 | 13.3 |
| HWF | July | 6 | 14.6 |
| HWF | July | 8 | 7.6 |
| HWF | July | 10 | 10.8 |

Table B-7. Depth profile of THg concentration in porewater and water column.

| Site | Month | Depth (cm) | THg ($ng\ L^{-1}$) |
|---|---|---|---|
| HWF | July | -22 | 22.1 |
| HWF | July | -20 | 29.5 |
| HWF | July | -18 | 22.1 |
| HWF | July | -16 | 19.0 |
| HWF | July | -12 | 16.6 |
| HWF | July | -10 | 18.2 |
| HWF | July | -8 | 16.1 |
| HWF | July | -6 | 14.6 |
| HWF | July | -4 | 20.1 |
| HWF | July | 0 | 23.1 |
| HWF | July | 2 | 16.3 |
| HWF | July | 4 | 11.2 |
| HWF | July | 6 | 16.4 |
| HWF | July | 8 | 11.7 |
| HWF | July | 10 | 21.0 |
| HWF | July | 12 | 33.0 |
| HWF | July | 14 | 10.4 |

Table B-8. Depth profile of THg concentration in porewater and water column.

| Site | Month | Depth (cm) | THg ($ng\ L^{-1}$) |
|---|---|---|---|
| HWF | July | -20 | 6.45 |
| HWF | July | -18 | 25.37 |
| HWF | July | -16 | 18.72 |
| HWF | July | -14 | 13.59 |
| HWF | July | -12 | 18.45 |
| HWF | July | -10 | 18.30 |
| HWF | July | -8 | 21.14 |
| HWF | July | -6 | 11.41 |
| HWF | July | -4 | 18.09 |
| HWF | July | -2 | 19.58 |
| HWF | July | 0 | 25.15 |
| HWF | July | 2 | 10.78 |
| HWF | July | 4 | 11.05 |
| HWF | July | 6 | 16.88 |
| HWF | July | 8 | 14.65 |
| HWF | July | 10 | 8.74 |
| HWF | July | 12 | 9.54 |
| HWF | July | 14 | 12.13 |

Table B-9. Depth profile of THg concentration in porewater and water column.

| Site | Month | Depth (cm) | THg (ng $L^{-1}$) |
|---|---|---|---|
| LWF | July | -24 | 9.5 |
| LWF | July | -22 | 11.5 |
| LWF | July | -18 | 15.7 |
| LWF | July | -16 | 21.1 |
| LWF | July | -14 | 17.6 |
| LWF | July | -12 | 29.6 |
| LWF | July | -10 | 19.9 |
| LWF | July | -8 | 16.7 |
| LWF | July | -6 | 14.0 |
| LWF | July | -4 | 17.0 |
| LWF | July | -2 | 57.1 |
| LWF | July | 0 | 31.8 |
| LWF | July | 2 | 16.1 |
| LWF | July | 4 | 9.9 |
| LWF | July | 6 | 8.2 |
| LWF | July | 8 | 13.4 |

Table B-10. Depth profile of THg concentration in porewater and water column.

| Site | Month | Depth (cm) | THg ($ng\ L^{-1}$) |
|---|---|---|---|
| LWF | July | -20 | 14.5 |
| LWF | July | -18 | 15.0 |
| LWF | July | -16 | 13.8 |
| LWF | July | -14 | 11.8 |
| LWF | July | -12 | 10.3 |
| LWF | July | -10 | 29.2 |
| LWF | July | -8 | 42.1 |
| LWF | July | -6 | 19.1 |
| LWF | July | -4 | 26.8 |
| LWF | July | -2 | 21.7 |
| LWF | July | 0 | 12.2 |
| LWF | July | 2 | 12.3 |
| LWF | July | 4 | 19.1 |
| LWF | July | 6 | 15.7 |
| LWF | July | 8 | 13.8 |
| LWF | July | 10 | 10.4 |
| LWF | July | 12 | 10.1 |
| LWF | July | 14 | 13.9 |
| LWF | July | 16 | 11.2 |

Table B-11. Depth profile of THg concentration in porewater and water column.

| Site | Month | Depth (cm) | THg ($ng\ L^{-1}$) |
|---|---|---|---|
| LWF | July | -14 | 19.8 |
| LWF | July | -12 | 17.1 |
| LWF | July | -10 | 21.7 |
| LWF | July | -8 | 21.1 |
| LWF | July | -6 | 27.6 |
| LWF | July | -4 | 11.9 |
| LWF | July | -2 | 11.5 |
| LWF | July | 4 | 29.2 |
| LWF | July | 8 | 18.4 |
| LWF | July | 10 | 15.5 |

Table B-12. Depth profile of THg concentration in porewater and water column.

| Site | Month | Depth (cm) | THg ($ng\ L^{-1}$) |
|---|---|---|---|
| HWF | August | -20 | 15.0 |
| HWF | August | -18 | 24.5 |
| HWF | August | -16 | 18.4 |
| HWF | August | -14 | 18.3 |
| HWF | August | -12 | 10.1 |
| HWF | August | -10 | 8.9 |
| HWF | August | -8 | 10.2 |
| HWF | August | -6 | 12.9 |
| HWF | August | -4 | 15.1 |
| HWF | August | -2 | 17.4 |
| HWF | August | 0 | 11.9 |
| HWF | August | 2 | 8.1 |
| HWF | August | 4 | 7.8 |
| HWF | August | 6 | 7.8 |
| HWF | August | 8 | 6.8 |
| HWF | August | 10 | 8.8 |
| HWF | August | 12 | 8.2 |
| HWF | August | 14 | 7.1 |

Table B-13. Depth profile of THg concentration in porewater and water column.

| Site | Month | Depth (cm) | THg ($ng\ L^{-1}$) |
|---|---|---|---|
| HWF | August | -24 | 33.3 |
| HWF | August | -22 | 28.1 |
| HWF | August | -18 | 13.8 |
| HWF | August | -16 | 22.0 |
| HWF | August | -14 | 13.4 |
| HWF | August | -12 | 12.6 |
| HWF | August | -10 | 13.4 |
| HWF | August | -8 | 13.9 |
| HWF | August | -6 | 20.2 |
| HWF | August | -4 | 33.0 |
| HWF | August | -2 | 29.6 |
| HWF | August | 0 | 19.6 |
| HWF | August | 2 | 14.7 |
| HWF | August | 4 | 15.0 |
| HWF | August | 6 | 8.6 |
| HWF | August | 8 | 11.8 |
| HWF | August | 10 | 9.5 |
| HWF | August | 12 | 9.8 |

Table B-14. Depth profile of THg concentration in porewater and water column.

| Site | Month | Depth (cm) | THg ($ng\ L^{-1}$) |
|---|---|---|---|
| HWF | August | -18 | 15.3 |
| HWF | August | -16 | 10.8 |
| HWF | August | -14 | 13.6 |
| HWF | August | -12 | 12.7 |
| HWF | August | -10 | 9.8 |
| HWF | August | -8 | 10.7 |
| HWF | August | -4 | 13.5 |
| HWF | August | -2 | 16.2 |
| HWF | August | 0 | 18.8 |
| HWF | August | 2 | 12.4 |
| HWF | August | 4 | 7.4 |
| HWF | August | 6 | 5.6 |
| HWF | August | 8 | 6.9 |
| HWF | August | 10 | 5.1 |
| HWF | August | 12 | 5.5 |
| HWF | August | 14 | 4.4 |
| HWF | August | 16 | 5.5 |

Table B-15. Depth profile of THg concentration in porewater and water column.

| Site | Month | Depth (cm) | THg ($ng\ L^{-1}$) |
|---|---|---|---|
| LWF | August | -18 | 28.6 |
| LWF | August | -16 | 12.9 |
| LWF | August | -14 | 12.2 |
| LWF | August | -12 | 11.4 |
| LWF | August | -10 | 14.0 |
| LWF | August | -8 | 14.0 |
| LWF | August | -6 | 16.4 |
| LWF | August | -4 | 76.9 |
| LWF | August | -2 | 50.6 |
| LWF | August | 2 | 16.8 |
| LWF | August | 4 | 14.1 |
| LWF | August | 6 | 13.7 |
| LWF | August | 8 | 7.1 |
| LWF | August | 10 | 7.2 |
| LWF | August | 12 | 8.2 |
| LWF | August | 14 | 7.4 |
| LWF | August | 16 | 6.5 |
| LWF | August | 18 | 7.5 |

Table B-16. Depth profile of THg concentration in porewater and water column.

| Site | Month | Depth (cm) | THg ($ng\ L^{-1}$) |
|---|---|---|---|
| LWF | August | -22 | 26.8 |
| LWF | August | -20 | 12.3 |
| LWF | August | -18 | 8.6 |
| LWF | August | -16 | 11.3 |
| LWF | August | -14 | 10.9 |
| LWF | August | -12 | 11.4 |
| LWF | August | -10 | 11.3 |
| LWF | August | -8 | 9.9 |
| LWF | August | -6 | 13.3 |
| LWF | August | -4 | 16.0 |
| LWF | August | -2 | 13.8 |
| LWF | August | 0 | 13.2 |
| LWF | August | 2 | 26.1 |
| LWF | August | 4 | 10.7 |
| LWF | August | 6 | 13.1 |
| LWF | August | 8 | 7.3 |
| LWF | August | 10 | 9.1 |
| LWF | August | 12 | 7.5 |
| LWF | August | 14 | 8.6 |

Table B-17. Depth profile of THg concentration in porewater and water column.

| Site | Month | Depth (cm) | THg (ng $L^{-1}$) |
|---|---|---|---|
| LWF | August | -22 | 16.0 |
| LWF | August | -20 | 12.1 |
| LWF | August | -18 | 13.0 |
| LWF | August | -16 | 11.7 |
| LWF | August | -14 | 13.6 |
| LWF | August | -12 | 14.1 |
| LWF | August | -10 | 15.0 |
| LWF | August | -8 | 15.8 |
| LWF | August | -6 | 16.2 |
| LWF | August | -4 | 18.6 |
| LWF | August | -2 | 16.2 |
| LWF | August | 0 | 17.6 |
| LWF | August | 2 | 43.7 |
| LWF | August | 4 | 21.6 |
| LWF | August | 6 | 24.8 |
| LWF | August | 8 | 24.8 |
| LWF | August | 10 | 21.1 |
| LWF | August | 12 | 13.0 |
| LWF | August | 14 | 15.2 |

Table B-18. Depth profile of MeHg concentration in porewater and water column.

| Site | Month | Depth (cm) | MeHg ($ng\ L^{-1}$) |
|---|---|---|---|
| HWF | June | -24 | 2.26 |
| HWF | June | -22 | 2.48 |
| HWF | June | -20 | 3.79 |
| HWF | June | -18 | 3.84 |
| HWF | June | -16 | 3.41 |
| HWF | June | -14 | 4.83 |
| HWF | June | -12 | 5.48 |
| HWF | June | -10 | 2.78 |
| HWF | June | -8 | 2.69 |
| HWF | June | -6 | 3.44 |
| HWF | June | -4 | 4.04 |
| HWF | June | -2 | 4.19 |
| HWF | June | 0 | 1.38 |
| HWF | June | 2 | 2.83 |
| HWF | June | 4 | 2.94 |
| HWF | June | 6 | 3.00 |
| HWF | June | 8 | 1.66 |
| HWF | June | 10 | 2.57 |
| HWF | June | 12 | 1.74 |

Table B-19. Depth profile of MeHg concentration in porewater and water column.

| Site | Month | Depth (cm) | MeHg ($ng\ L^{-1}$) |
|---|---|---|---|
| HWF | June | -22 | 4.42 |
| HWF | June | -20 | 2.40 |
| HWF | June | -18 | 2.17 |
| HWF | June | -16 | 5.21 |
| HWF | June | -14 | 4.97 |
| HWF | June | -12 | 3.97 |
| HWF | June | -10 | 4.01 |
| HWF | June | -8 | 5.82 |
| HWF | June | -6 | 8.43 |
| HWF | June | -4 | 5.88 |
| HWF | June | -2 | 3.27 |
| HWF | June | 0 | 2.12 |
| HWF | June | 2 | 3.06 |
| HWF | June | 4 | 1.71 |
| HWF | June | 6 | 2.53 |
| HWF | June | 8 | 3.76 |
| HWF | June | 10 | 2.22 |
| HWF | June | 12 | 3.41 |

Table B-20. Depth profile of MeHg concentration in porewater and water column.

| Site | Month | Depth (cm) | MeHg ($ng\ L^{-1}$) |
|---|---|---|---|
| LWF | June | -22 | 6.19 |
| LWF | June | -20 | 3.46 |
| LWF | June | -18 | 2.44 |
| LWF | June | -16 | 4.02 |
| LWF | June | -12 | 3.82 |
| LWF | June | -10 | 3.35 |
| LWF | June | -8 | 3.84 |
| LWF | June | -6 | 6.51 |
| LWF | June | -4 | 4.83 |
| LWF | June | -2 | 8.10 |
| LWF | June | 0 | 6.52 |
| LWF | June | 2 | 2.12 |
| LWF | June | 4 | 6.79 |
| LWF | June | 6 | 2.87 |
| LWF | June | 8 | 3.67 |
| LWF | June | 10 | 2.64 |
| LWF | June | 12 | 3.58 |
| LWF | June | 14 | 5.91 |

Table B-21. Depth profile of MeHg concentration in porewater and water column.

| Site | Month | Depth (cm) | MeHg ($ng\ L^{-1}$) |
|---|---|---|---|
| HWF | July | -22 | 11.6 |
| HWF | July | -18 | 12.54 |
| HWF | July | -16 | 13.06 |
| HWF | July | -14 | 11.66 |
| HWF | July | -12 | 8.21 |
| HWF | July | -10 | 8.01 |
| HWF | July | -8 | 8.02 |
| HWF | July | -6 | 4.27 |
| HWF | July | -4 | 20.98 |
| HWF | July | -2 | 19.82 |
| HWF | July | 0 | 9.34 |
| HWF | July | 2 | 7.15 |
| HWF | July | 4 | 16.21 |
| HWF | July | 6 | 27.87 |
| HWF | July | 8 | 8.25 |
| HWF | July | 10 | 3.35 |
| HWF | July | 12 | 9.66 |
| HWF | July | 14 | 8.58 |

Table B-22. Depth profile of MeHg concentration in porewater and water column.

| Site | Month | Depth (cm) | MeHg ($ng\ L^{-1}$) |
|---|---|---|---|
| LWF | July | -20 | 8.3 |
| LWF | July | -18 | 5.0 |
| LWF | July | -16 | 3.4 |
| LWF | July | -14 | 4.9 |
| LWF | July | -12 | 0.7 |
| LWF | July | -10 | 7.3 |
| LWF | July | -8 | 6.5 |
| LWF | July | -6 | 4.0 |
| LWF | July | -4 | 3.0 |
| LWF | July | -2 | 3.5 |
| LWF | July | 0 | 4.4 |
| LWF | July | 2 | 4.4 |
| LWF | July | 4 | 2.5 |
| LWF | July | 6 | 10.3 |
| LWF | July | 8 | 3.5 |
| LWF | July | 10 | 2.5 |
| LWF | July | 12 | 2.1 |
| LWF | July | 14 | 1.4 |
| LWF | July | 16 | 8.8 |

Table B-23. Depth profile of MeHg concentration in porewater and water column.

| Site | Month | Depth (cm) | MeHg ($ng\ L^{-1}$) |
|---|---|---|---|
| HWF | August | -20 | 8.4 |
| HWF | August | -18 | 8.6 |
| HWF | August | -14 | 7.3 |
| HWF | August | -12 | 10.5 |
| HWF | August | -10 | 3.4 |
| HWF | August | -8 | 11.5 |
| HWF | August | -6 | 6.6 |
| HWF | August | -4 | 7.0 |
| HWF | August | -2 | 9.2 |
| HWF | August | 0 | 6.3 |
| HWF | August | 2 | 2.4 |
| HWF | August | 4 | 1.3 |
| HWF | August | 6 | 0.5 |
| HWF | August | 8 | 2.8 |
| HWF | August | 10 | 1.3 |
| HWF | August | 12 | 2.8 |
| HWF | August | 14 | 1.8 |

Table B-24. Depth profile of MeHg concentration in porewater and water column.

| Site | Month | Depth (cm) | MeHg ($ng\ L^{-1}$) |
|---|---|---|---|
| LWF | August | -22 | 3.60 |
| LWF | August | -20 | 9.34 |
| LWF | August | -18 | 2.10 |
| LWF | August | -16 | 3.53 |
| LWF | August | -14 | 10.19 |
| LWF | August | -12 | 4.79 |
| LWF | August | -10 | 8.87 |
| LWF | August | -8 | 19.44 |
| LWF | August | -6 | 2.86 |
| LWF | August | -4 | 6.51 |
| LWF | August | -2 | 6.62 |
| LWF | August | 0 | 5.98 |
| LWF | August | 2 | 4.14 |
| LWF | August | 4 | 11.29 |
| LWF | August | 6 | 1.45 |
| LWF | August | 8 | 1.45 |
| LWF | August | 10 | 4.03 |
| LWF | August | 12 | 2.24 |
| LWF | August | 14 | 3.99 |

# APPENDIX C

# Redox – dependent

# Variables

# Porewater Profiles

Table C-1. Redox- dependent variables concentration in porewater and water column.

| Site | Month | Depth (cm) | $Fe^{2+}$(mg $L^{-1}$) | $S^{2-}$(mg $L^{-1}$) | $SO_4^{2-}$ (mg $L^{-1}$) |
|---|---|---|---|---|---|
| HWF | June | -25 | 8.7 | — | 0 |
| HWF | June | -24 | 8.69 | 0.07 | 0 |
| HWF | June | -23 | 6.91 | 0.12 | 0 |
| HWF | June | -22 | 5.74 | 0.13 | 0 |
| HWF | June | -21 | 5.18 | 0.08 | 0 |
| HWF | June | -20 | 5.44 | 0.03 | 0.82 |
| HWF | June | -19 | 5.14 | 0.01 | 1.29 |
| HWF | June | -18 | 3.37 | 0.03 | 0.52 |
| HWF | June | -17 | 2.48 | 0.10 | 2.17 |
| HWF | June | -16 | 2.38 | 0.14 | 9.77 |
| HWF | June | -15 | 1.59 | 0.16 | 13.58 |
| HWF | June | -14 | 0.79 | 0.13 | 16.42 |
| HWF | June | -13 | 0.04 | 0.18 | 17.42 |
| HWF | June | -12 | 0.27 | 0.06 | 22.31 |
| HWF | June | -11 | 0.48 | 0.03 | 17.49 |
| HWF | June | -10 | 0.82 | 0.01 | 16.44 |
| HWF | June | -9 | 0.86 | 0.03 | 8.92 |
| HWF | June | -8 | 0.93 | 0.04 | 11.09 |
| HWF | June | -7 | 1.07 | 0.08 | 8.74 |
| HWF | June | -6 | 1.31 | 0.06 | 7.81 |
| HWF | June | -5 | 1.64 | 0.01 | 6.95 |
| HWF | June | -4 | 0.23 | 0.00 | 15.12 |
| HWF | June | -3 | 0.88 | 0.01 | 29.14 |
| HWF | June | -2 | 0.98 | 0.00 | 16.23 |
| HWF | June | -1 | 0.61 | 0.00 | 15.28 |
| HWF | June | 0 | 0.02 | 0.00 | 18.57 |
| HWF | June | 1 | 0.01 | 0.01 | 18.04 |
| HWF | June | 2 | 0.01 | 0.00 | 19.94 |
| HWF | June | 3 | 0 | 0.00 | 18.1 |
| HWF | June | 4 | 0 | 0.00 | 18.73 |
| HWF | June | 5 | 0 | 0.00 | 18.28 |
| HWF | June | 6 | 0 | 0.00 | 22.05 |
| HWF | June | 7 | 0 | 0.00 | 17.88 |
| HWF | June | 8 | 0 | 0.00 | 20.06 |
| HWF | June | 9 | 0 | 0.00 | 17.25 |
| HWF | June | 10 | 0 | 0.00 | 16.72 |
| HWF | June | 11 | 0 | 0.00 | 18.87 |

Table C-2. Redox- dependent variables concentration in porewater and water column.

| Site | Month | Depth(cm) | $Fe^{2+}$(mg $L^{-1}$) | $S^{2-}$(mg $L^{-1}$) | $SO_4^{2-}$ (mg $L^{-1}$) |
|---|---|---|---|---|---|
| HWF | July | -24 | 7.79 | 0.894 | 0.61 |
| HWF | July | -23 | 5.22 | 1.248 | 0 |
| HWF | July | -22 | 5.61 | 0.797 | 0.15 |
| HWF | July | -21 | 0 | 0.676 | 1.78 |
| HWF | July | -20 | 2.48 | 0.27 | 1.85 |
| HWF | July | -19 | 7.83 | 0.863 | 2.67 |
| HWF | July | -18 | 6.93 | 1.108 | 1.21 |
| HWF | July | -17 | 4.36 | 0.938 | 1.12 |
| HWF | July | -16 | 2.89 | 0.307 | 1.21 |
| HWF | July | -15 | 1.96 | 0.293 | 1.69 |
| HWF | July | -14 | 0.64 | 0.091 | 1.05 |
| HWF | July | -13 | 1.86 | 0.323 | 1.61 |
| HWF | July | -12 | 1.72 | 0.145 | 1.1 |
| HWF | July | -11 | 1.88 | 0.237 | 2.21 |
| HWF | July | -10 | 1.75 | 0.253 | 1.58 |
| HWF | July | -9 | 0.47 | 0.317 | 1.25 |
| HWF | July | -8 | — | 0.069 | 6.68 |
| HWF | July | -7 | 1 | 0.126 | 1.32 |
| HWF | July | -6 | 0.28 | 0.157 | 2.9 |
| HWF | July | -5 | 0.05 | 1.01 | 8.58 |
| HWF | July | -4 | 0.05 | 0.178 | 13.65 |
| HWF | July | -3 | 0.05 | 0.222 | 19.59 |
| HWF | July | -2 | 0.09 | 0.078 | 17.67 |
| HWF | July | -1 | 0 | 0.017 | 19.36 |
| HWF | July | 0 | 0 | 0.006 | 20.36 |
| HWF | July | 1 | 0 | 0.374 | 21.82 |
| HWF | July | 2 | 0.63 | 0.004 | 20.07 |
| HWF | July | 3 | 0 | 0.003 | 22.11 |
| HWF | July | 4 | 0 | 0.023 | 21.1 |
| HWF | July | 5 | 0.02 | 0.002 | 20.36 |
| HWF | July | 6 | 0.01 | 0.075 | 19.25 |
| HWF | July | 7 | 0 | 0.013 | 20.82 |
| HWF | July | 8 | 0 | 0.032 | 20.38 |
| HWF | July | 9 | 0.04 | 0.017 | 21.3 |
| HWF | July | 10 | 0 | 0 | 21.2 |
| HWF | July | 11 | 0 | 0.01 | 21.33 |
| HWF | July | 12 | 0 | 0.018 | 18.67 |
| HWF | July | 13 | 0 | 0.039 | 20.95 |

Table C-3. Redox- dependent variables concentration in porewater and water column.

| Site | Month | Depth(cm) | $Fe^{2+}$(mg $L^{-1}$) | $S^{2-}$(mg $L^{-1}$) | $SO_4^{2-}$ (mg $L^{-1}$) |
|---|---|---|---|---|---|
| HWF | August | -24 | 8.19 | 0.74 | 3.3 |
| HWF | August | -23 | 8.15 | — | 0 |
| HWF | August | -22 | 0 | 0.48 | 0 |
| HWF | August | -21 | 7.97 | 0.42 | 0 |
| HWF | August | -20 | 0 | 0.63 | 0 |
| HWF | August | -19 | 8.15 | 0.8 | 0 |
| HWF | August | -18 | 8.08 | 0.63 | 0 |
| HWF | August | -17 | 8 | 0.47 | 0 |
| HWF | August | -16 | 7.45 | 0.64 | 0 |
| HWF | August | -15 | 6.33 | 0.55 | 0 |
| HWF | August | -14 | 4.96 | 0.26 | 0 |
| HWF | August | -13 | 1.45 | — | 0 |
| HWF | August | -12 | — | 0.1 | 0 |
| HWF | August | -11 | 4.47 | 0.2 | 0 |
| HWF | August | -10 | 4.64 | 0.3 | 0 |
| HWF | August | -9 | 5.57 | 1.5 | 0 |
| HWF | August | -8 | 6.52 | 0.73 | 1.32 |
| HWF | August | -7 | 6.18 | 0.69 | — |
| HWF | August | -6 | 5.63 | 0.25 | 0.48 |
| HWF | August | -5 | 5.13 | 0.17 | 0 |
| HWF | August | -4 | 3.37 | — | 0.44 |
| HWF | August | -3 | 4.89 | 0.01 | 0 |
| HWF | August | -2 | 2.62 | 0.15 | 0.25 |
| HWF | August | -1 | 1.17 | 0 | 0.38 |
| HWF | August | 0 | 0 | 0 | 2.9 |
| HWF | August | 1 | 0 | 0 | 18.97 |
| HWF | August | 2 | 0 | 0 | 21.67 |
| HWF | August | 3 | 0.04 | — | 22.67 |
| HWF | August | 4 | 0 | 0 | 21.06 |
| HWF | August | 5 | 0 | 0 | 22.55 |
| HWF | August | 6 | 0 | 0 | 21.45 |
| HWF | August | 7 | 0 | 0 | 21.81 |
| HWF | August | 8 | 0 | 0 | 22.53 |
| HWF | August | 9 | 0 | 0 | 24.5 |
| HWF | August | 10 | 0 | 0 | 23.75 |
| HWF | August | 11 | 0 | 0.07 | 25.42 |
| HWF | August | 12 | 0 | 0 | 22.56 |
| HWF | August | 13 | 0 | 0.48 | 23.72 |

Table C-4. Redox- dependent variables concentration in porewater and water column.

| Site | Month | Depth(cm) | $Fe^{2+}$(mg $L^{-1}$) | $S^{2-}$(mg $L^{-1}$) | $SO_4^{2-}$ (mg $L^{-1}$) |
|---|---|---|---|---|---|
| LWF | June | -27 | 8.13 | 0.188 | — |
| LWF | June | -26 | 7.77 | 0.000 | 0.84 |
| LWF | June | -25 | 7.13 | 0.000 | 0.49 |
| LWF | June | -24 | 5.23 | 0.000 | 0.7 |
| LWF | June | -23 | 2.51 | 0.000 | 2.96 |
| LWF | June | -22 | 4.79 | 0.000 | 3.64 |
| LWF | June | -21 | 3.64 | 0.000 | 3.81 |
| LWF | June | -20 | 3.34 | 0.000 | — |
| LWF | June | -19 | 2.96 | 0.000 | 2.02 |
| LWF | June | -18 | 3.49 | 0.000 | 1.55 |
| LWF | June | -17 | 2.93 | 0.009 | 1.09 |
| LWF | June | -16 | 2.46 | 0.000 | 0.96 |
| LWF | June | -15 | 2.35 | 0.000 | 1.75 |
| LWF | June | -14 | 2.47 | 0.000 | 2.12 |
| LWF | June | -13 | 2.33 | 0.000 | 1.33 |
| LWF | June | -12 | 1.76 | 0.000 | 1.27 |
| LWF | June | -11 | 1.65 | 0.000 | 1.06 |
| LWF | June | -10 | 1.7 | 0.000 | 3.65 |
| LWF | June | -9 | 1.7 | 0.000 | 1.34 |
| LWF | June | -8 | 1.76 | 0.000 | 1.53 |
| LWF | June | -7 | 1.92 | 0.000 | 1.78 |
| LWF | June | -6 | 2.01 | 0.000 | 2.02 |
| LWF | June | -5 | 2.02 | 0.000 | 1.56 |
| LWF | June | -4 | 2.17 | 0.000 | — |
| LWF | June | -3 | 3.35 | 0.000 | 1.76 |
| LWF | June | -2 | 4.01 | 0.000 | 6.94 |
| LWF | June | -1 | 1.16 | 0.000 | 2.55 |
| LWF | June | 0 | 1.33 | 0.000 | 54.18 |
| LWF | June | 1 | 1.21 | 0.000 | 9.59 |
| LWF | June | 2 | 0.5 | 0.002 | 17.22 |
| LWF | June | 3 | 0 | 0.002 | 33.9 |
| LWF | June | 4 | 0 | 0.001 | 44.42 |
| LWF | June | 5 | 0 | 0.000 | 22.78 |
| LWF | June | 6 | 0 | 0.000 | 21.99 |
| LWF | June | 7 | 0 | 0.000 | 35.33 |
| LWF | June | 8 | 0 | 0.000 | 25.89 |
| LWF | June | 9 | 0 | 0.000 | 23.25 |
| LWF | June | 10 | 0 | 0.000 | 23.09 |

Table C-5. Redox- dependent variables concentration in porewater and water column.

| Site | Month | Depth(cm) | $Fe^{2+}$(mg $L^{-1}$) | $S^{2-}$(mg $L^{-1}$) | $SO_4^{2-}$ (mg $L^{-1}$) |
|---|---|---|---|---|---|
| LWF | July | -20 | 7.81 | 0.253 | 0.9 |
| LWF | July | -19 | 0 | 1.039 | 0.23 |
| LWF | July | -18 | 7.55 | 0.929 | 0.49 |
| LWF | July | -17 | 4.17 | 1.091 | 0.01 |
| LWF | July | -16 | 6.8 | 0.715 | 0 |
| LWF | July | -15 | 7.59 | 0.525 | 0.26 |
| LWF | July | -14 | 6.66 | 2.597 | 0.19 |
| LWF | July | -13 | 5.51 | 0 | 0.24 |
| LWF | July | -12 | 4.98 | 0.085 | 0.76 |
| LWF | July | -11 | 4.88 | 0.049 | 1.18 |
| LWF | July | -10 | 4.14 | 0.378 | 1 |
| LWF | July | -9 | 3.84 | 0 | 0.49 |
| LWF | July | -8 | 3.18 | 0 | 0.39 |
| LWF | July | -7 | 2.53 | 0.047 | 0.72 |
| LWF | July | -6 | 2.2 | 1.556 | 0.87 |
| LWF | July | -5 | 1.57 | 1.595 | 0.68 |
| LWF | July | -4 | 1.01 | 0.4 | 3.8 |
| LWF | July | -3 | 0.49 | 0.157 | 4.88 |
| LWF | July | -2 | 0.65 | 0.09 | 9.05 |
| LWF | July | -1 | 0.14 | 0 | 12.65 |
| LWF | July | 0 | — | 0.022 | 16.99 |
| LWF | July | 1 | 0.05 | 0.044 | 21.4 |
| LWF | July | 2 | 0.05 | 0.013 | 21.51 |
| LWF | July | 3 | 0.05 | 0.079 | 20.69 |
| LWF | July | 4 | 0.04 | 0.072 | 20.38 |
| LWF | July | 5 | 0.04 | 0 | 19.6 |
| LWF | July | 6 | 0.04 | 0 | 20.96 |
| LWF | July | 7 | 0.05 | 0 | 19.83 |
| LWF | July | 8 | 0.06 | 0 | 19.36 |
| LWF | July | 9 | 0.04 | 0 | 19.22 |
| LWF | July | 10 | 0.04 | 0.226 | 22.56 |
| LWF | July | 11 | 0.04 | 0 | 24.53 |
| LWF | July | 12 | 0.04 | 0 | 20.65 |
| LWF | July | 13 | 0.04 | 0 | 19.81 |
| LWF | July | 14 | 0.04 | 0 | — |
| LWF | July | 15 | 0.05 | 0 | — |
| LWF | July | 16 | 0.03 | 0 | — |
| LWF | July | 17 | 0.04 | 0 | — |

Table C-6. Redox- dependent variables concentration in porewater and water column.

| Site | Month | Depth(cm) | $Fe^{2+}$(mg $L^{-1}$) | $S^{2-}$(mg $L^{-1}$) | $SO_4^{2-}$ (mg $L^{-1}$) |
|---|---|---|---|---|---|
| LWF | August | -24 | 8.13 | 0.53 | 0 |
| LWF | August | -23 | 8.17 | 0.37 | 2.21 |
| LWF | August | -22 | 8.04 | 0.78 | 0 |
| LWF | August | -21 | 7.1 | 2.22 | 0 |
| LWF | August | -20 | 8.11 | 1.52 | — |
| LWF | August | -19 | — | — | 0 |
| LWF | August | -18 | 7.89 | 1.98 | 0 |
| LWF | August | -17 | 7.54 | 1.41 | — |
| LWF | August | -16 | 6.4 | 1.01 | 0.2 |
| LWF | August | -15 | 6.74 | 1.79 | 0 |
| LWF | August | -14 | 6.13 | 1.99 | 0 |
| LWF | August | -13 | 5.76 | 2.16 | 0 |
| LWF | August | -12 | 3.79 | 2.53 | 0 |
| LWF | August | -11 | 4.7 | — | — |
| LWF | August | -10 | 4.49 | 2.98 | 0 |
| LWF | August | -9 | 4.00 | 2.06 | 0 |
| LWF | August | -8 | 3.43 | 2.02 | 2.11 |
| LWF | August | -7 | 3.41 | 1.14 | 1.28 |
| LWF | August | -6 | 2.81 | 0.96 | 0 |
| LWF | August | -5 | 1.69 | 0.59 | 2.57 |
| LWF | August | -4 | 0.49 | 0.57 | 7.74 |
| LWF | August | -3 | 1.00 | 0.46 | 4.59 |
| LWF | August | -2 | 0.95 | 0.31 | 4.57 |
| LWF | August | -1 | 0.81 | 0.18 | 2.91 |
| LWF | August | 0 | 0.82 | 0.13 | 2.69 |
| LWF | August | 1 | 0.65 | 0.21 | 8.54 |
| LWF | August | 2 | 0.03 | 0.07 | 20.43 |
| LWF | August | 3 | 0.03 | 0.06 | 24 |
| LWF | August | 4 | 0.01 | 0.05 | 22.05 |
| LWF | August | 5 | 0.01 | 0 | 23.55 |
| LWF | August | 6 | 0.01 | 0 | 21.13 |
| LWF | August | 7 | 0.01 | 0 | 22.23 |
| LWF | August | 8 | 0.01 | 0 | 23.69 |
| LWF | August | 9 | 0.02 | 0.01 | 21.5 |
| LWF | August | 10 | 0.01 | 0.22 | 23.38 |
| LWF | August | 11 | 0.01 | 0.01 | 22.95 |
| LWF | August | 12 | 0.01 | 0.07 | 20.92 |
| LWF | August | 13 | 0.01 | 0.01 | 20.9 |

Table C-7. Total Mn concentration in porewater and water column.

| Site | Month | Depth (cm) | Mn (mg $L^{-1}$) |
|---|---|---|---|
| HWF | June | -24 | 11.1128 |
| HWF | June | -22 | 8.6247 |
| HWF | June | -20 | 8.4682 |
| HWF | June | -18 | 9.8905 |
| HWF | June | -16 | 7.0882 |
| HWF | June | -14 | 3.7948 |
| HWF | June | -12 | 3.4758 |
| HWF | June | -10 | 3.4749 |
| HWF | June | -8 | 3.0015 |
| HWF | June | -6 | 3.67 |
| HWF | June | -4 | 1.9436 |
| HWF | June | -2 | 2.1272 |
| HWF | June | 0 | 1.1069 |
| HWF | June | 2 | 0.1237 |
| HWF | June | 4 | 0.0819 |
| HWF | June | 6 | 0.0371 |
| HWF | June | 8 | 0.0303 |
| HWF | June | 10 | 0.0223 |
| HWF | June | 12 | 0.0407 |
| LWF | June | -24 | 7.9748 |
| LWF | June | -22 | 4.271 |
| LWF | June | -20 | 3.5096 |
| LWF | June | -18 | 2.8799 |
| LWF | June | -16 | 2.5712 |
| LWF | June | -14 | 2.4209 |
| LWF | June | -12 | 2.2946 |
| LWF | June | -10 | 1.5187 |
| LWF | June | -8 | 1.7175 |
| LWF | June | -6 | 2.2033 |
| LWF | June | -4 | 2.3386 |
| LWF | June | -2 | 1.6102 |
| LWF | June | 0 | 0.7857 |
| LWF | June | 2 | 0.4549 |
| LWF | June | 4 | 0.0767 |
| LWF | June | 6 | 0.0264 |
| LWF | June | 8 | 0.0219 |
| LWF | June | 10 | 0.0376 |
| LWF | June | 12 | 0.0822 |

Table C-8. Total Mn concentration in porewater and water column.

| Site | Month | Depth (cm) | Mn (mg $L^{-1}$) |
|---|---|---|---|
| LWF | July | -20 | 0.522 |
| LWF | July | -18 | 0.4768 |
| LWF | July | -16 | |
| LWF | July | -14 | 0.4159 |
| LWF | July | -12 | 0.3609 |
| LWF | July | -10 | 0.3282 |
| LWF | July | -8 | 0.2683 |
| LWF | July | -6 | 0.2245 |
| LWF | July | -4 | 0.1596 |
| LWF | July | -2 | 0.1328 |
| LWF | July | 0 | 0.1159 |
| LWF | July | 2 | 0.0245 |
| LWF | July | 4 | 0.0166 |
| LWF | July | 6 | 0.0099 |
| LWF | July | 8 | 0.0078 |
| LWF | July | 10 | 0.0061 |
| LWF | July | 12 | 0.005 |
| LWF | July | 14 | 0.0046 |
| LWF | July | 16 | 0.0569 |

Table C-9. Total Mn concentration in porewater and water column.

| Site | Month | Depth (cm) | Mn (mg $L^{-1}$) |
|---|---|---|---|
| HWF | August | -22 | 0.8449 |
| HWF | August | -20 | 0.7703 |
| HWF | August | -18 | 0.4615 |
| HWF | August | -16 | 0.6054 |
| HWF | August | -14 | 0.5364 |
| HWF | August | -12 | 0.4685 |
| HWF | August | -10 | 0.3944 |
| HWF | August | -8 | 0.3567 |
| HWF | August | -6 | 0.3439 |
| HWF | August | -4 | 0.4478 |
| HWF | August | -2 | 0.5853 |
| HWF | August | 0 | 0.7065 |
| HWF | August | 2 | 0.2015 |
| HWF | August | 4 | 0.005 |
| HWF | August | 6 | 0.0031 |
| HWF | August | 8 | 0.0028 |
| HWF | August | 10 | 0.0024 |
| HWF | August | 12 | 0.0033 |
| HWF | August | 14 | 0.0043 |
| LWF | August | -22 | 0.5801 |
| LWF | August | -20 | 0.4945 |
| LWF | August | -18 | 0.4295 |
| LWF | August | -16 | 0.3937 |
| LWF | August | -14 | 0.3626 |
| LWF | August | -12 | 0.3554 |
| LWF | August | -10 | 0.3406 |
| LWF | August | -8 | 0.3799 |
| LWF | August | -6 | 0.3351 |
| LWF | August | -4 | 0.2409 |
| LWF | August | -2 | 0.2475 |
| LWF | August | 0 | 0.2797 |
| LWF | August | 2 | 0.0103 |
| LWF | August | 4 | 0.0025 |
| LWF | August | 6 | 0.0039 |
| LWF | August | 8 | 0.003 |
| LWF | August | 10 | 0.0032 |
| LWF | August | 12 | 0.0033 |
| LWF | August | 14 | 0.0039 |

# APPENDIX D

# ANOVA Analyses

Table D.1. Three-factor Anova for THg in porewater.

| Source | Type III SS | df | Mean Squares | F-ratio | p-value |
|---|---|---|---|---|---|
| Site | 0.006 | 1 | 0.006 | 0.257 | 0.617 |
| Month | 0.011 | 2 | 0.005 | 0.229 | 0.797 |
| Level | 0.073 | 1 | 0.073 | 3.081 | 0.093 |
| Month*Level | 0.043 | 2 | 0.022 | 0.912 | 0.416 |
| Site*Level | 0.022 | 1 | 0.022 | 0.940 | 0.343 |
| Month*Site | 0.037 | 2 | 0.018 | 0.781 | 0.470 |
| Site*Month*Level | 0.035 | 2 | 0.018 | 0.745 | 0.486 |
| Error | 0.520 | 22 | 0.024 | | |

Table D.2. Two-factor ANOVA for MeHg in porewater.

| Source | Type III SS | df | Mean Squares | F-ratio | p-value |
|---|---|---|---|---|---|
| Site | 0.006 | 1 | 0.006 | 0.257 | 0.617 |
| Month | 0.011 | 2 | 0.005 | 0.229 | 0.797 |
| Level | 0.073 | 1 | 0.073 | 3.081 | 0.093 |
| Month*Level | 0.043 | 2 | 0.022 | 0.912 | 0.416 |
| Site*Level | 0.022 | 1 | 0.022 | 0.940 | 0.343 |
| Month*Site | 0.037 | 2 | 0.018 | 0.781 | 0.470 |
| Site*Month*Level | 0.035 | 2 | 0.018 | 0.745 | 0.486 |
| Error | 0.520 | 22 | 0.024 | | |